ADAPTATION OF THE RADIAL FLOW ENERGY DISSIPATOR FOR USE WITH CIRCULAR OR BOX CULVERTS

by

Walter L. Moore
Khosrow Meshgin

Research Report Number 116-1

Performance of Circular Culverts on Steep Grades
Research Project 3-5-69-116

conducted for

The Texas Highway Department

in cooperation with the
U. S. Department of Transportation
Federal Highway Administration
Bureau of Public Roads

by the

CENTER FOR HIGHWAY RESEARCH
THE UNIVERSITY OF TEXAS AT AUSTIN

ACKNOWLEDGMENT

The research work presented herein is the continuation of Research Project No. 3-5-69-116, entitled "Performance of Circular Culverts on Steep Grades - Part II Exploratory Study of Energy Dissipator for Culvert Outlets."

The authors are grateful for helpful comments and suggestions by staff members of the Texas Highway Department and the U. S. Bureau of Public Roads, Mr. Samuel V. Fox, Mr. William J. Dallas, and Mr. Frank Johnson, and for financial support from these agencies as well as general assistance from the University of Texas Center for Highway Research.

The experimental work was conducted in the Hydraulic Laboratory of the University of Texas. Assisting the writers in the model construction, data collection and reduction were Engineering students, William Henderson, Phillip Cook, and Raymond K. Lamb. Laboratory assistance was also provided by Mr. Edward Bruce during the early stages of construction of the models. Many of the drawings for the report were prepared by Mr. Emede Garcia. Acknowledgment is made to Mrs. Patricia Harris for typing the final manuscript.

The authors are grateful to all individuals and agencies who were instrumental in the preparation and completion of this report.

The opinions, findings, and conclusions expressed in this publication are those of the authors and not necessarily those of the Bureau of Public Roads.

ABSTRACT

The investigation reported herein was undertaken to explore methods of adapting the radial flow energy dissipator previously developed for a box culvert for use with a circular culvert. Some of the geometric arrangements developed for use with circular culverts were also studied to see if they would be better than the arrangements originally developed for box culverts.

The basic criteria used in investigating the effectiveness of various geometric arrangements as energy dissipator were the stability of hydraulic jump, the efficiency of the spreading action, and the degree of velocity reduction in the jump.

The overall comparison of the performance characteristics of seven different structural configurations indicated a small difference in the performance of various arrangements. These structures included variations in the distance along the centerline from the end of the circular culvert to the beginning of the curved bottom drop section, variations in the shape of the curved bottom channel, and the elimination of the curved drop section replacing it with a simple vertical wall.

The more complex geometric forms showed no particular improvement over the simple curved drop section. From the evaluated results it appeared that the relative simplicity of construction was a strong argument in favor of the arrangements with the simple curved drop and straight horizontal transverse elements.

SUMMARY

Research Report 116-1 deals with studies made at the Hydraulic Laboratory of the Department of Civil Engineering at The University of Texas at Austin to develop the geometric form for a proposed new type of energy dissipator for use at the outlets of highway culverts. Two previous reports on another project (Refs 2 and 3) had indicated the feasibility of the new concept for an energy dissipator.

The basic concept for the new energy dissipator was to devise a means by which the flow at the culvert outlet could be spread in width to several times the width of the culvert. This was accomplished by incorporating a downward-curved entrance channel near the culvert outlet, followed by a sharp upward curve at the beginning of a horizontal basin. The upward vertical curve produced a pressure field causing the supercritical flow to spread in a radial direction between flared wingwalls, and with proper tailwater conditions a circular hydraulic jump was formed on the horizontal apron.

Water from a head tank was led into a six-inch culvert three feet long. Provision was made for installing either a circular culvert or a square box culvert and for controlling and measuring the discharge as well as independently setting the depth of flow. In this way, it was possible to reproduce a desired rate of discharge and Froude number at the culvert outlet.

A number of different forms of the entrance channel leading from the culvert outlet down an incline to the horizontal floor of the stilling basin were tried. The model stilling basin had wingwalls, flared 45^{o} from the

centerline, leading into a channel three feet wide, or six times the width of the culvert.

For a limited range of Froude numbers and a number of different entrance channel geometries, measurements were made to determine the performance of the stilling basin. Criteria used in judging the performance included the stability of the hydraulic jump for varying tailwater, the efficiency of the spreading action, and the degree of velocity reduction after the flow had passed through the hydraulic jump.

It had been anticipated that the geometry of the stilling basin for use with a circular culvert would be different from that for use with a box culvert. A rather large number of experiments indicated, however, that the simplest form of geometry for the entrance channel (which was developed to provide economy of construction) worked satisfactorily for both the circular and box culvert. Variations in the performance of the structures were small for rather drastic variations in the geometric form of the entrance channel. It was therefore decided that the simplest geometric form should be used in future investigations.

IMPLEMENTATION STATEMENT

It was expected that at the conclusion of this phase of the investigation additional development work would be necessary before the proposed structure would be considered for field tests or field application. Additional investigation is needed on the effect of flare angle of the wingwalls, the required length of the stilling basin, and a means to adapt the new type of energy dissipator for use with a downstream channel having a trapezoidal cross section. Consideration will also be given to designing the structure so it will operate satisfactorily with no tailwater requirements, that is, when the flow leaves the stilling basin at the critical depth. Additional work is scheduled to explore these variables.

TABLE OF CONTENTS

LIST OF FIGURES

LIST OF SYMBOLS

a	Distance along the centerline from end of the circular or box culvert to the beginning of the curved bottom drop section.
b	Width of the curved bottom drop section.
B	Width of the downstream channel.
F_t	Froude number at the upstream end of flat section curved bottom.
g	Acceleration of gravity.
L_x	Distance along the channel centerline from leading edge of the hydraulic jump to the section of velocity measurements.
P.C.	Point of curvature.
P.T.	Point of tangency.
Q	Discharge.
r	Radius of curvature of the curved drop section.
V	Measured variable velocity in the downstream channel.
V_m	Mean velocity in downstream channel.
V_t	Velocity of flow at the upstream end of the curved drop section.
x	Distance along the centerline from the upstream end of the flaring wingwalls to the leading edge of hydraulic jump.
Y_t	Depth of flow at the upstream end of curved drop section.
Y_2	Downstream or sequent depth of the hydraulic jump.
Z	Height of drop of curved bottom channel section.
α	Deflection angle between tangent to the downstream end of the curved bottom drop section and the horizontal apron.
θ	Angle between flaring wingwalls and the centerline of the channel.

CHAPTER 1

Introduction

Culverts for carrying surface drainage through the highway embankment are an important part of the drainage system for any highway. It has been estimated that the total cost of culverts commonly amounts to over 15% of the total cost of many highways [1] *.

In moderately steep topography, the water flowing through culverts frequently acquires a high kinetic energy at the outlet, and the high velocity flow causes serious problems of local scour in the region of the culvert outlet. This severe localized scour frequently causes damage in the downstream channel either on or off of the right-of-way, damage to the highway embankment, or it may endanger and damage the culvert structure itself. Repairing this damage results in costly maintenance expense.

Although the increase in kinetic energy in the culvert is an important factor in causing damage near the outlet, it is apparent that an additional cause of the damage is the concentration of the flow into a deep and narrow stream. In order to minimize problems created at culvert outlets it would be desirable to destroy the excess kinetic energy in the flow and also cause the flow to spread laterally so that when it

---

* Numbers in parenthesis refer to references listed at the end of of the report.

leaves the culvert outlet it is as near as possible at the same conditions of width, depth, and velocity as would have occurred in the stream had the culvert not been built.

Numerous attempts have been made to devise culvert outlet structures that will reduce the problems created by local scour at the culvert outlet. Some of these were reviewed by Aguirre[2], who reported on the initial investigation of a new type outlet structure based on the principle of radial flow. His investigation demonstrated the feasibility of designing an outlet structure for a box culvert which effectively spread the flow between flared wingwalls at 45 degrees from the centerline to produce a flow with six times the width of the culvert. Robert Wear[3] explored the effect of a partial transverse sill and a solid end sill on the performance of a radial flow energy dissipator for a box culvert with the flare angle and width ratio the same as for Aguirre's investigation. This report, the third in the series, deals with the adaptation of the radial flow outlet structure for use with circular culverts and records the results of studies with some novel modifications of the geometry of the outlet structure.

Objectives

This study was undertaken to explore methods of adapting the radial flow outlet structure for use at the outlet of a circular culvert in place of the box culvert for which it was originally developed. Further, some novel geometric arrangements suggested by the adaptations to the circular culvert were studied to see if they would produce a significant improvement in the performance of the radial flow energy dissipator when used with a box culvert.

CHAPTER 2

Experimental Arrangement and Procedure

The experiments were performed in the Hydraulic Laboratory of the Civil Engineering Department at The University of Texas using apparatus similar to that used by Aguirre[2] and Wear[3]. It was a new arrangement, however, incorporating a large head tank open at the top and containing several baffles to quiet the disturbance from the supply pipe. A diagram of the test arrangement is shown in Figure 2-1. A horizontal culvert, 3 feet long, either circular or square could be installed to lead the flow from the stilling tank to the stilling basin structure. The circular culvert was formed from a piece of aluminum sheet metal rolled to a 0.5 foot diameter. The edges of the sheet metal formed a butt joint which was held in place with tape and placed at the top of the pipe where it caused no leakage. At the upstream end of the pipe an adjustable sluice gate was used to set the depth of flow in the model culvert.

The downstream channel was three feet wide as for the previous experiments performed, but was 8.5 feet long as measured from the upstream end of the flared wingwalls. This was 3.0 feet longer than the one used in the previous experiments which helped to minimize any possible influence of the downstream control gate on the flow conditions in the model.

Flow for the experiments was supplied by a low head pump from the laboratory sump directly into the laboratory distribution system. Flow

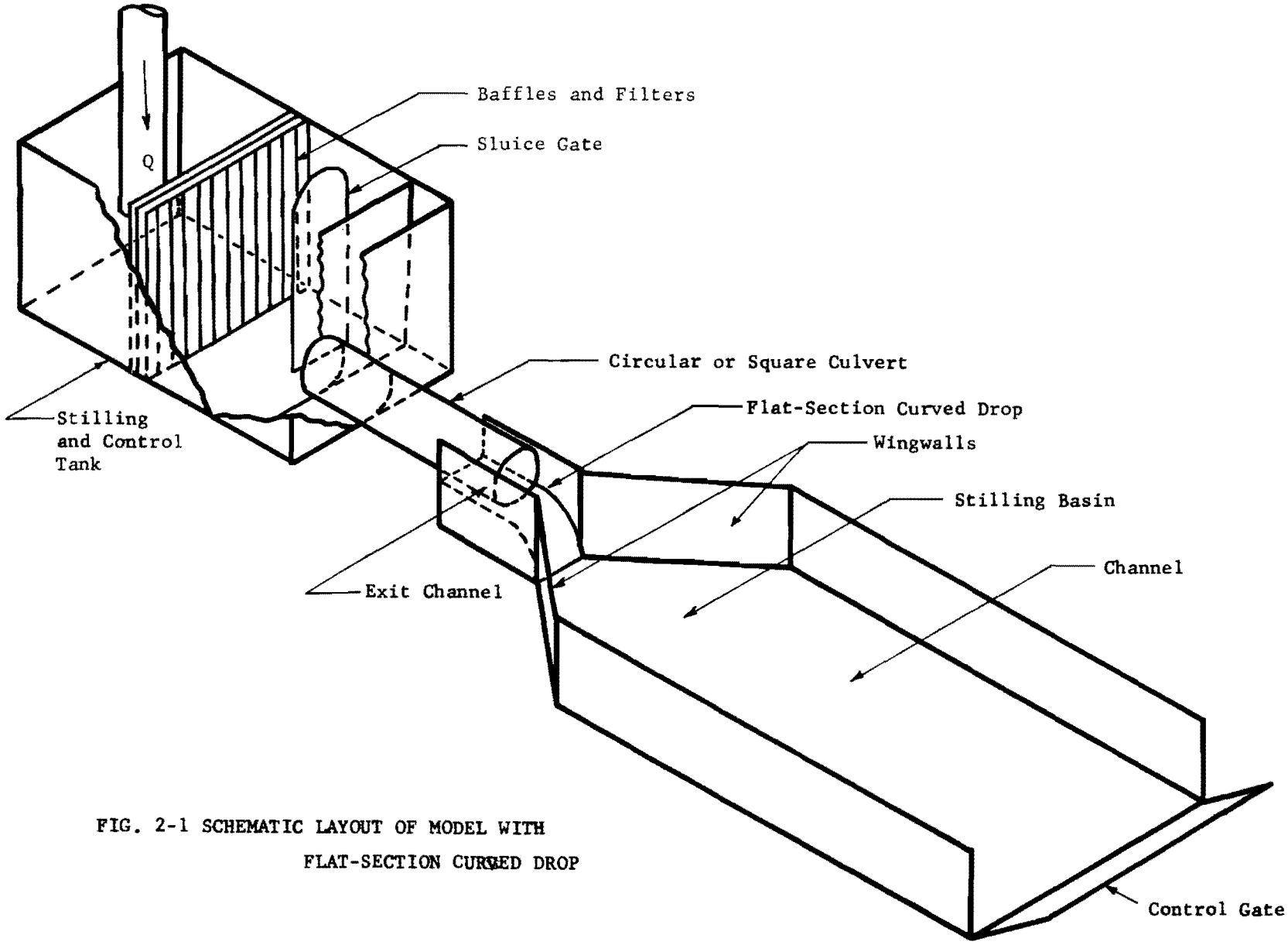

FIG. 2-1 SCHEMATIC LAYOUT OF MODEL WITH FLAT-SECTION CURVED DROP

was regulated by a three inch gate valve and measured by a calibrated-in-place three inch elbow meter. The piezometric head difference from the elbow meter was measured with a precision differential water manometer with a vernier reading to 0.001 foot.

Water surface elevations were measured with a Lory type point gage reading to 0.001 foot mounted on a rigid instrument carriage moving on horizontal rails over the model. Velocities in the downstream channel were measured with a one quarter inch diameter prandtl-type Pitot tube and a differential water manometer. The locations of velocity and water surface profile measurements are shown in Figure 2-2.

Measurements were made for several different arrangements of the outlet structure. Normally for each arrangement, measurements were made of the water surface elevation with shooting flow in the downstream channel, of the position of the hydraulic jump as a function of tailwater elevation and of velocities in the downstream channel measured both very near the bottom (at y = 0.03 foot) and at 0.6 depth ($0.4y_2$ from the floor). A schedule included as Table 2-1 shows the outlet structure arrangements tested with their designations and the pages where the results are presented.

Three basic configurations were investigated as possible adaptations of the radial flow energy dissipator for use with a circular pipe. One configuration made use of the same design as developed for the box culvert, that is, with a flat section curved drop leading from the end of the culvert to the apron of the structure. It was reasoned that as the flow went from the circular conduit into the flat section rectangular

TABLE 2-1 - SCHEDULE OF TEST CONDITIONS AND LOCATION OF RESULTS

Designation of Various Arrangements	Arrangement of Outlet Structures		Location of Results - Figures		
	Description	Figures	Water Surface Elevation	Jump Stability	Velocity in Downstream Channel
	Group I Structures - Circular Culvert and Flat Section Curved Drop b = 0.5 ft., B = 3.0 ft. $\theta = 45^{o}$, r = 0.75 ft.				
CIR1	a = 0.0 ft.	2-3	3-1	3-3	3-6 to 3-11
CIR2	a = 0.25 ft.	2-3		3-4	3-12 to 3-17
CIR3	a = 0.50 ft.	2-3	3-2	3-5	3-18 & 3-19
	Group II Structures - Circular Culvert b = 0.5 ft., B = 3.0 ft $\theta = 45^{o}$, r = 0.75 ft.				
CIR4	a = 0.0---V-Section Curved Drop with Sloping Wingwalls	2-6	3-20	3-22	3-24 to 3-29
CIR5	a = 0.0---Abrupt Drop	2-8	3-21	3-23	3-30 to 3-34
	Group III Structures - Box Culvert b = 0.5 ft., B = 3.0 ft. $\theta = 45^{o}$				
BOX1	Gradual V-Section Curved Drop with Vertical Wingwalls	2-9	3-35	3-37	3-39 to 3-44
BOX2	Gradual V-Section Curved Drop with Sloping Wingwalls		3-36	3-38	3-45 to 3-50

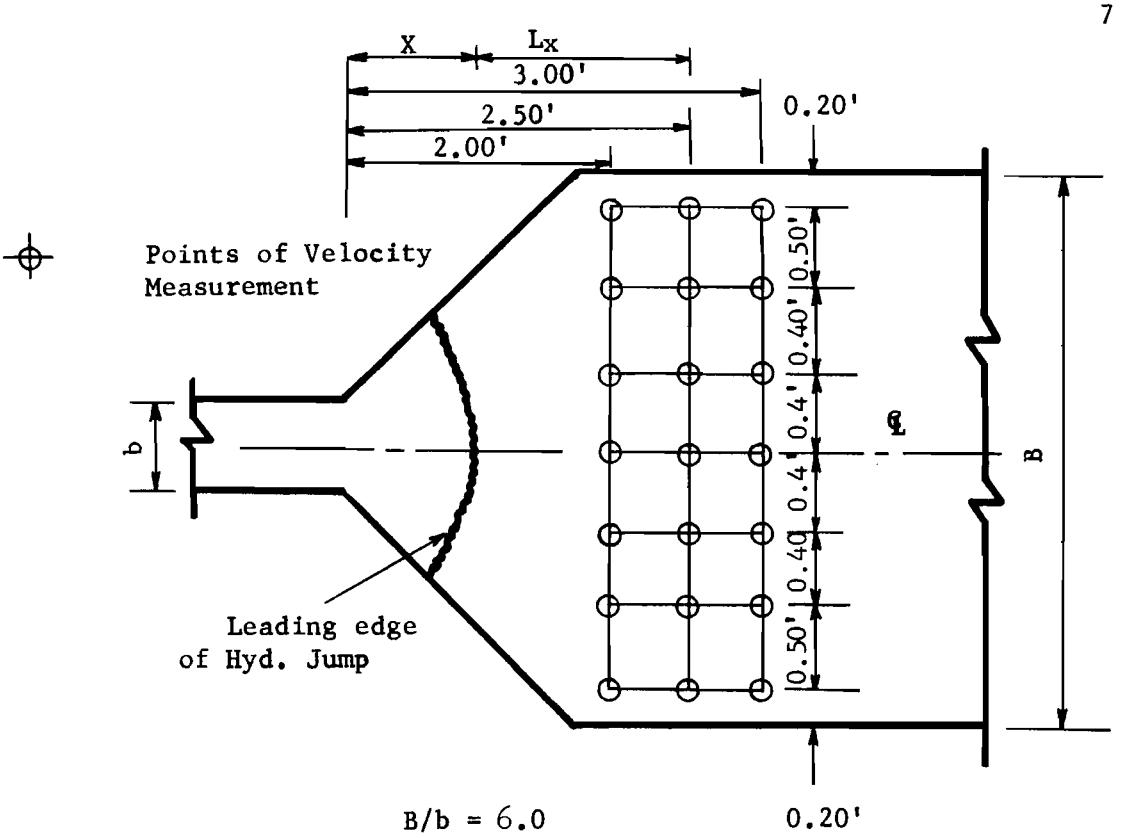

FIG. 2-2(a) LOCATION OF VELOCITY MEASUREMENTS

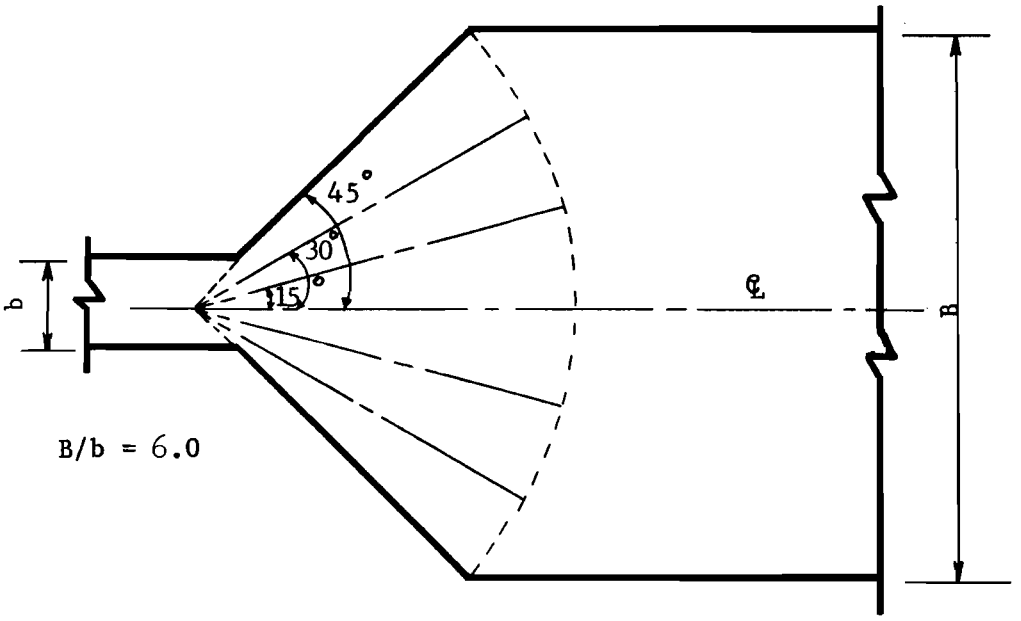

FIG. 2-2(b) LOCATION OF WATER SURFACE PROFILE MEASUREMENTS

channel the flow near the sides would drop and spread toward the sides. To explore this effect, measurements were made with the circular culvert ending at three different positions, one, with a = 0, (with the pipe ending at the point of tangency) and the other conditions with a = 0.25 ft., and a = 0.50 ft. This arrangement is shown in Figures 2-3, 4, and 5. Figure 2-3 also serves as a definition diagram for pertinent variables.

Another configuration studies incorporated a 90^{o} V cross section (see Figure 2-6). The curved drop was formed from concrete so that all radial sections in the drop had a 90^{o} V bottom intersecting parallel sides 0.5 foot apart. With this arrangement of the curved drop its intersection with the horizontal apron of the stilling basin nearly coincided with the upstream extension of the flared wingwalls. It appeared that this arrangement might make for a better distribution of the radial flow on the horizontal apron. The flared wingwalls were sloped backward so they were continuations of the two planes forming the V section channel drop at the bottom end of the drop. Figure 2-7 shows a close-up photograph of this arrangement with shooting flow away from the drop and a general view with a circular jump forming near the drop.

Observations were made to investigate the possibility of eliminating the curved drop, replacing it with a simple vertical wall. This arrangement is shown in Figure 2-8. It appeared desirable that the falling jet impinge on the apron at the same location in relation to the flared wingwalls as would have occurred with the curved drop. With the flow over the drop unventilated it would be expected that the region

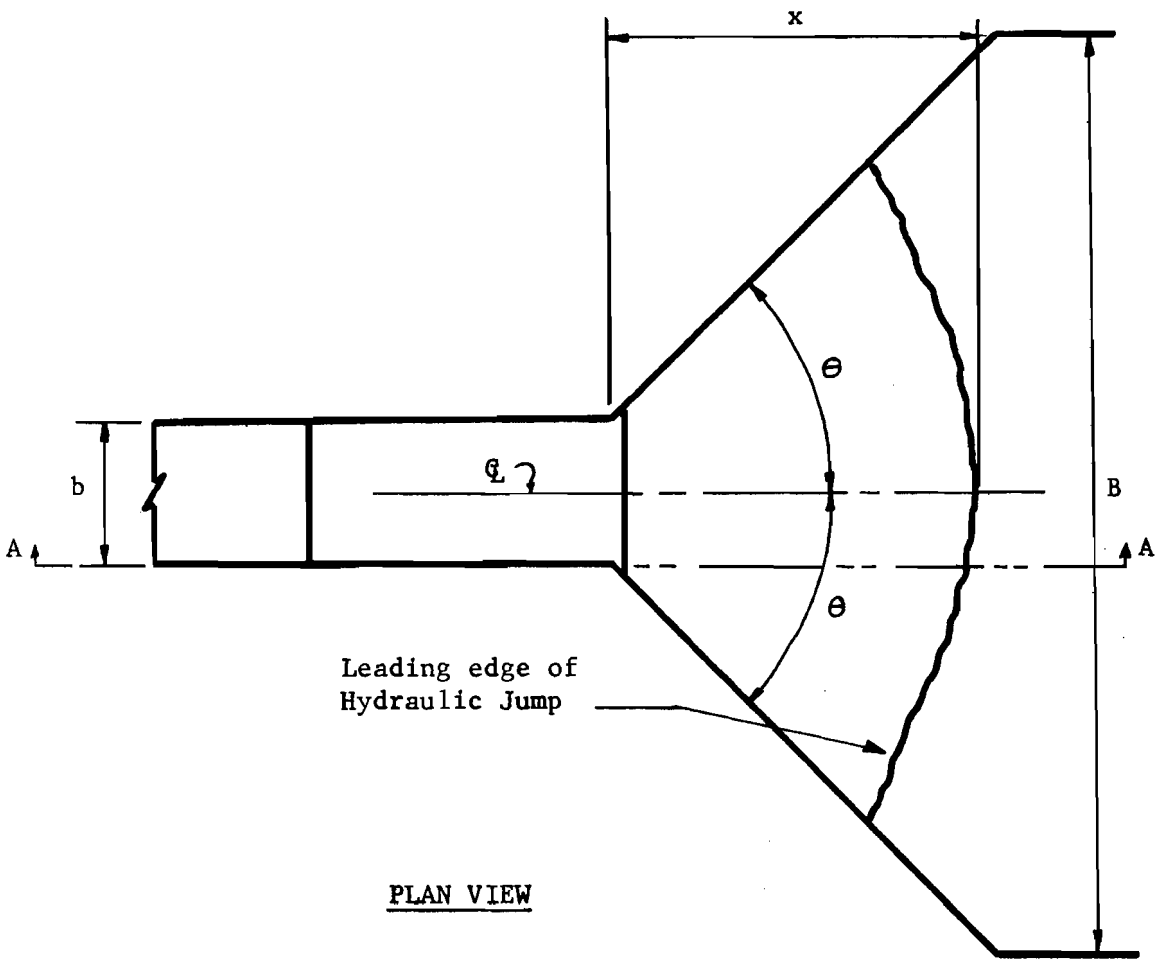

PLAN VIEW

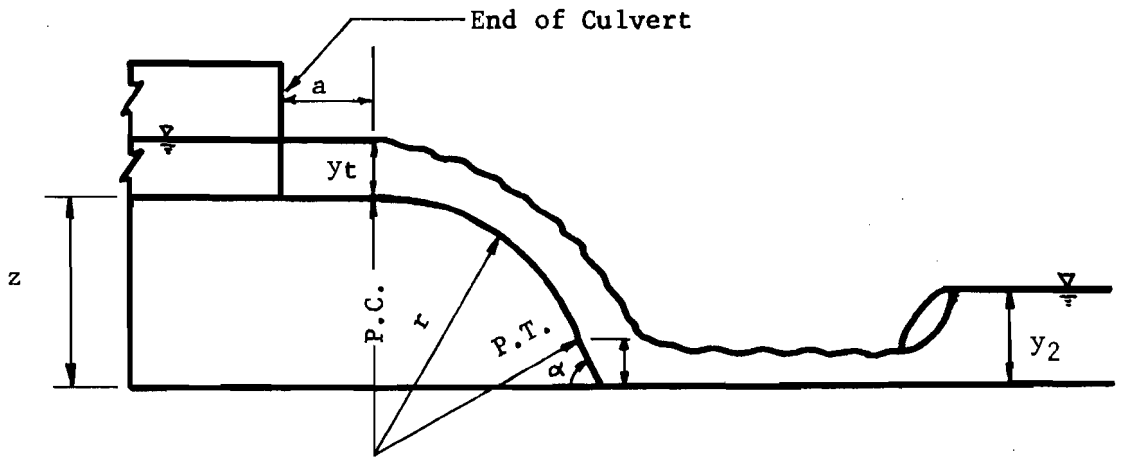

ELEVATION AA

FIG. 2-3 CIRCULAR CULVERT WITH FLAT-SECTION CURVED DROP

(Arrangement CIR1, 2, 3)

No Flow

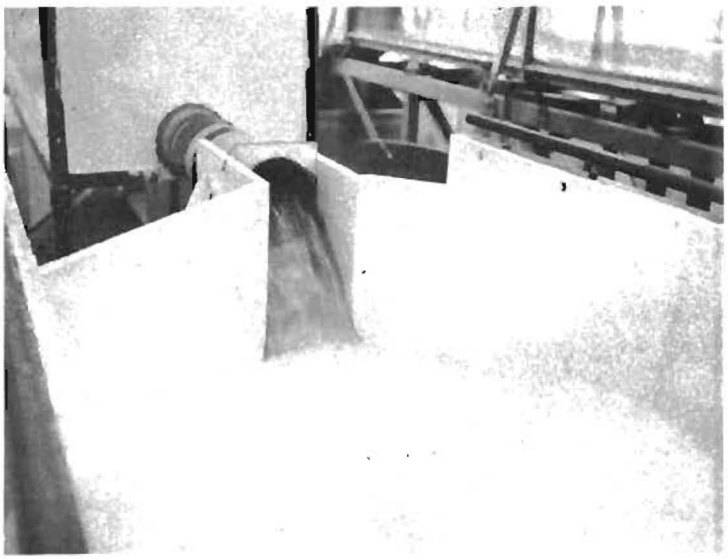

With Flow

FIG. 2-4 CIRCULAR CULVERT WITH FLAT-SECTION CURVED DROP CLOSE-UP
(Arrangement CIR1)

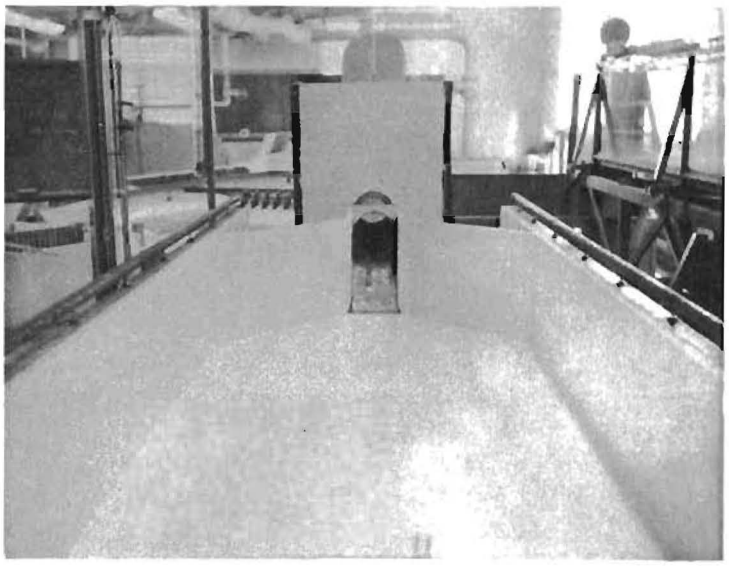

No Flow

With Flow

FIG. 2-5 CIRCULAR CULVERT WITH FLAT-SECTION CURVED DROP - GENERAL VIEW
(Arrangement CIR1)

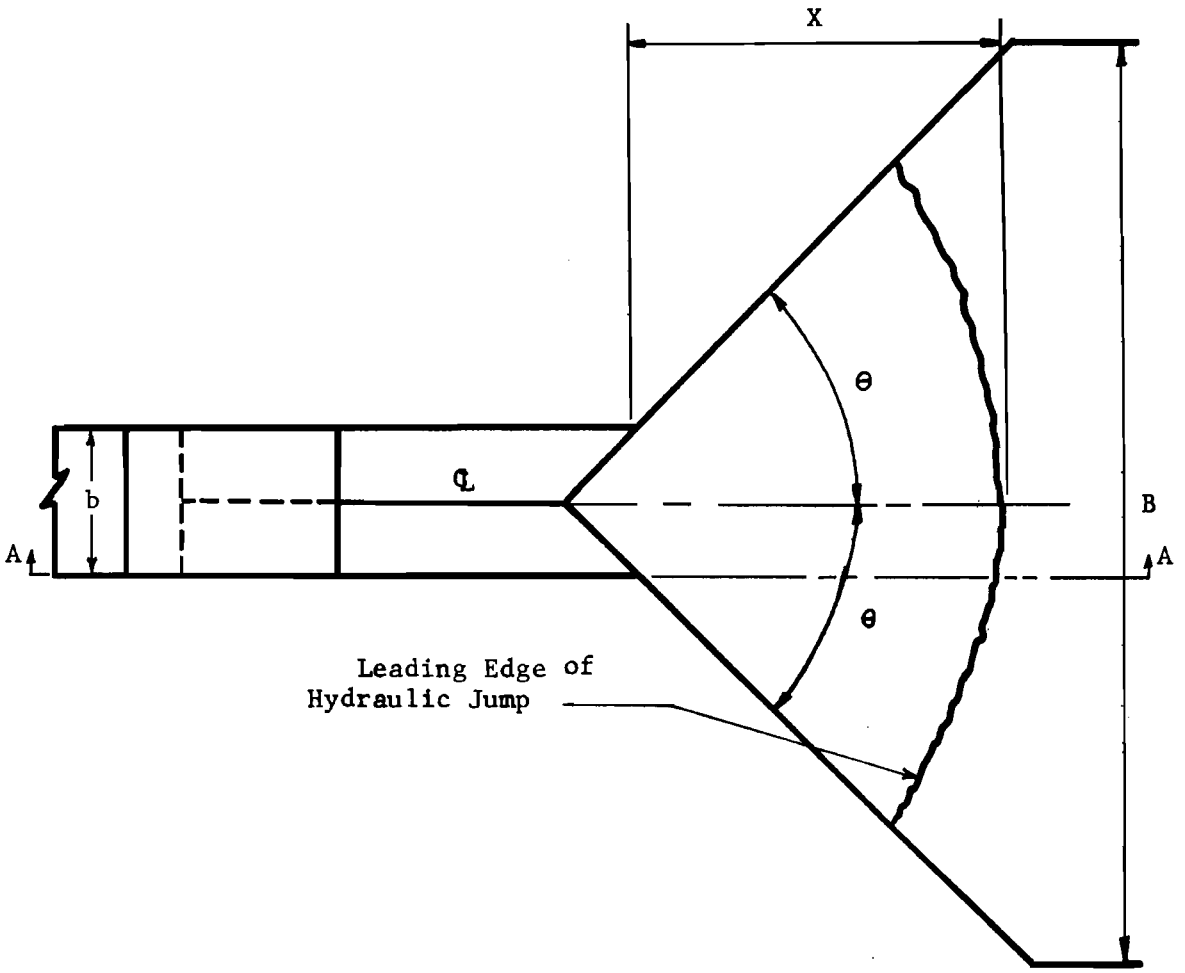

PLAN VIEW

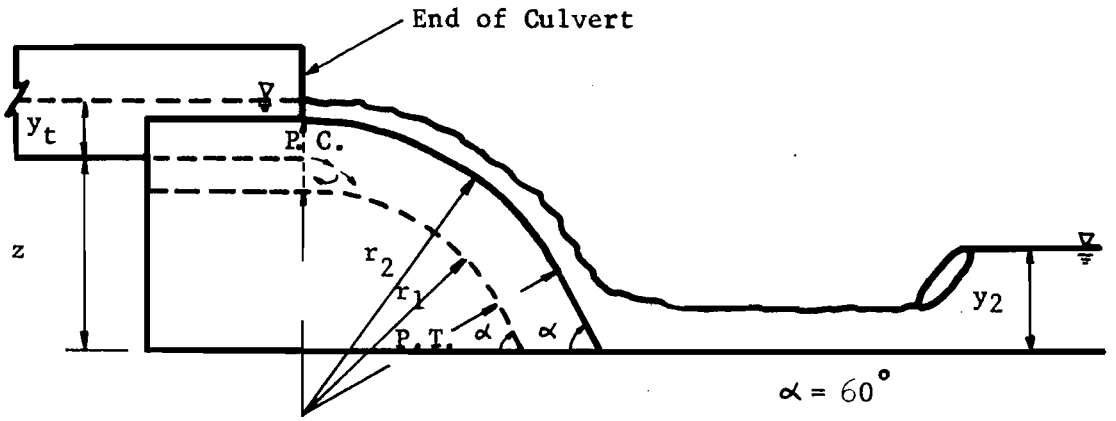

ELEVATION AA

FIG. 2-6 CIRCULAR CULVERT WITH V-SECTION CURVED DROP
(Arrangement CIR4)

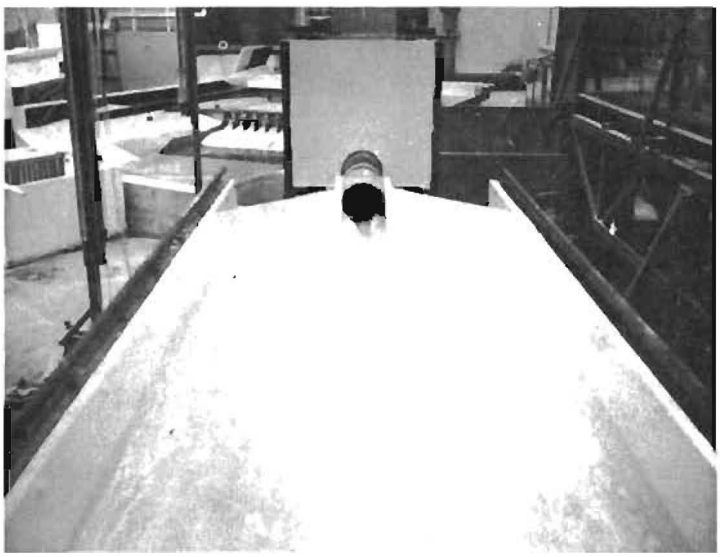

General View

(Arrangement CIR4)

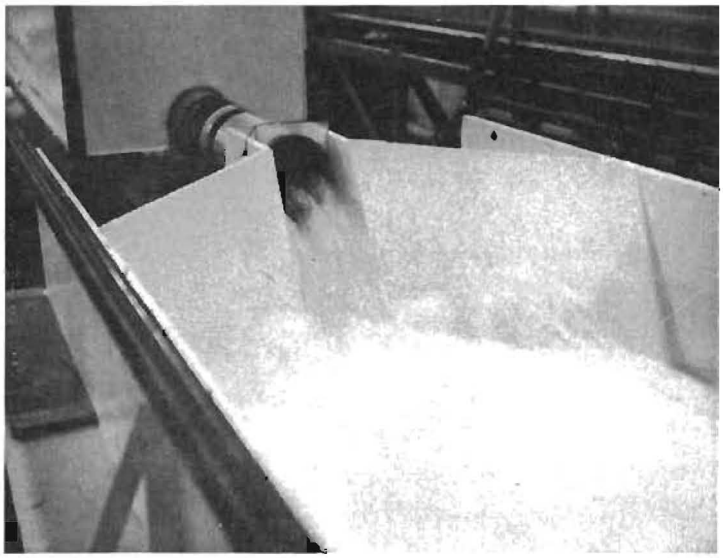

Close up View

FIG. 2-7 CIRCULAR CULVERT WITH V-SECTION CURVED DROP AND SLOPING WING WALLS

under the falling nappe would gradually fill with water as the air under the nappe was entrained and carried downstream. Thus, it seemed desirable that the vertical drop be located at the same place as the upper point of tangency for the curved drop. The arrangement investigated was constructed in this manner.

Drawing on the idea of the V section curved drop for the circular pipe, an adaptation of this arrangement was explored for use with a box culvert. The geometrical configuration of this structure is shown in Figure 2-9. The V section in the curved drop developed gradually from a flat section at the top of the drop to a full 90^{o} V at the bottom of the drop. This was accomplished by molding the curved drop section in concrete with the outer edges following templets cut to the same curve as used for the earlier tests and the center templet displaced horizontally upstream so that the V section formed by the intersection of the curved drop in the horizontal apron was an upstream continuation of the flared wingwalls. In this drop section the V was so formed that its intersection with a horizontal plane always formed a 90^{o} V. One series of measurements was made with the wingwalls vertical, and in another series with the wingwalls sloping backward so they were continuations of the two planes forming the lower section of the V bottomed drop.

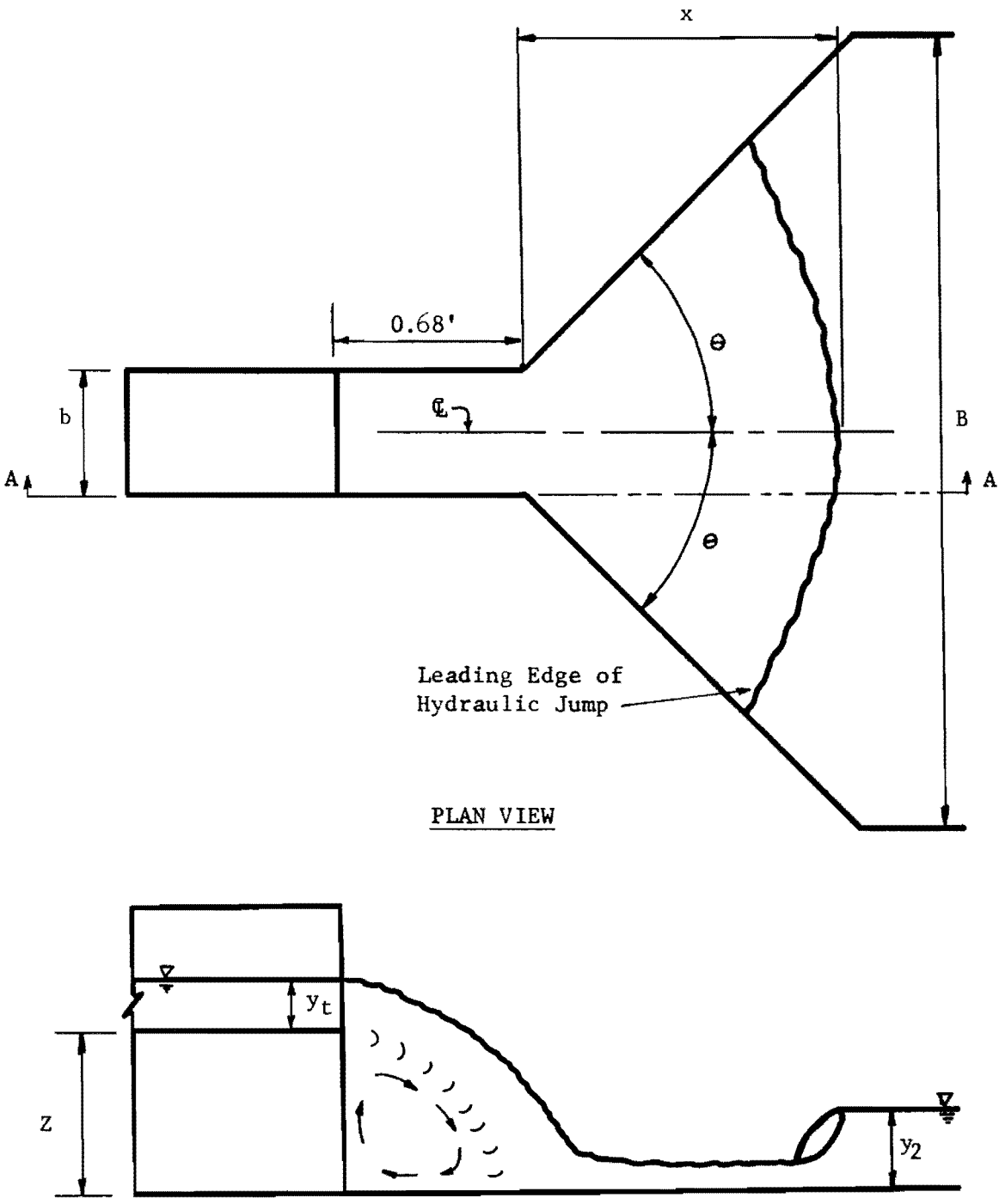

FIG. 2-8 CIRCULAR CULVERT WITH ABRUPT DROP

(Arrangement CIR5)

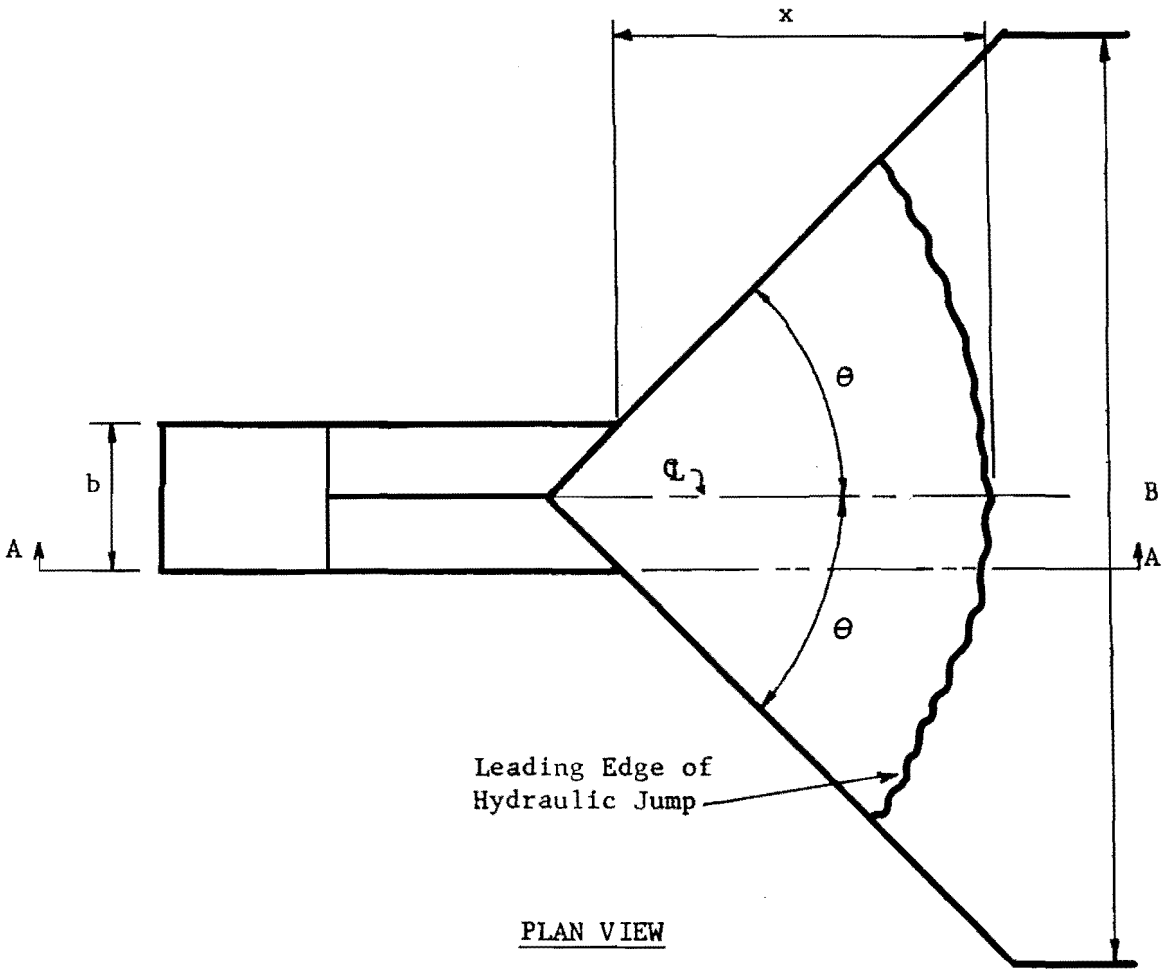

PLAN VIEW

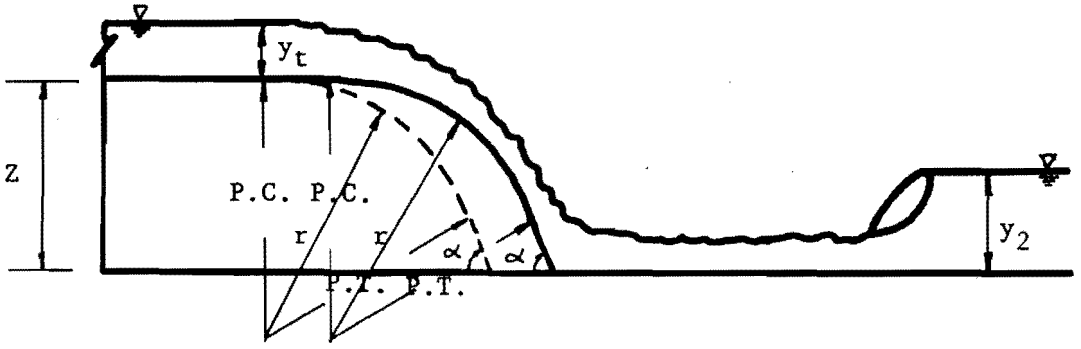

ELEVATION AA

FIG. 2-9 BOX CULVERT WITH GRADUAL V-SECTION CURVED DROP AND VERTICAL WINGWALLS

(Arrangement BOX1)

CHAPTER 3

Experimental Results and Procedure

The basic criteria used in investigating the effectiveness of various geometric arrangements as energy dissipator were the stability of the hydraulic jump, the efficiency of the spreading action and the degree of velocity reduction in the jump, and the degree of angular uniformity of the supercritical flow within the basin.

The degree of angular uniformity of the supercritical flow was estimated from the water surface profile when the tailwater conditions were such that no hydraulic jump was formed within the basin. In order to determine the angular uniformity of flow, surface profile measurements were made along radial lines in the basin. These lines were set at 15^{o}, 30^{o}, and 45^{o} from the centerline, and on the centerline. It was observed that the depth of flow decreased as the fluid advanced downstream. Of course, this is a characteristic of a radial flow basin. A relatively high flow depth was created adjacent to the flaring wingwalls, especially in the beginning portion of the basin. The formation of the high depth on the sides may be attributed to the wall effect and the pressure build up where the flow impinged on the horizontal apron.

An indicator of the stability of hydraulic jump was the magnitude of the longitudinal change in the position of the jump as a result of a change in the tailwater depth. The position of the jump was defined as the distance x along the channel centerline from the beginning of the

flared wingwalls to the leading edge of the hydraulic jump. Since the leading edge of the jump exhibited a considerable amount of fluctuation, the jump position was obtained as the visual temporal average of the position for each fixed tailwater condition. An increase in the tailwater depth was accompanied by a decrease in distance x. In order to investigate the jump stability, the parameters x and Y_2 were varied over a specific range while V_t and Y_t were held constants. Y_2 was the depth of flow in the downstream channel, V_t and Y_t were the velocity and flow depth respectively at the upstream end of the curved bottom channel section. The degree of stability of the hydraulic jump at a given position could be determined from the absolute value of the slope of the curves of Y_2/Y_t vs. x/Y_t for each geometric arrangement.

The degree of velocity reduction as a measure of the efficiency of the stilling basin was evaluated from the velocity measurements obtained in the downstream channel. The velocities were determined at various transverse sections having a particular value of L_x, where L_x was the distance along the centerline from the leading edge of the hydraulic jump downstream to the section of velocity measurements (see Figure 2-2a). Prior to making the velocity measurements a suitable F_t, Froude number at the upstream end of the curved channel, was selected and the position of the jump was stabilized at x = 0.4 ft., x = 1.0 ft., and x = 1.50 ft. For each jump position the velocities were measured in three different transverse sections with $X + L_x$ equal to 2.0, 2.5, and 3.0 feet respectively. The velocity magnitude and distribution in each section was represented by a dimensionless parameter V/V_m, where V was the velocity

measured at a particular point and V_m was the mean velocity in the downstream channel. The magnitudes of V/V_m and the position of velocity measurements for each configuration at various flow conditions are presented later in this report when individual arrangements are discussed and analyzed.

Hydraulic performance of various structures will be discussed separately for three groups of arrangements as follows:

I - Structures with a Circular Conduit Ending at Different Positions

These structures consisted of arrangements CIR1, CIR2, and CIR3. As mentioned previously, the criteria used in evaluating the performance characteristics of each structure were the general appearance of the water surface profile, the jump stability, and the degree of velocity reduction.

Water Surface Profile

The representative water surface profiles in radial directions for arrangements CIR1 and CIR3 are shown in Figures 3-1 and 3-2 respectively. These figures indicate the surface profiles when the structures operated at F_t of 1.78. At any given section the flow depth at the centerline was higher than the depths at the intermediate lines. The centerline depth was extremely high in arrangement CIR3. In this configuration the flow of water with high kinetic energy entered the basin and upon impact with basin floor caused a considerable disturbance with a high rise in the flow depth at the centerline. The centerline depth in this arrangement was more than 100% higher than the depth in the intermediate lines. Along the flared wingwalls, a high wave formed in all cases especially in the upstream portion of the basin. However, the depth of flow in this region was higher for arrangement CIR3 than CIR1 when all hydraulic parameters were constant. It was observed that in all experiments the depth of flow decreased as

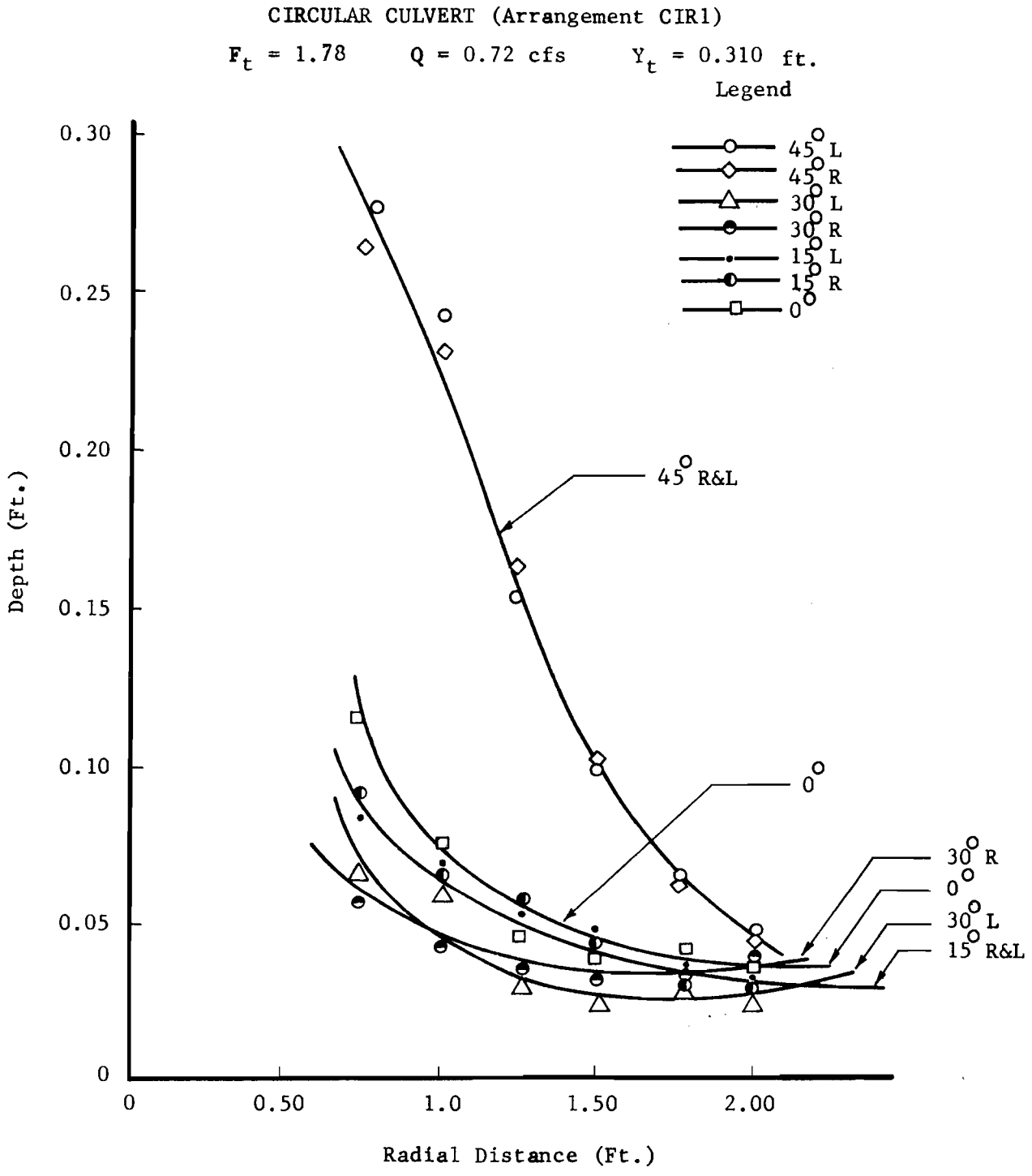

FIG. 3-1 WATER SURFACE ELEVATION OF SUPERCRITICAL FLOW ON APRON

CIRCULAR CULVERT (Arrangement CIR3)

F_t = 1.78 Q = 0.72 cfs Y_t = 0.306 ft.

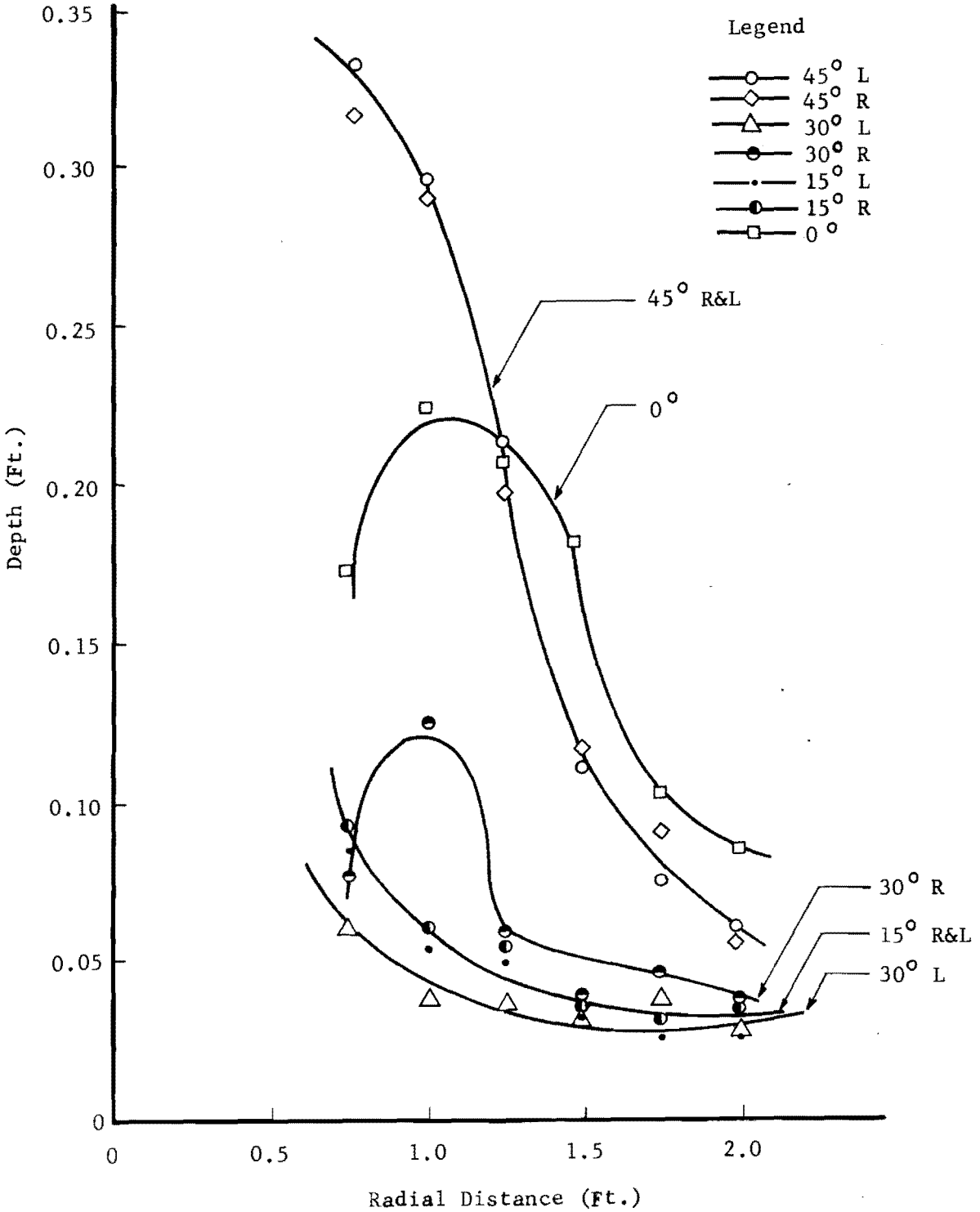

FIG. 3-2 WATER SURFACE ELEVATION OF SUPERCRITICAL FLOW ON APRON

the flow advanced downstream before reaching the leading edge of the jump. The comparison of the results obtained for three arrangements shows that as the distance "a" increased the degree of the uniformity of the supercritical flow was reduced and when the value of "a" was 0.5 ft. the performance of the basin was considered unsatisfactory.

Stability of the Hydraulic Jump

The stability of the hydraulic jump for different geometric arrangements could be determined from the slope of the curves of Y_2/Y_t vs. x/Y_t. Several of these curves were plotted in Figures 3-3, 4, and 5 for arrangement CIR1, CIR2, and CIR3 respectively. Analyses of these curves show that the hydraulic jump was highly stable within the region of the basin with flared wingwalls. As the value of x/Y_t increased, the absolute value of the slope of the curve decreased until the curve became nearly horizontal. The higher the absolute value of the slope of Y_2/Y_t vs. x/Y_t curve the more stable the jump position.

Although, when the jump moved into the downstream channel, the absolute value of the slope of the Y_2/Y_t vs. x/Y_t curve decreased rapidly, it did not immediately reach its minimum value corresponding to the parallel wall channel. Hence, the stabilizing effect of the radial basin was present to certain degree even in the downstream channel section. The reason behind this performance was that the flow entered the parallel wall channel in radial direction and continued to do so until sufficient momentum buildup changed its direction from radial to parallel. A view of the laboratory stilling basin operating with a hydraulic jump is shown in Figure 2-5.

CIRCULAR CULVERT (Arrangement CIR1)

F_t = 1.90 Q = 0.72 cfs Y_t = 0.300 ft.
F_t = 1.76 Q = 0.64 cfs Y_t = 0.293 ft.

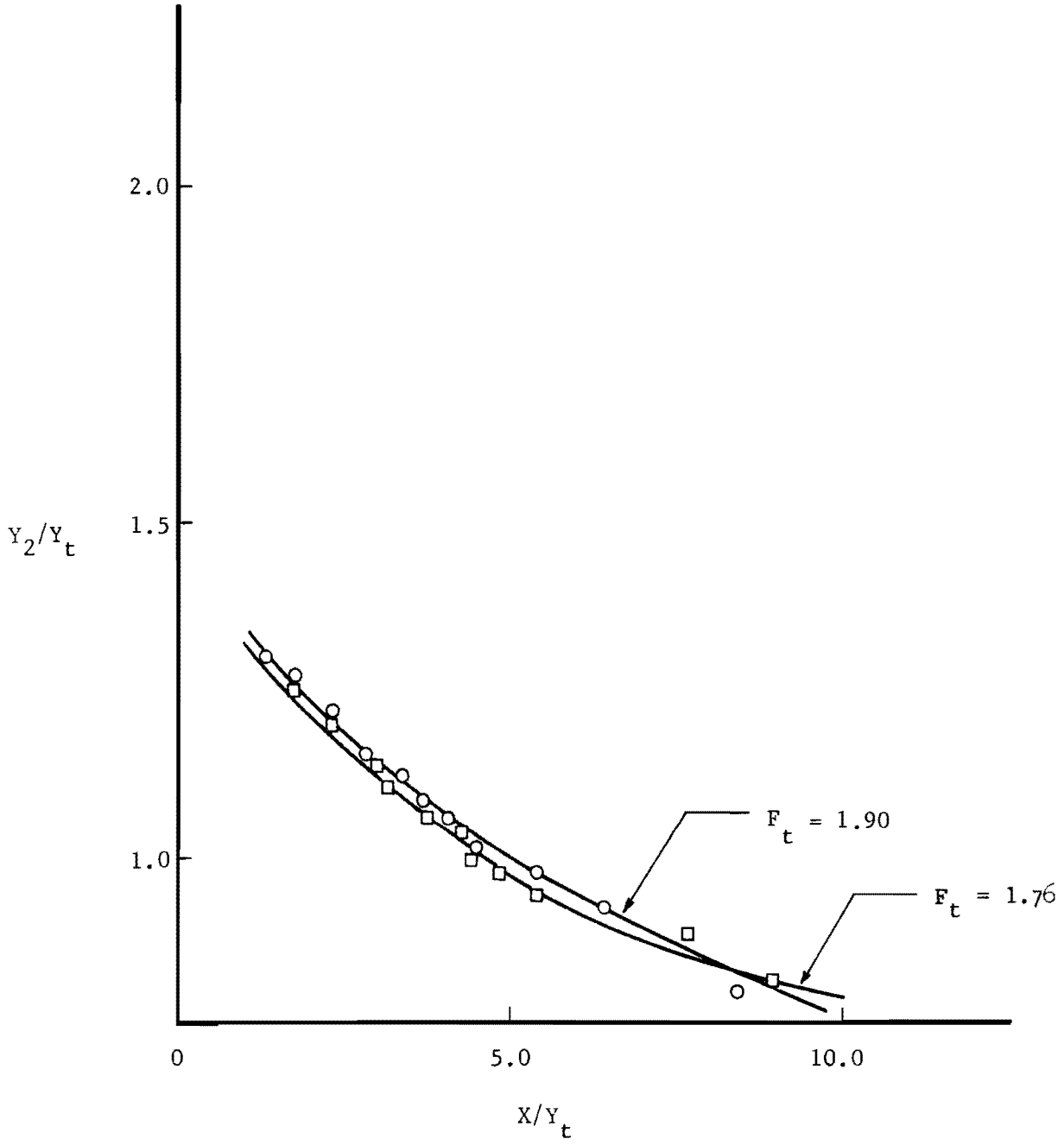

FIG. 3-3 TAILWATER DEPTH vs. JUMP POSITION

CIRCULAR CULVERT (Arrangement CIR2)

F_t = 2.87 Q = 0.72 cfs Y_t = 0.234 ft.
F_t = 2.33 Q = 0.72 cfs Y_t = 0.264 ft.

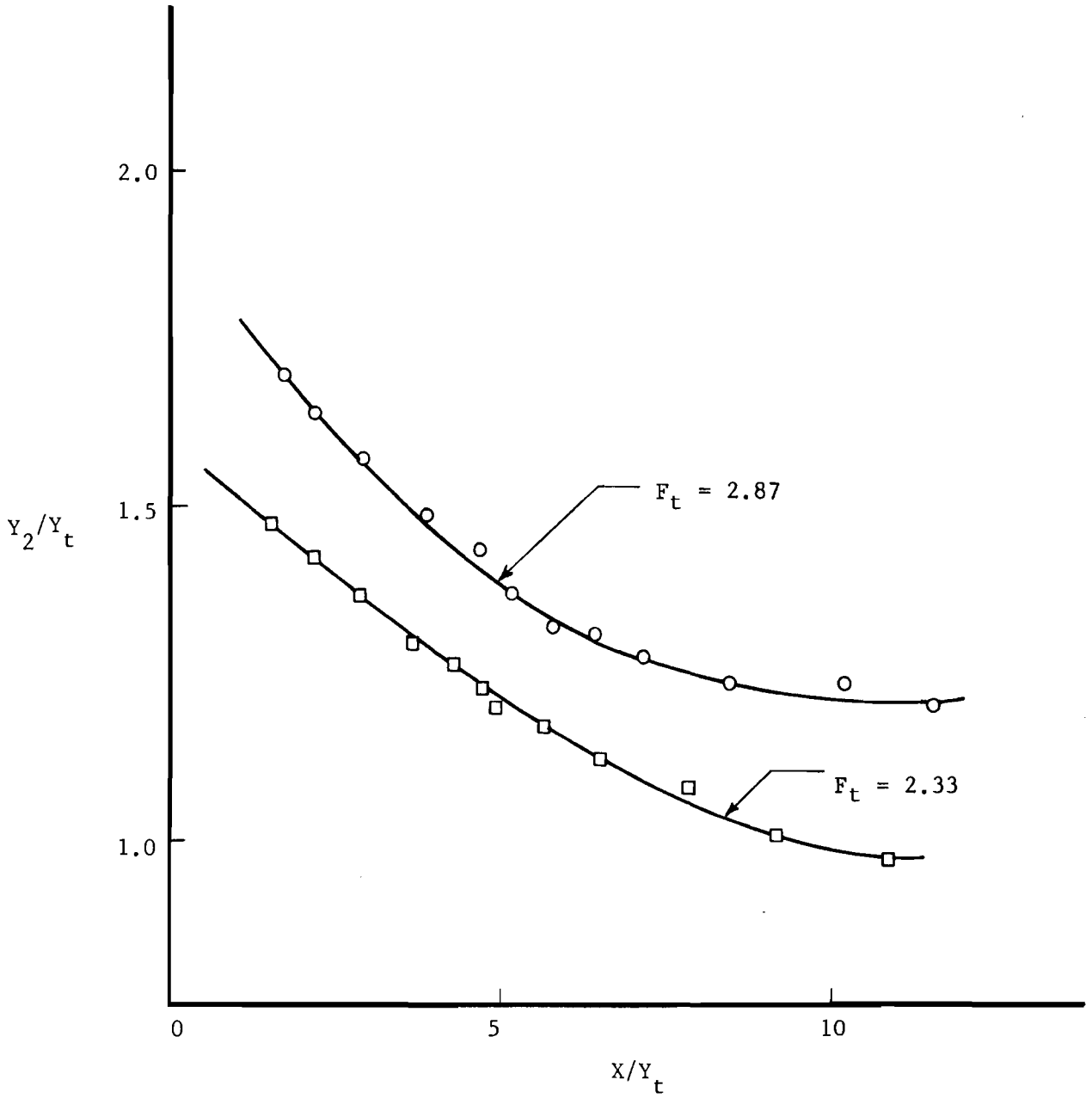

FIG. 3-4 TAILWATER DEPTH vs. JUMP POSITION

CIRCULAR CULVERT (Arrangement CIR3)

F_t = 3.85 Q = 0.72 cfs Y_t = 0.202 ft.
F_t = 2.59 Q = 0.72 cfs Y_t = 0.250 ft.

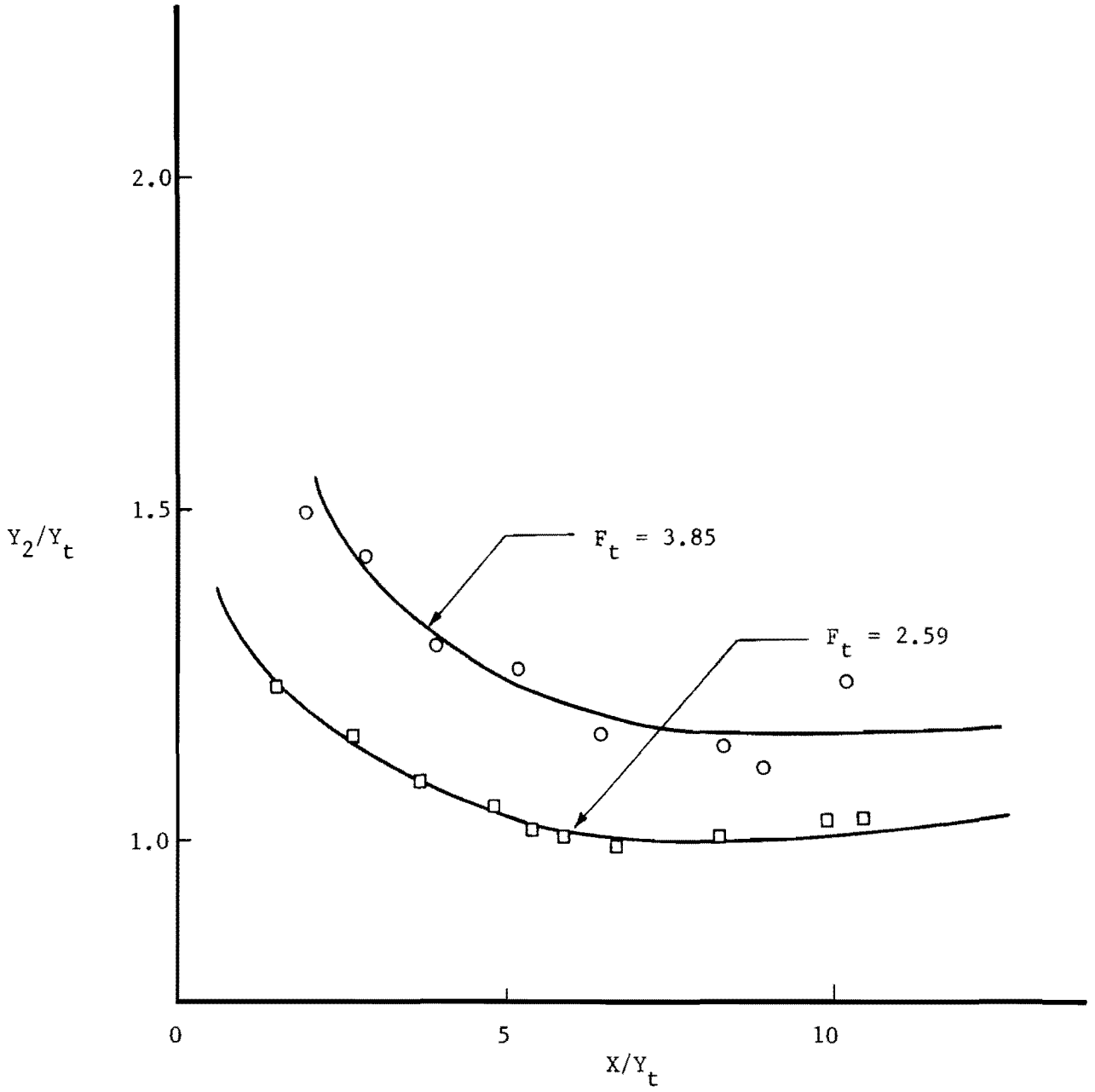

FIG. 3-5 TAILWATER DEPTH vs. JUMP POSITION

Comparison of Figures 3-3 through 3-5 shows that arrangement CIR1 preserved a much larger range of x/Y_t for stable jump position than that of arrangements CIR2 and CIR3. Arrangement CIR3 did not perform satisfactorily, because when the value of x/Y_t exceeded 5.0 the jump lost its stability completely, moved downstream quickly and was eventually washed out. This undesirable performance characteristic is shown in Figure 3-5. Furthermore, the operating range of Y_2/Y_t was smaller for CIR3 than CIR1 and CIR2.

The effect of F_t on the stability of the jump could be detected from Figures 3-3 through 3-5. Within the region of wingwalls the higher the F_t the more stable was the jump position. However, outside of this region in the downstream channel an increase in F_t corresponded to a decrease in the jump stability. So far as the relative tailwater (Y_2/Y_t) requirements were concerned, arrangement CIR2 had the highest operating range in which the jump was still stable. On the otherhand, the evaluated results showed that arrangement CIR1 had the best stabilizing characteristics, and within the range of experimentation as the distance "a" increased the stability of the hydraulic jump decreased.

Velocity Distribution and Reduction

Velocity measurements were made at various transverse sections in the downstream channel to facilitate the determination of velocity reduction and distribution of flow in each arrangement. Values of V/V_m are plotted in Figures 3-6 through 3-19. These figures show the velocities measured at three different transverse sections. This system

of velocity representation provided the means for comparison of general pattern and magnitude of velocity variations for a given F_t and fixed jump position. The leading edge of the jump is marked in each figure with a small arc to indicate the relative location of the transverse sections to the jump position.

Analyses of these figures show that arrangement CIR1 had a fairly uniform distribution of velocity. The velocities in each section of this arrangement were less than two times the mean channel velocity, which is equivalent to less than 30 percent of V_t, average flow velocity at the upstream end of the curved bottom channel. This reduction in velocity held true in a zone immediately after the jump and as the flow advanced downstream from the jump the velocities became less than 1.5 times V_m corresponding to values smaller than 20 percent of V_t.

Arrangements CIR2 and CIR3 performed with considerably different velocity pattern than that of CIR1. The velocity distributions obtained in CIR2 and CIR3 showed that the velocities measured near the sides of the channel were very low, while at the center portion of the channel they were quite high. The velocities measured along the sides of the channel were usually zero indicating formation of eddies which resulted in improper velocity measurements by Pitot tube in its longitudinal direction. At the section nearest to the leading edge of the jump, the velocity at the center section varied within a range of 2 to 6 times V_m. This range corresponded to a velocity varying from 30 to 80 percent of V_t. The upper magnitude of the velocity in these arrangements was considered sufficiently high to be unsatisfactory.

The velocity distributions in CIR2 and CIR3 were skewed to one side of the channel disturbing their symmetry about the channel centerline. This skewness could have been due to the upstream disturbances in the flow or small deviations in the symmetry of the channel geometry.

The analyses of the results of this experimental study indicated that arrangement CIR1 was superior to arrangements CIR2 and CIR3 in respect of water surface profile, jump stability, and velocity distribution.

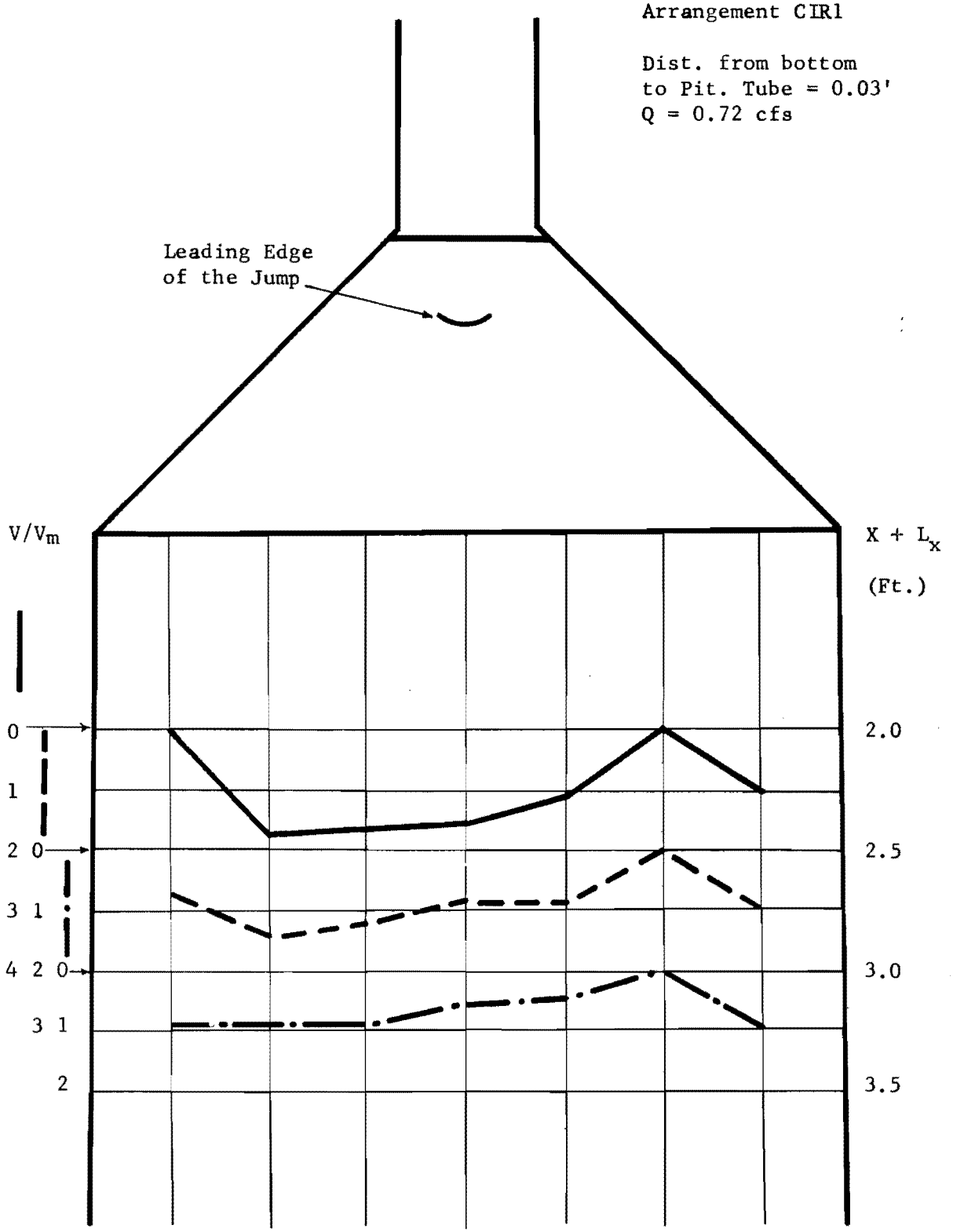

NOTE: Horizontal arrow along V/V_m scale indicates the section of velocity measurements in downstream channel.

FIG. 3-6 VELOCITIES IN DOWNSTREAM CHANNEL

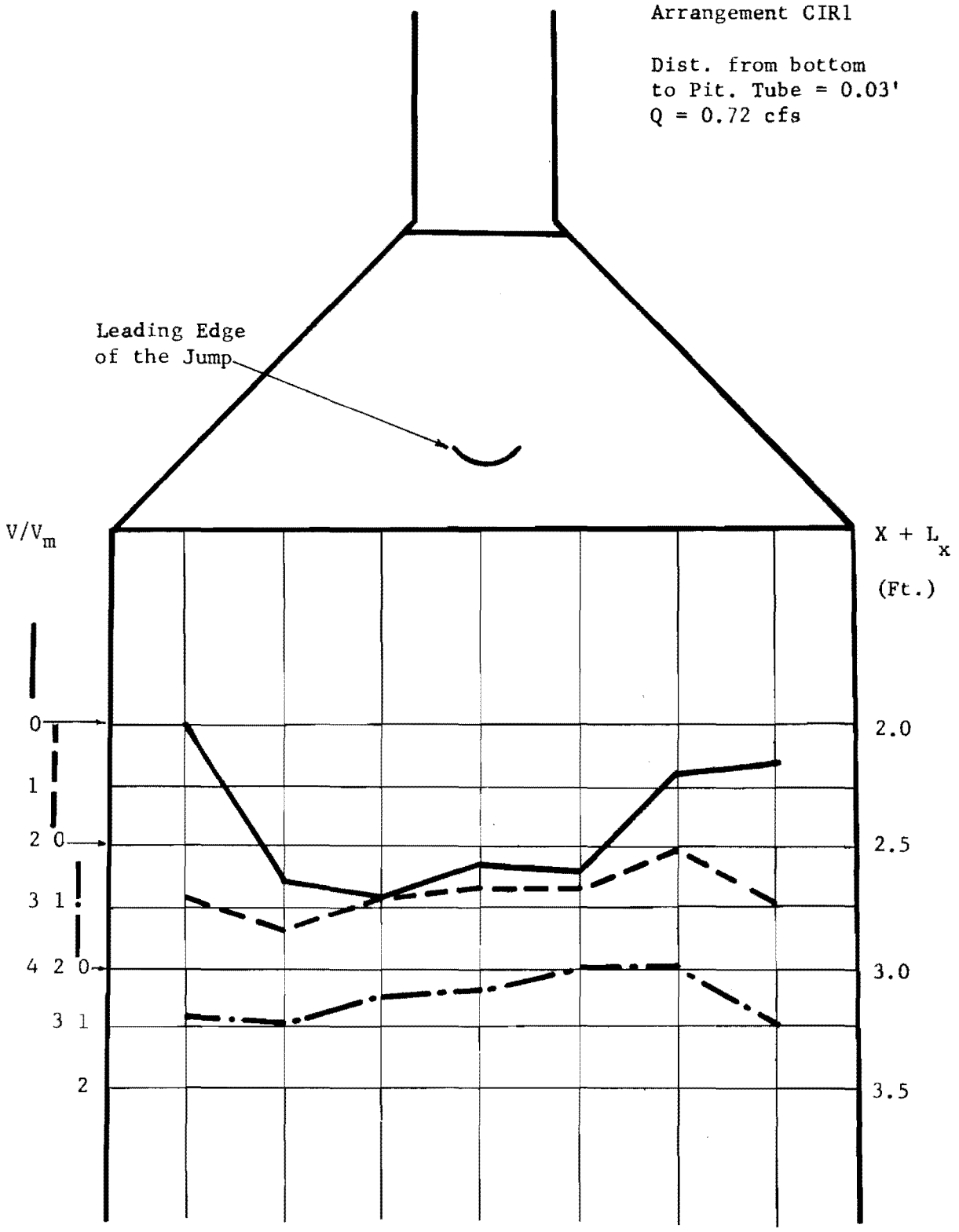

NOTE: Horizontal arrow along V/V_m scale indicates the section of velocity measurements in downstream channel.

FIG. 3-7 VELOCITIES IN DOWNSTREAM CHANNEL

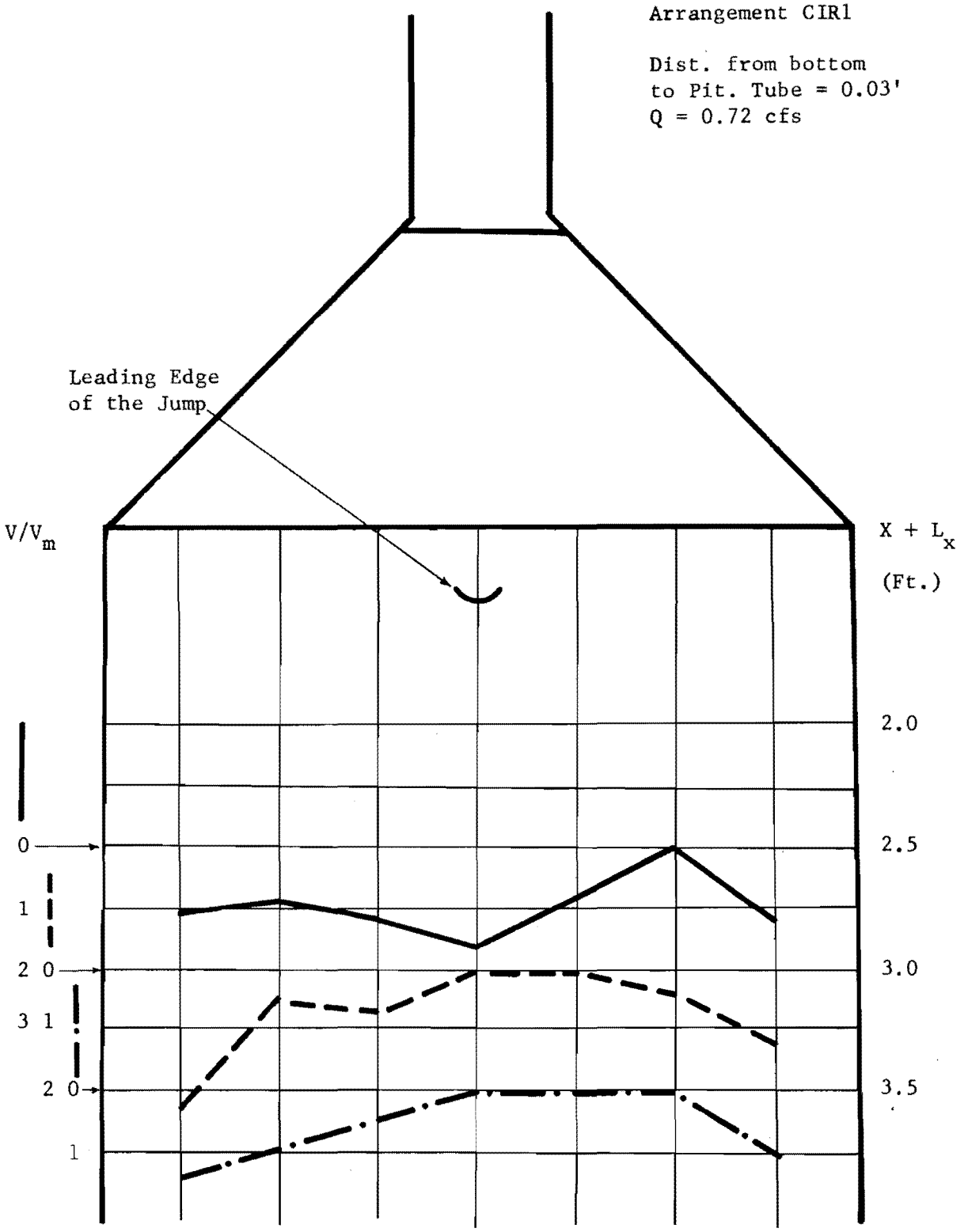

NOTE: Horizontal arrow along V/V_m scale indicates the section of velocity measurements in downstream channel.

FIG. 3-8 VELOCITIES IN DOWNSTREAM CHANNEL

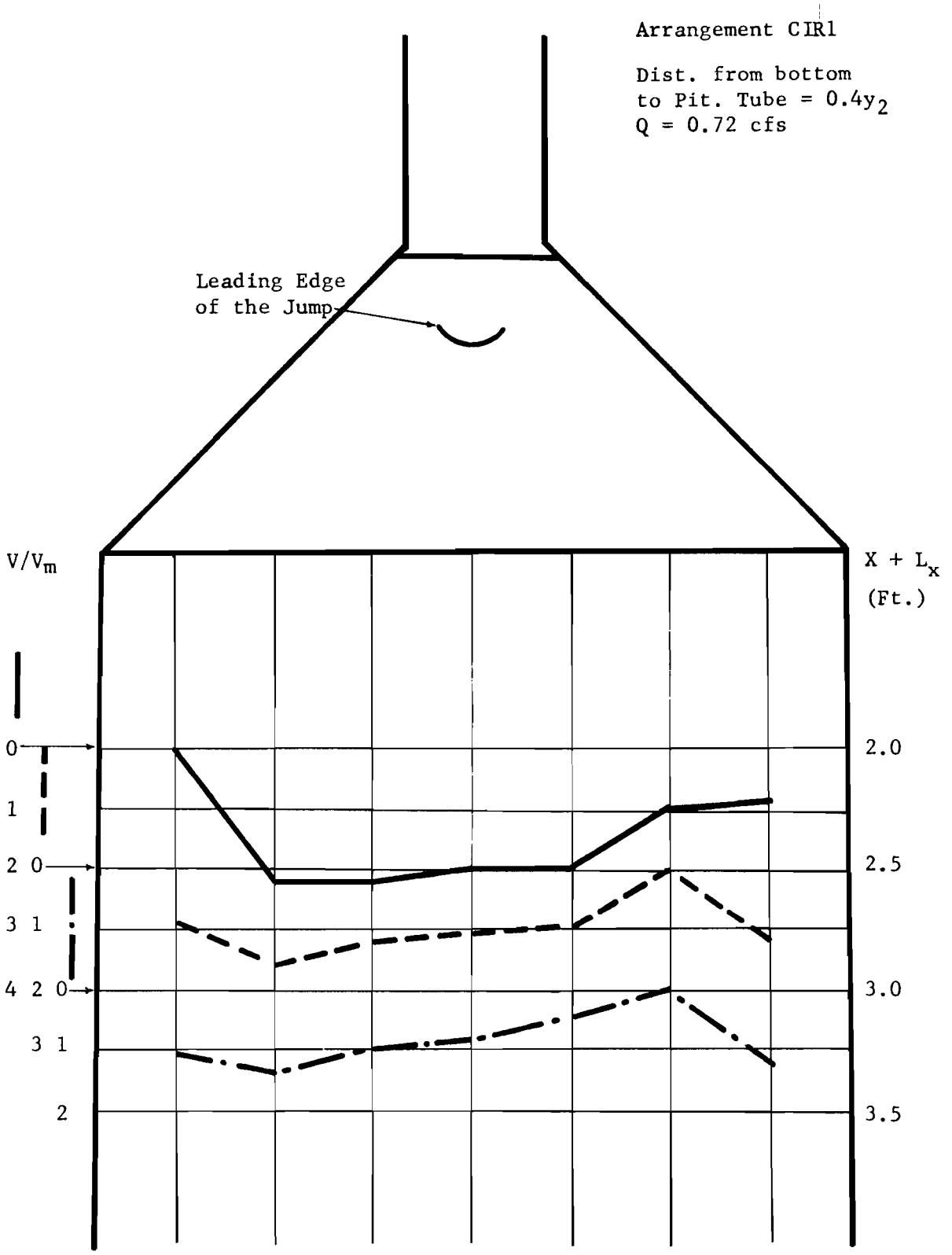

NOTE: Horizontal arrow along V/V_m scale indicates the section of velocity measurements in downstream channel.

FIG. 3-9 VELOCITIES IN DOWNSTREAM CHANNEL

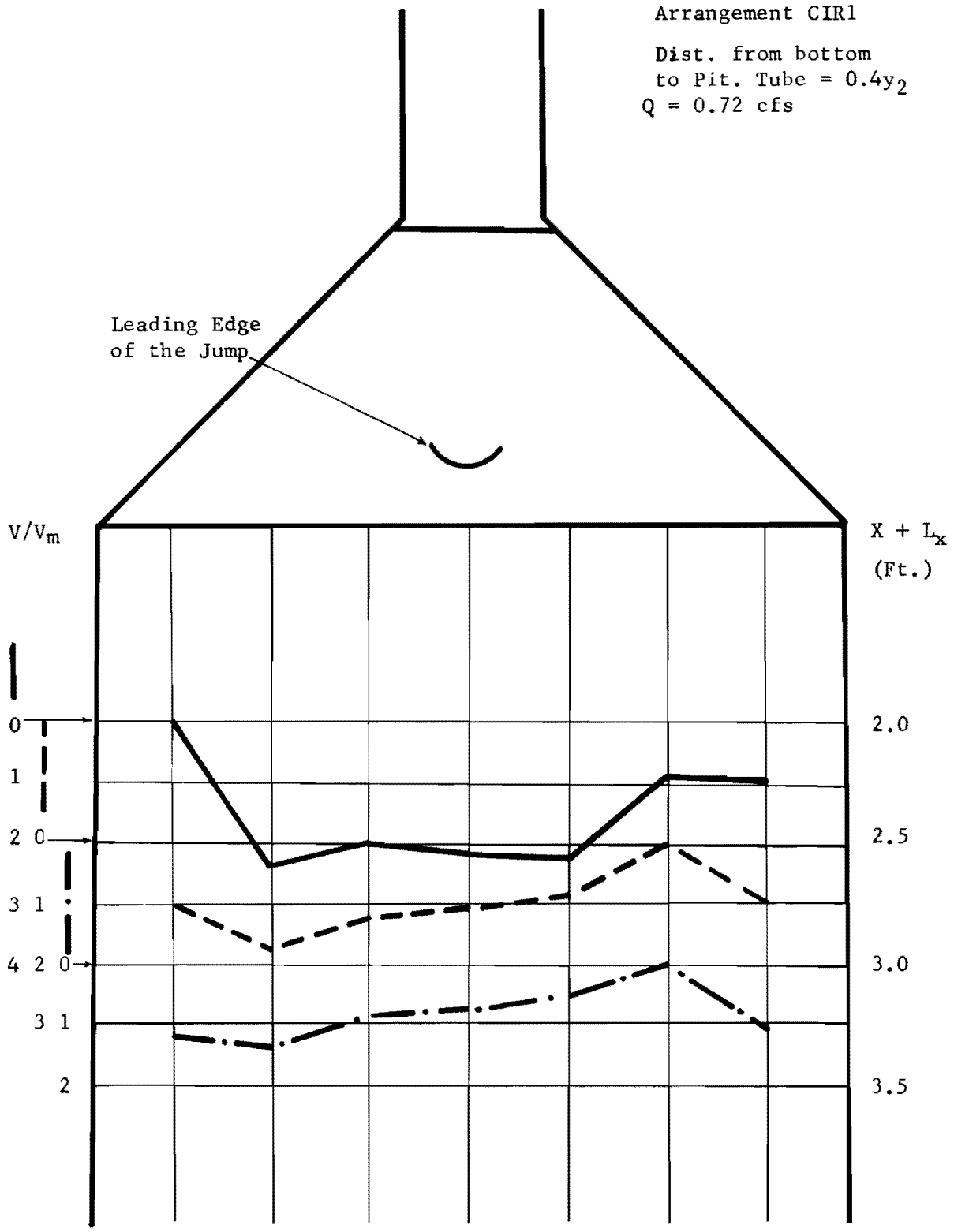

NOTE: Horizontal arrow along V/V_m scale indicates the section of velocity measurements in downstream channel.

FIG. 3-10 VELOCITIES IN DOWNSTREAM CHANNEL

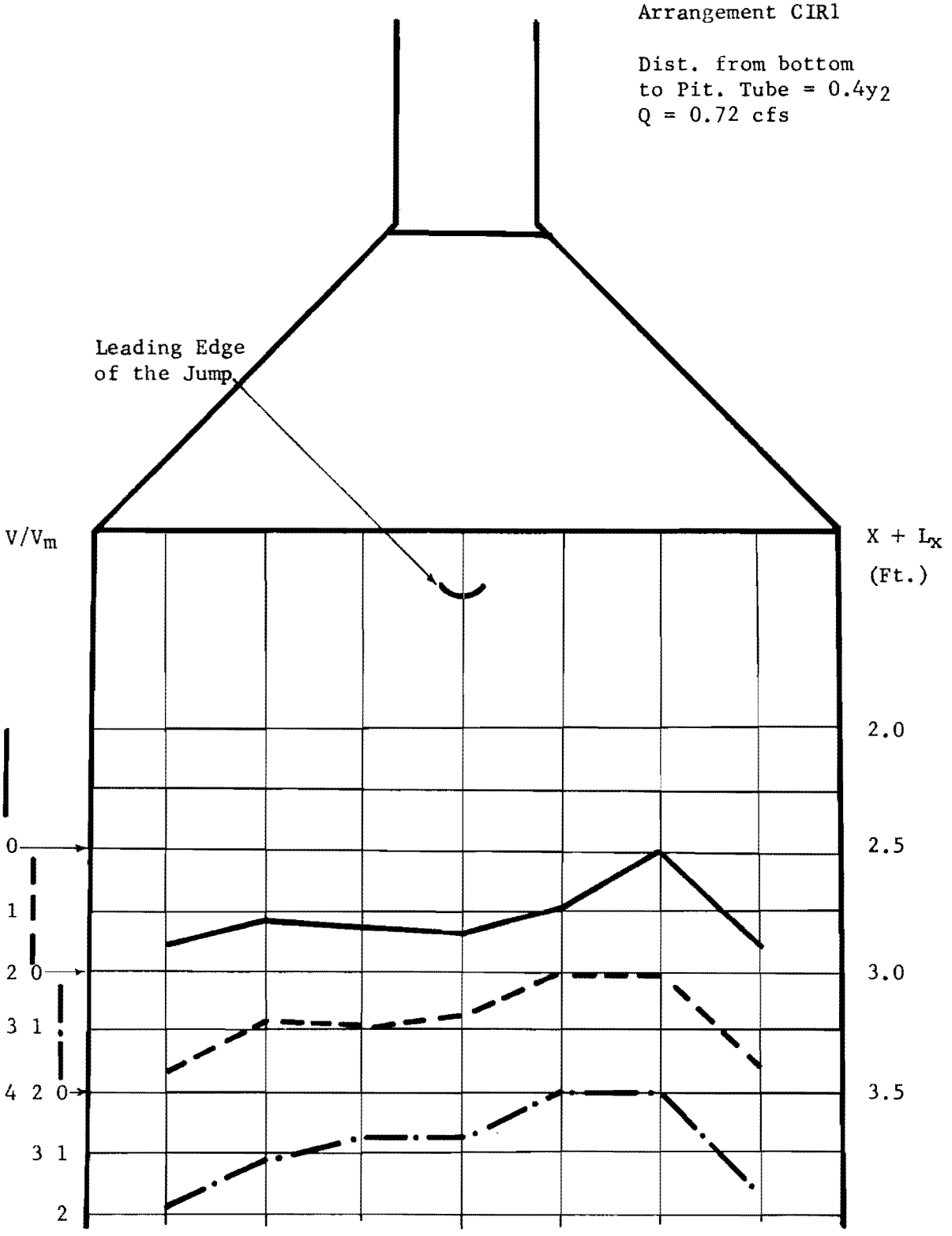

NOTE: Horizontal arrow along V/V_m scale indicates the section of velocity measurements in downstream channel.

FIG. 3-11 VELOCITIES IN DOWNSTREAM CHANNEL

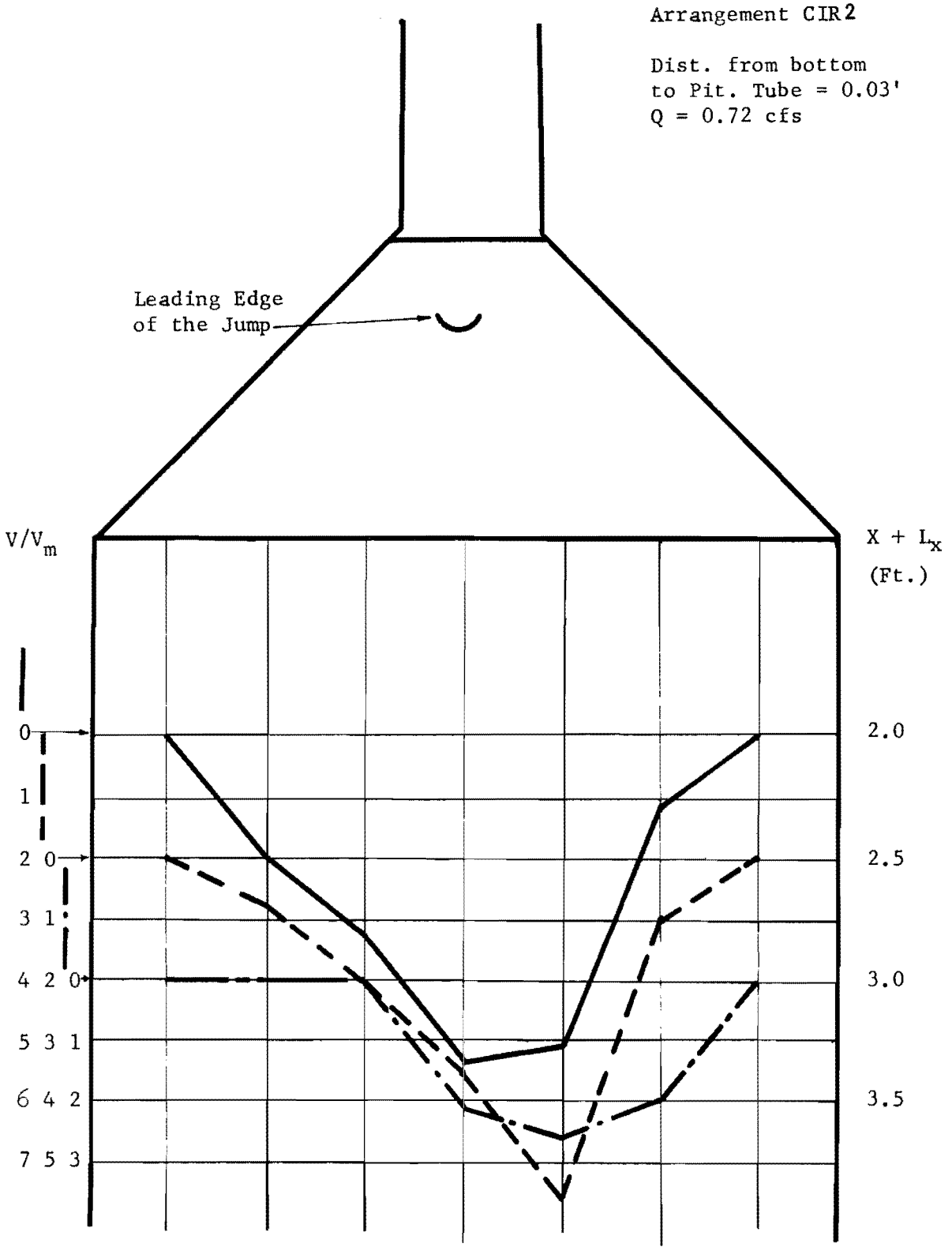

NOTE: Horizontal arrow along V/V_m scale indicates the section of velocity measurements in downstream channel.

FIG. 3-12 VELOCITIES IN DOWNSTREAM

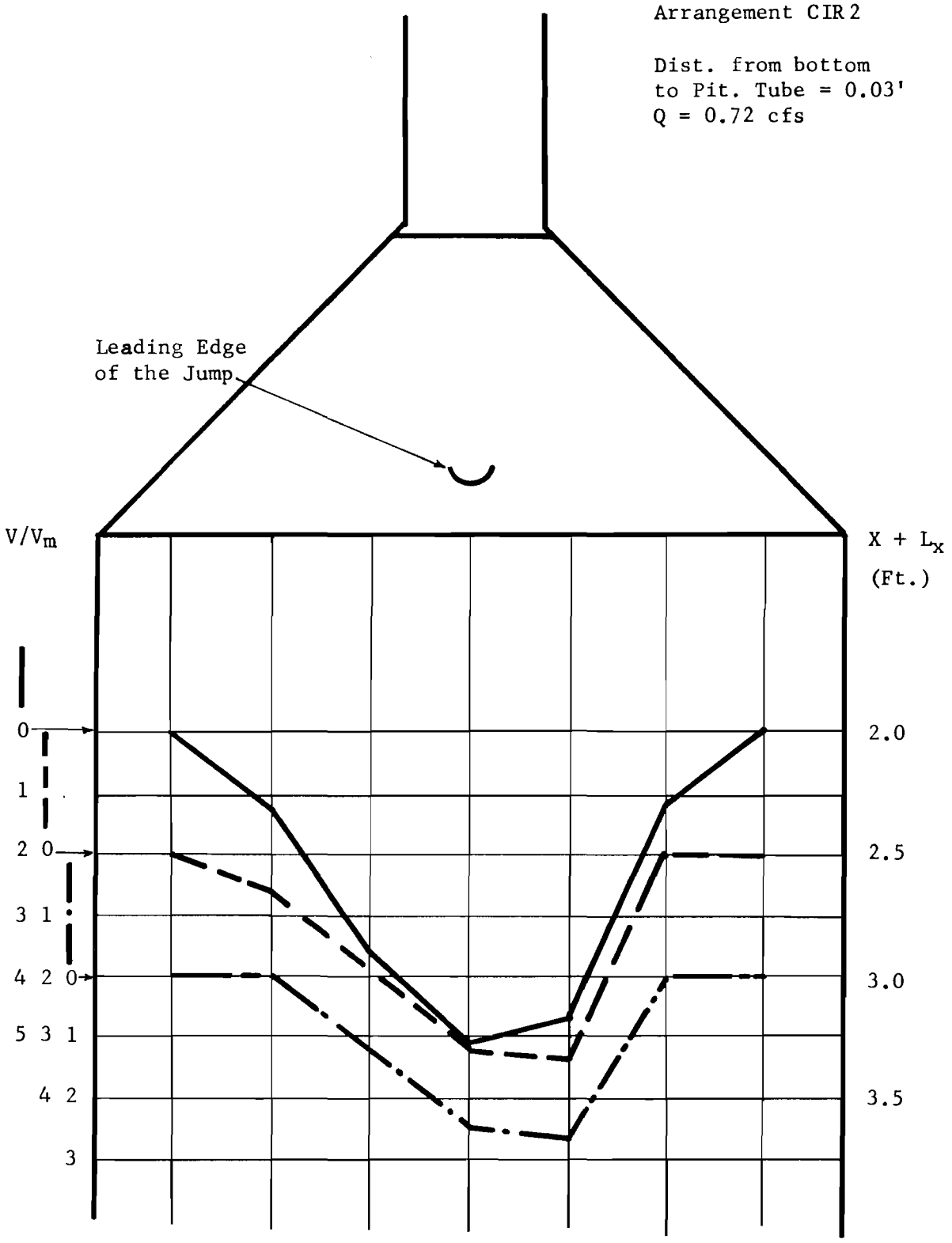

NOTE: Horizontal arrow along V/V_m scale indicates the section of velocity measurements in downstream channel.

FIG. 3-13 VELOCITIES IN DOWNSTREAM CHANNEL

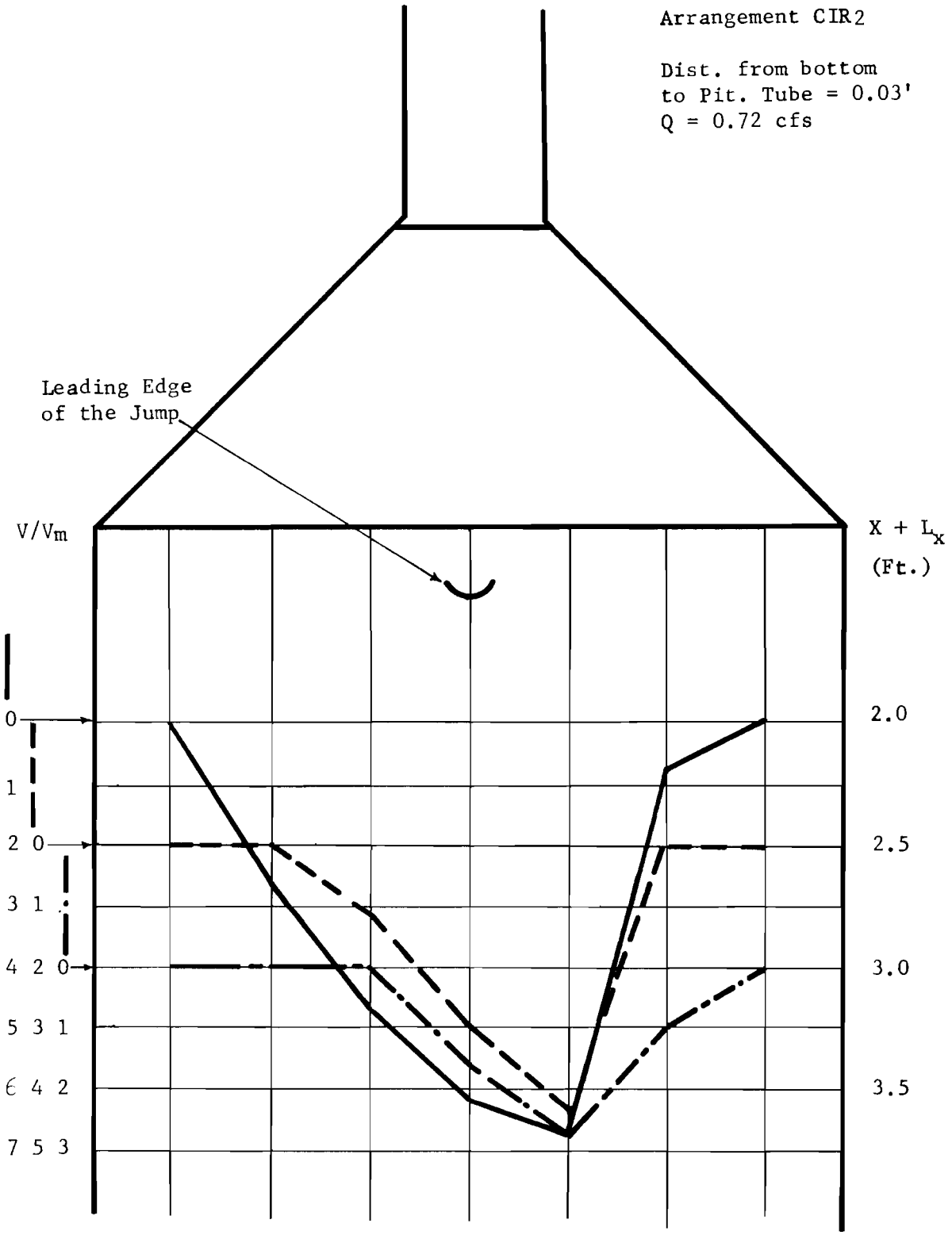

NOTE: Horizontal arrow along V/V_m scale indicates the section of velocity measurements in downstream channel.

FIG. 3-14 VELOCITIES IN DOWNSTREAM CHANNEL

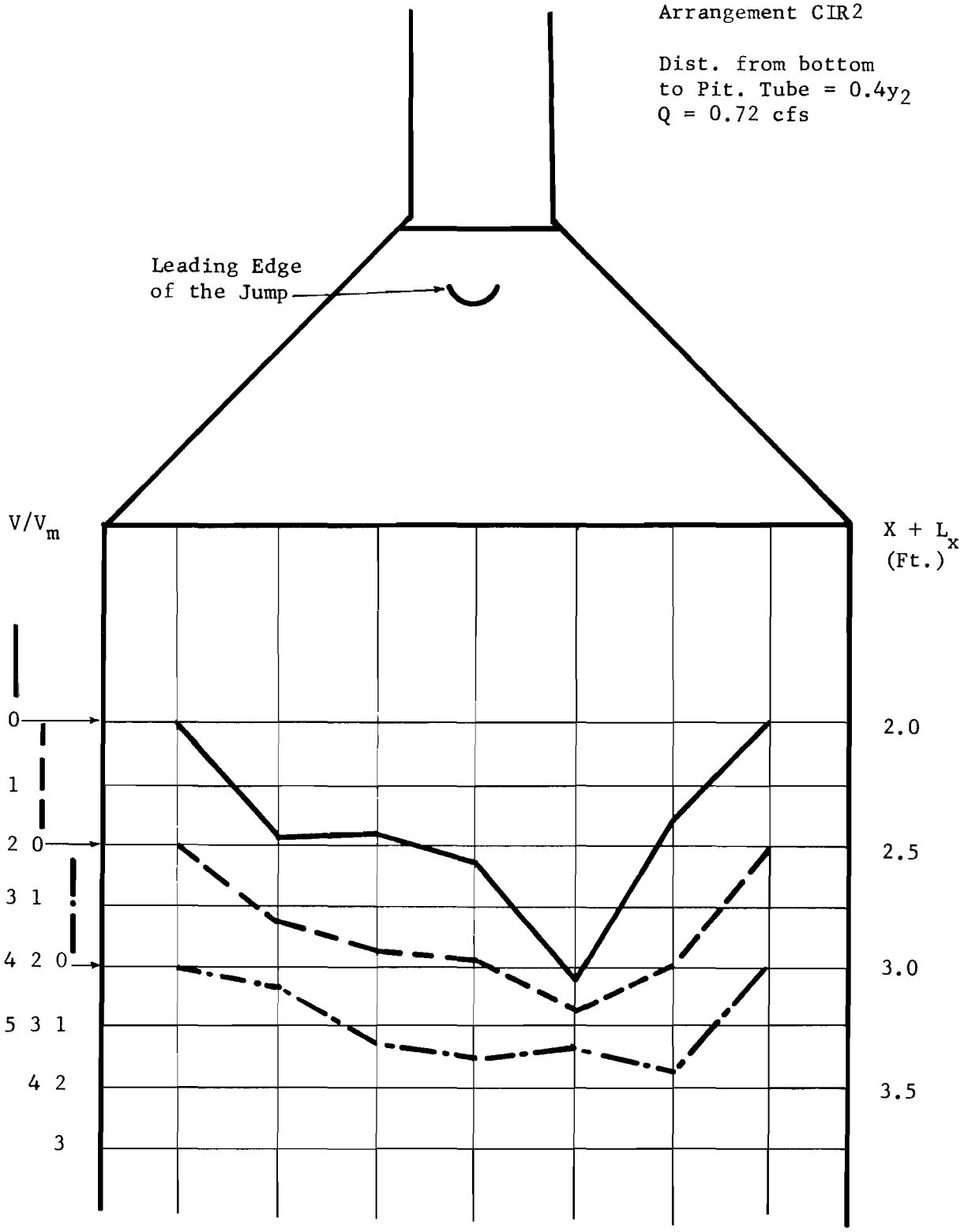

NOTE: Horizontal arrow along V/V_m scale indicates the section of velocity measurements in downstream channel.

FIG. 3-15 VELOCITIES IN DOWNSTREAM CHANNEL

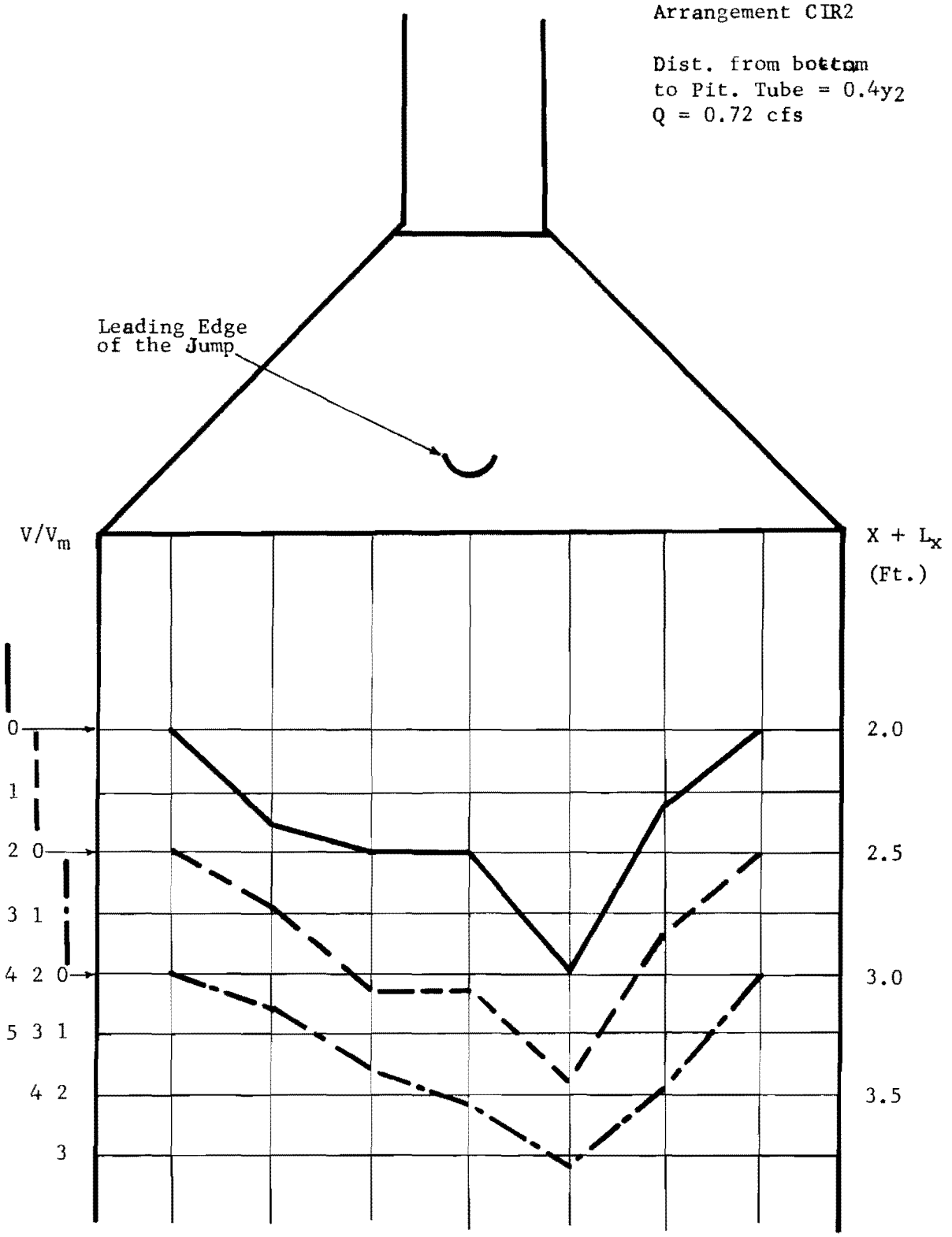

NOTE: Horizontal arrow along V/V_m scale indicates the section of velocity measurements in downstream channel.

FIG. 3-16 VELOCITIES IN DOWNSTREAM CHANNEL

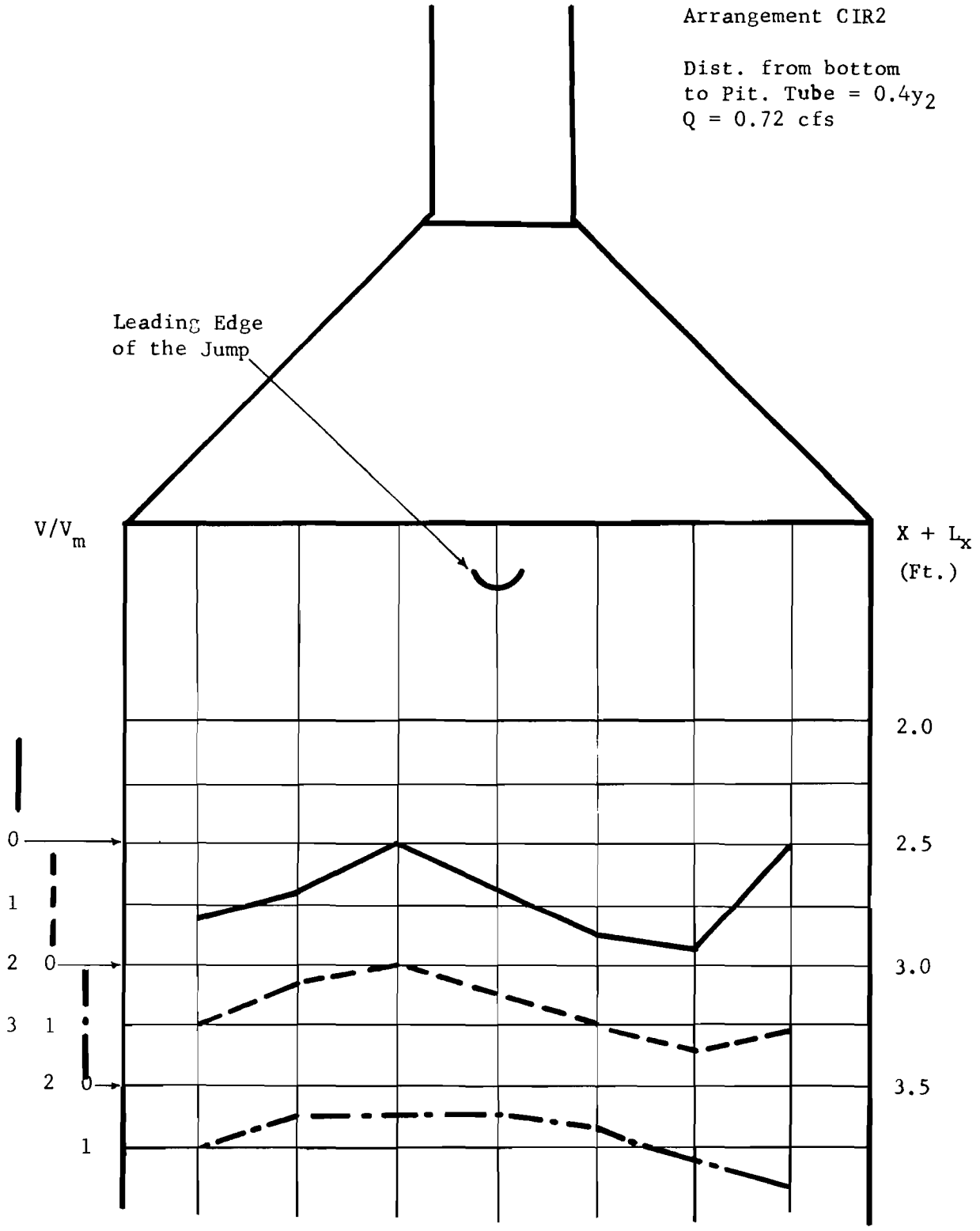

NOTE: Horizontal arrow along V/V_m scale indicates the section of velocity measurements in downstream channel.

FIG. 3-17 VELOCITIES IN DOWNSTREAM CHANNEL

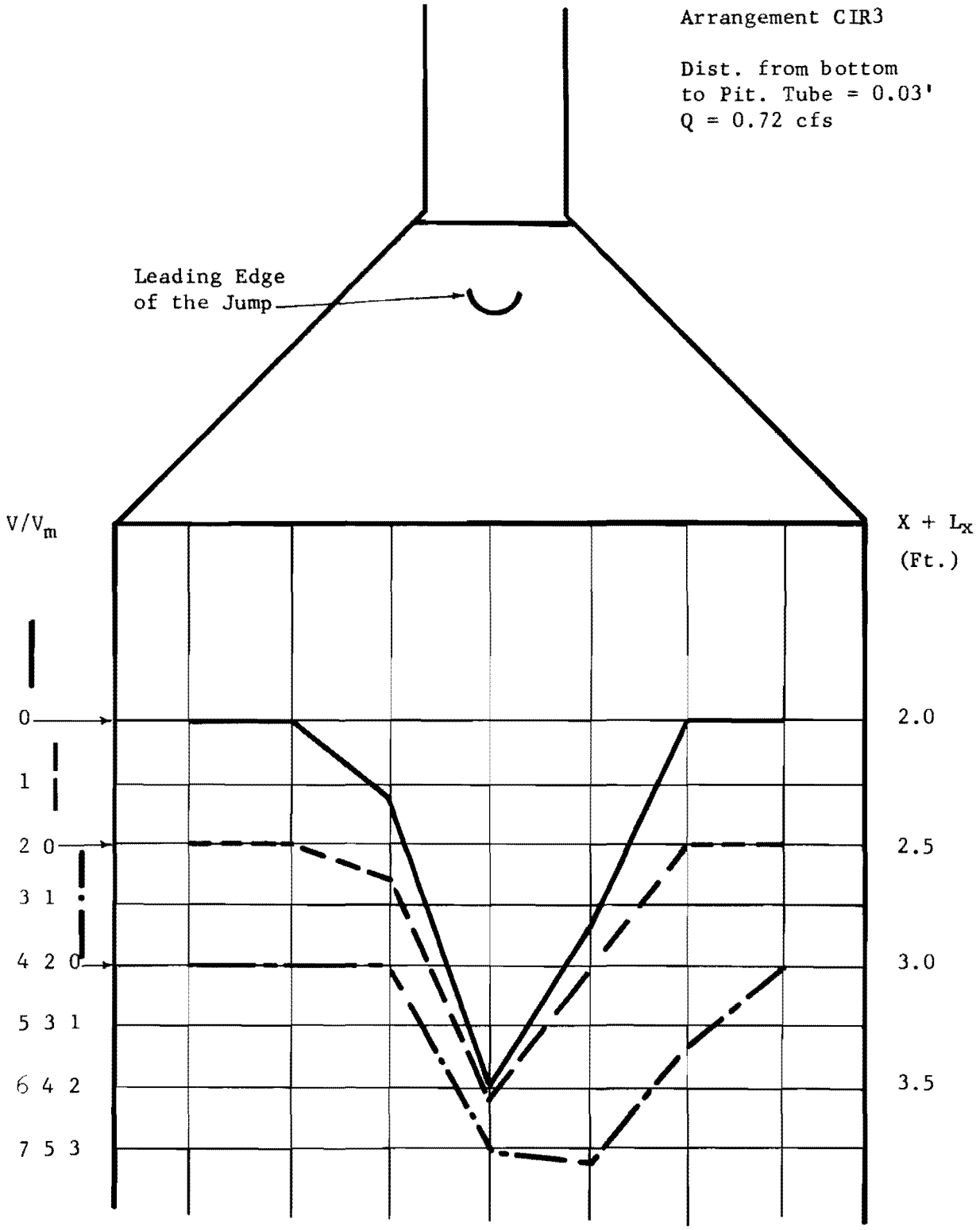

NOTE: Horizontal arrow along V/V_m scale indicates the section of velocity measurements in downstream channel.

FIG. 3-18 VELOCITIES IN DOWNSTREAM CHANNEL

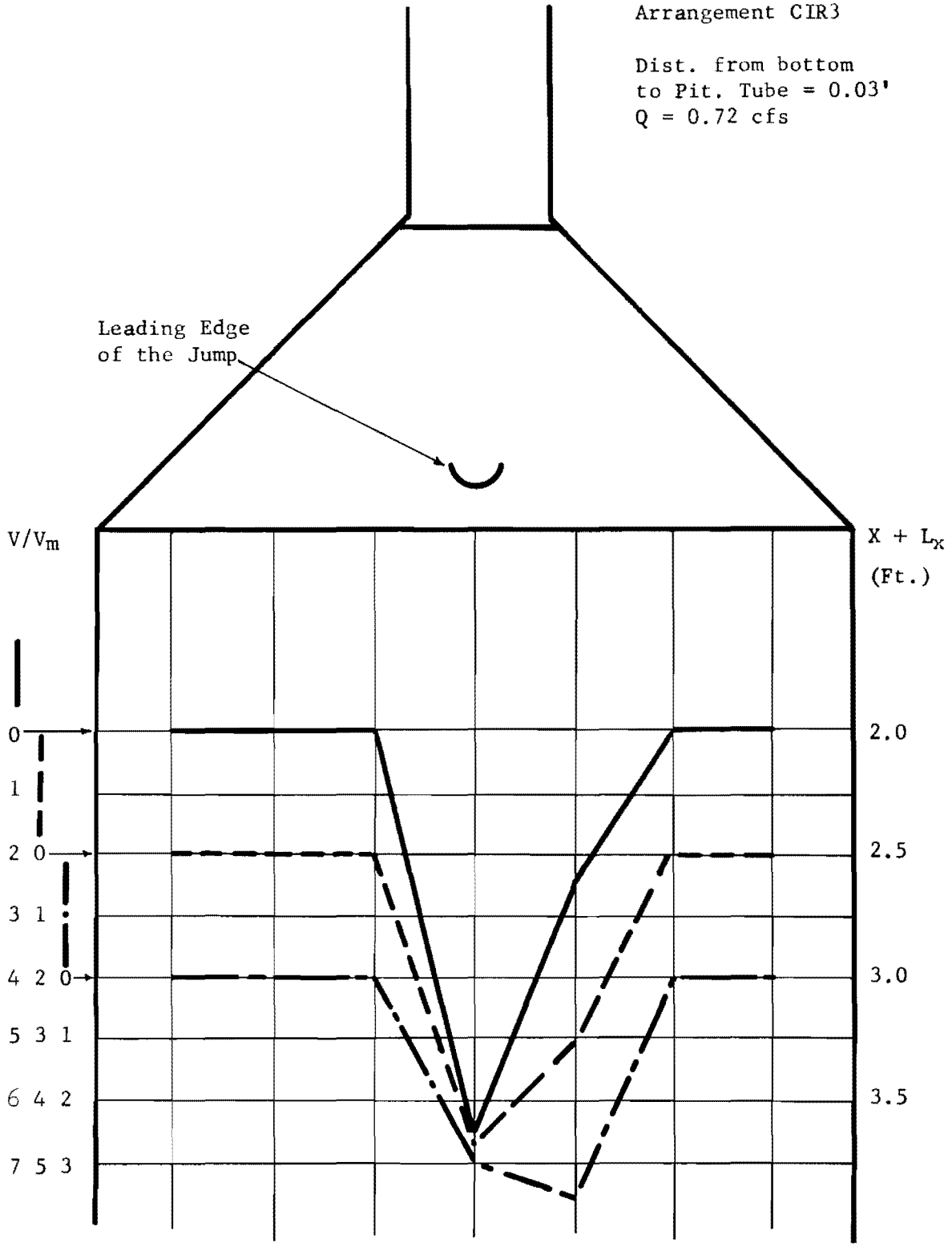

NOTE: Horizontal arrow along V/V_m scale indicates the section of velocity measurements in downstream channel.

FIG. 3-19 VELOCITIES IN DOWNSTREAM CHANNEL

II - Structures with Circular Culvert Incorporating a V Shape Curved Bottom Channel or an Abrupt Drop

The structures used for this study were arrangements CIR4 and CIR5, the geometric dimensions of which are shown in Table 2-1. In view of the observations made in the performance of group I structures, the distance "a" was selected to be zero in these arrangements. The criteria and the method of analyses in determining the efficiency of these basins are similar to that of group I structures. A discussion of the hydraulic performance of these configuration is followed.

Water Surface Profile

Figures 3-20 and 3-21 are representative water surface profiles for arrangements CIR4 and CIR5 respectively when operated at F_t of 1.90. Arrangement CIR4 performed with high wave flow in the vicinity of the flared wingwalls. Fluctuations occurred in the depth of flow in this region and the V-shape curved bottom channel section did not particularly improve the water surface profile. The flow depth in the region of flared wingwalls quickly decreased as the flow moved downstream, resulting in a fairly uniform flow depth across the downstream end of the stilling basin. The depth of flow decreased within the basin as the flow advanced downstream until the leading edge of the hydraulic jump was reached. Of course, this was characteristic of the radial flow basin, and it occurred in every arrangement. Arrangement CIR5 performed with lower water surface profile than that of arrangement CIR4 for the same hydraulic conditions. The high water depth in the region of flared wingwalls for CIR5 was considerably lower than all other previous

arrangements. The continuation of parallel wingwalls downstream from the abrupt drop in this arrangement confined the flow for some distance after reaching the basin floor and partially damped out the high waves on the sides of the flared wingwalls. It was noted that in arrangement CIR5 the depth of flow decreased within the basin as the flow advanced downstream at a faster rate than that of CIR4. In other words, the absolute value of the slope of tangent to the curves of depth vs. distance (Figures 3-20, 3-21) at a given section was higher for arrangement CIR5 than arrangement CIR4. Comparison of the experimental results for these structures shows that, so far as the water surface profile is concerned, arrangement CIR5 is somewhat preferable to arrangement CIR4.

Stability of the Hydraulic Jump

In order to determine the stability of the Hydraulic jump, the longitudinal change in position of the jump corresponding to a change in tailwater depth was recorded and curves of Y_2/Y_t vs. x/Y_t were plotted as shown in Figures 3-22 and 3-23. As shown in these figures when the value of x/Y_t was increased, the absolute value of the slope of Y_2/Y_t vs. x/Y_t curves decreased corresponding to a reduction in the stability of the hydraulic jump. The slope of the curve for arrangement CIR5 (Figure 3-23) was larger than that of arrangement CIR4 (Figure 3-22). This is an indication of more stable position of the jump in the basin of CIR5 when hydraulic conditions are unchanged. Furthermore, CIR5 could be operated at a higher range of tailwater variations than CIR4. Figures 3-22 and 3-23 show that an

CIRCULAR CULVERT (Arrangement CIR4)

F_t = 1.90 Q = 0.72 cfs Y_t = 0.30 ft.

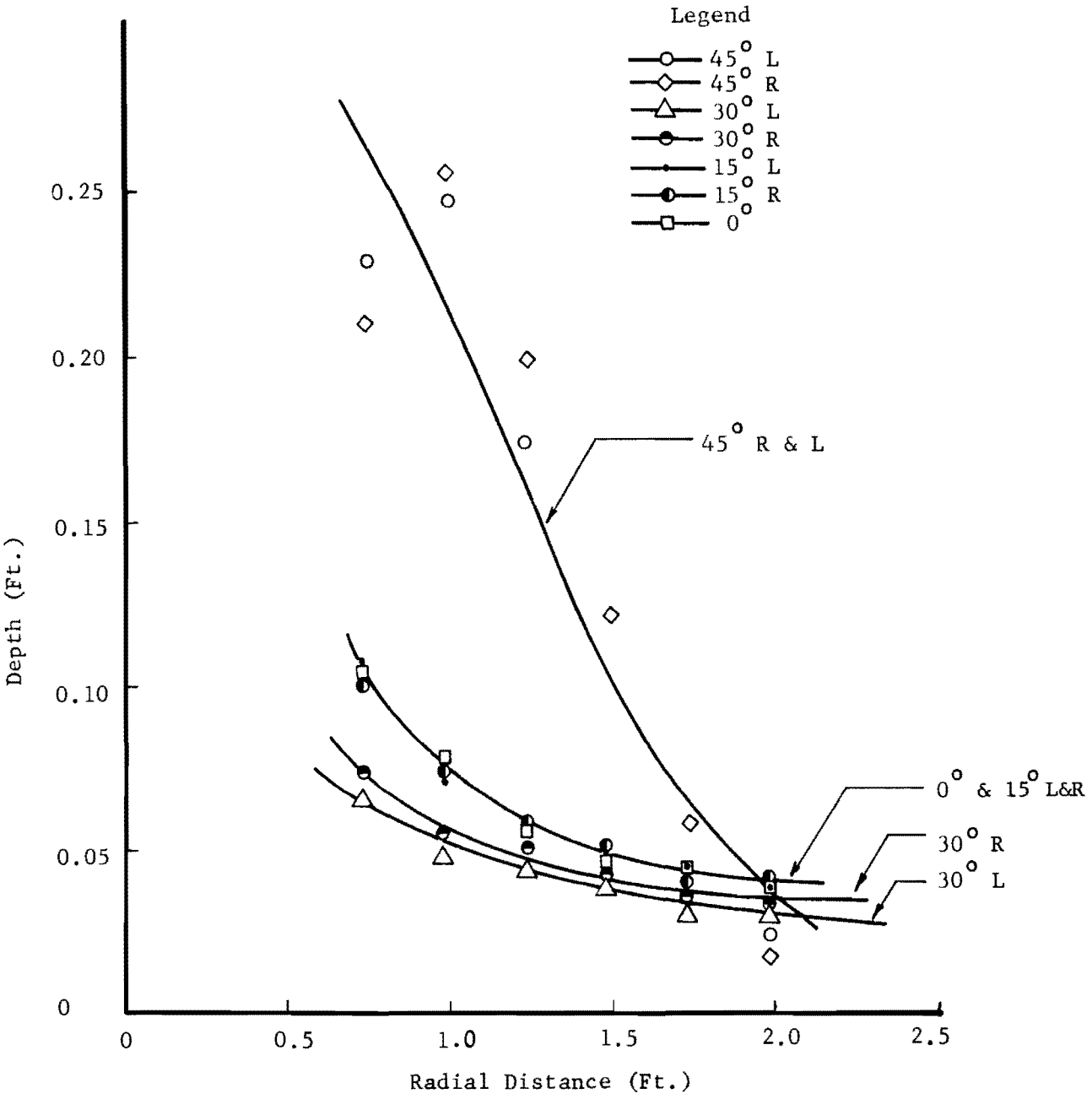

FIG. 3-20 WATER SURFACE ELEVATION OF SUPERCRITICAL FLOW ON APRON

CIRCULAR CULVERT (Arrangement CIR5)

F_t = 1.90 Q = 0.72 cfs Y_t = 0.30 ft.

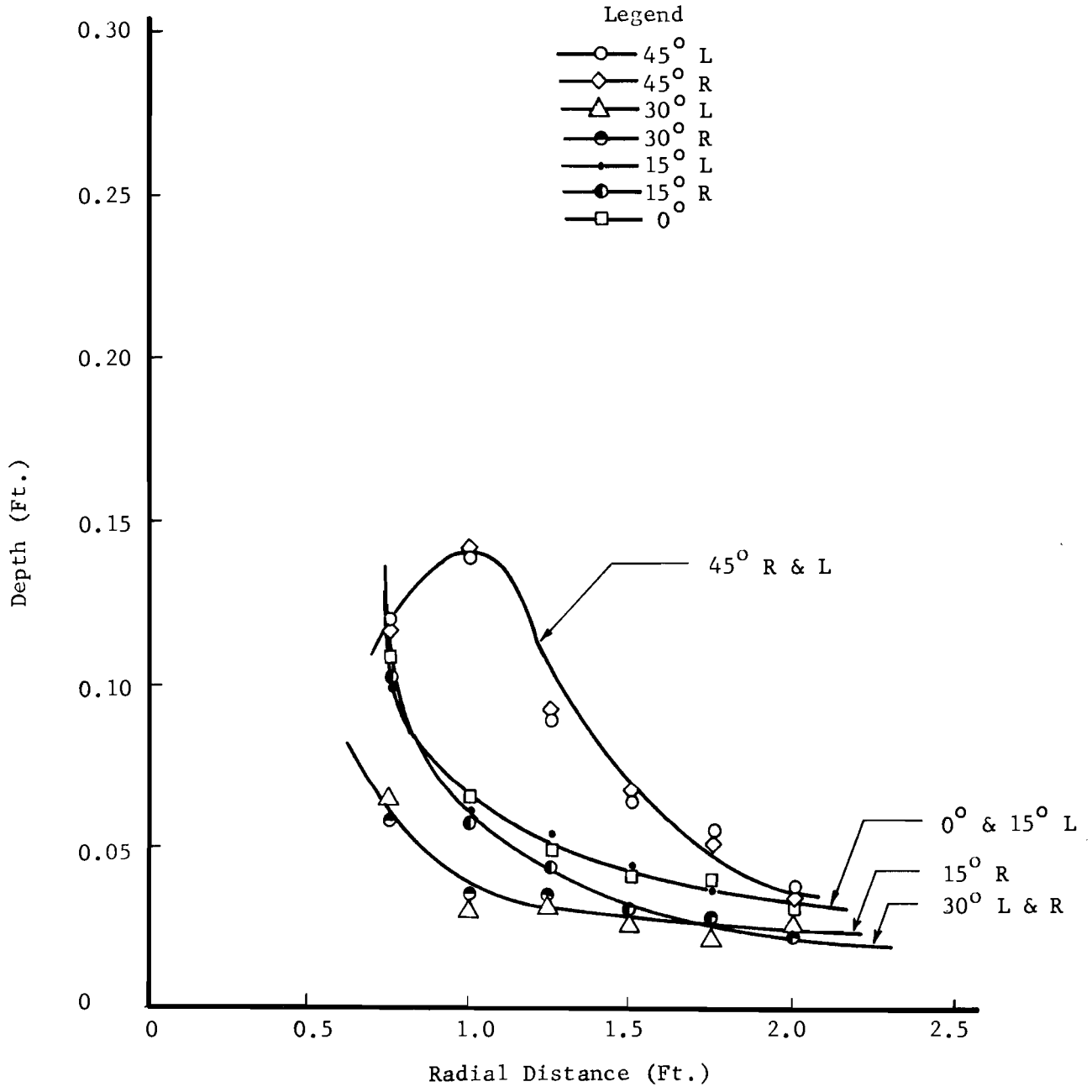

FIG. 3-21 WATER SURFACE ELEVATION OF SUPERCRITICAL FLOW ON APRON

incremental change in the tailwater depth resulted in a larger variation of x in arrangement CIR4 than CIR5.

The F_t for this experimental study was 1.90 in both structures. No attempt was made to explore the effect of F_t in these structures since such investigation was already conducted for radial flow basin in previous arrangements.

The evaluated results indicate that the basin with the best degree of jump stability is arrangement CIR5, because of higher absolute value of slope of curves Y_2/Y_t vs. x/Y_t and lower tailwater requirements at a given value of x/Y_t.

Velocity Distribution and Reduction

Velocity measurements were taken at the same sections in the downstream channel as that of group I structures. Measured values of V/V_m are shown in Figures 3-24 through 3-34. Prior to making the velocity measurements, the jump was stabilized at three different positions with F_t equal to 1.90. The leading edge of the jump is shown in each figure. The general pattern of velocity distribution showed concentration of flow velocities within the central portion of the channel and zero velocities on the sides of the channel. The nonuniform spreading of the supercritical flow within the radial basin and its reflection off of the flared wingwalls into the parallel flow section resulted in the concentration of flow velocities in the central portion of the downstream channel. Normally, the magnitude of V/V_m for a given section within the central portion of the channel in arrangement

CIRCULAR CULVERT (Arrangement CIR4)

F_t = 1.94 Q = 0.72 cfs Y_t = 0.297 ft.

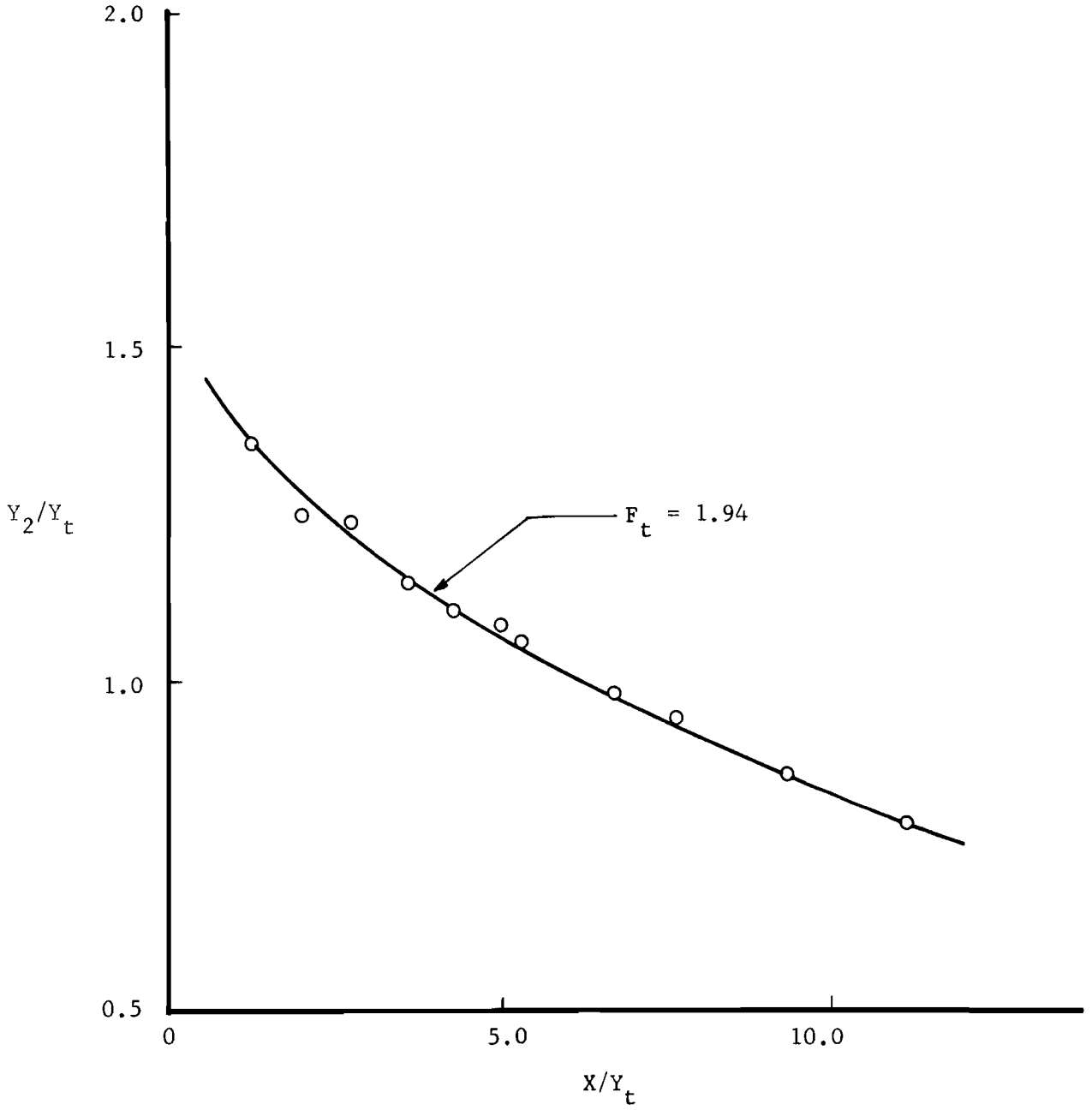

FIG. 3-22 TAILWATER DEPTH vs. JUMP POSITION

CIRCULAR CULVERT (Arrangement CIR5)

F_t = 1.90 Q = 0.72 cfs Y_t = 0.30 ft.
F_t = 1.78 Q = 0.72 cfs Y_t = 0.31 ft.

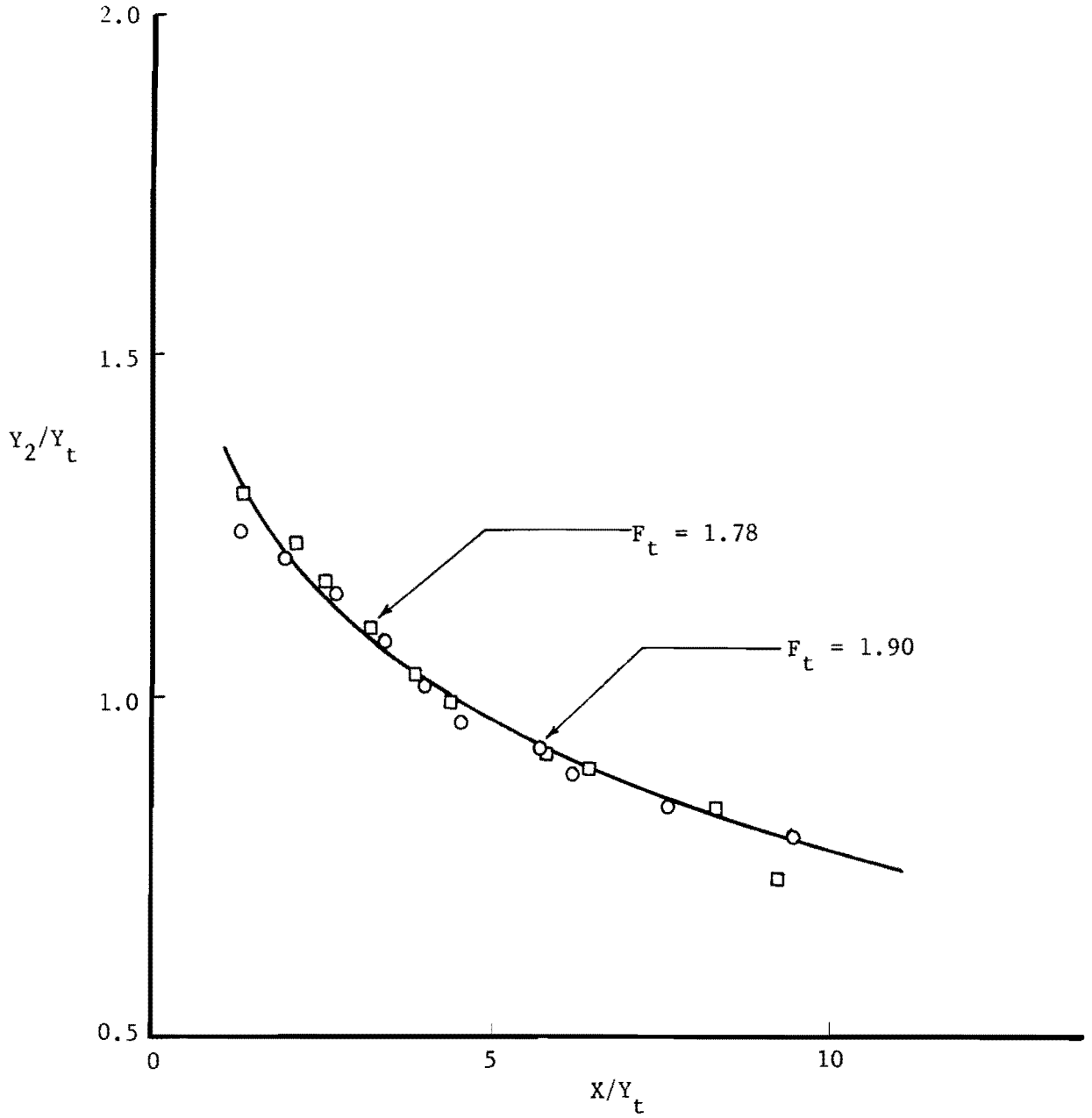

FIG. 3-23 TAILWATER DEPTH vs. JUMP POSITION

CIR4 increased as the leading edge of the jump moved downstream. Highest velocities along the channel centerline were recorded at points nearest to the leading edge of the jump.

Analyses of the velocity profiles show that for arrangement CIR4, at the sections nearest the leading edge of the jump, the maximum velocity at the center portion of the channel varied within a range of 1.5 to 5.5 times V_m. This range of velocity variation corresponded to an approximate range of 20 to 80 percent of V_t. For arrangement CIR5 the velocity for the same section as that of CIR4 varied within a range of 1 to 4 times V_m. This was equivalent to an approximate range of 15 to 80 percent of V_t. Velocity distribution in arrangement CIR5 was more shewed to the side of the channel than that of arrangement CIR4. Generally, the velocity of each section for a fixed F_t was lower in arrangement CIR5 than CIR4. However, arrangement CIR5 performed with high degree of skewness in velocity profile which is an undesirable characteristic of this basin.

It should be noted that the upper limit of these velocity magnitudes may require certain protective measures against scouring damage in the downstream channel. The suitability of a protected channel bottom depends to a large degree on the type of material in the natural channel bed. Furthermore, if the high velocity flow in the central portion of the channel could be slowed down by a suitable method, the required length of the channel protection may be reduced.

From a point-of-view of velocity reduction and uniformity, arrangement CIR5 performed with a higher efficiency than CIR4.

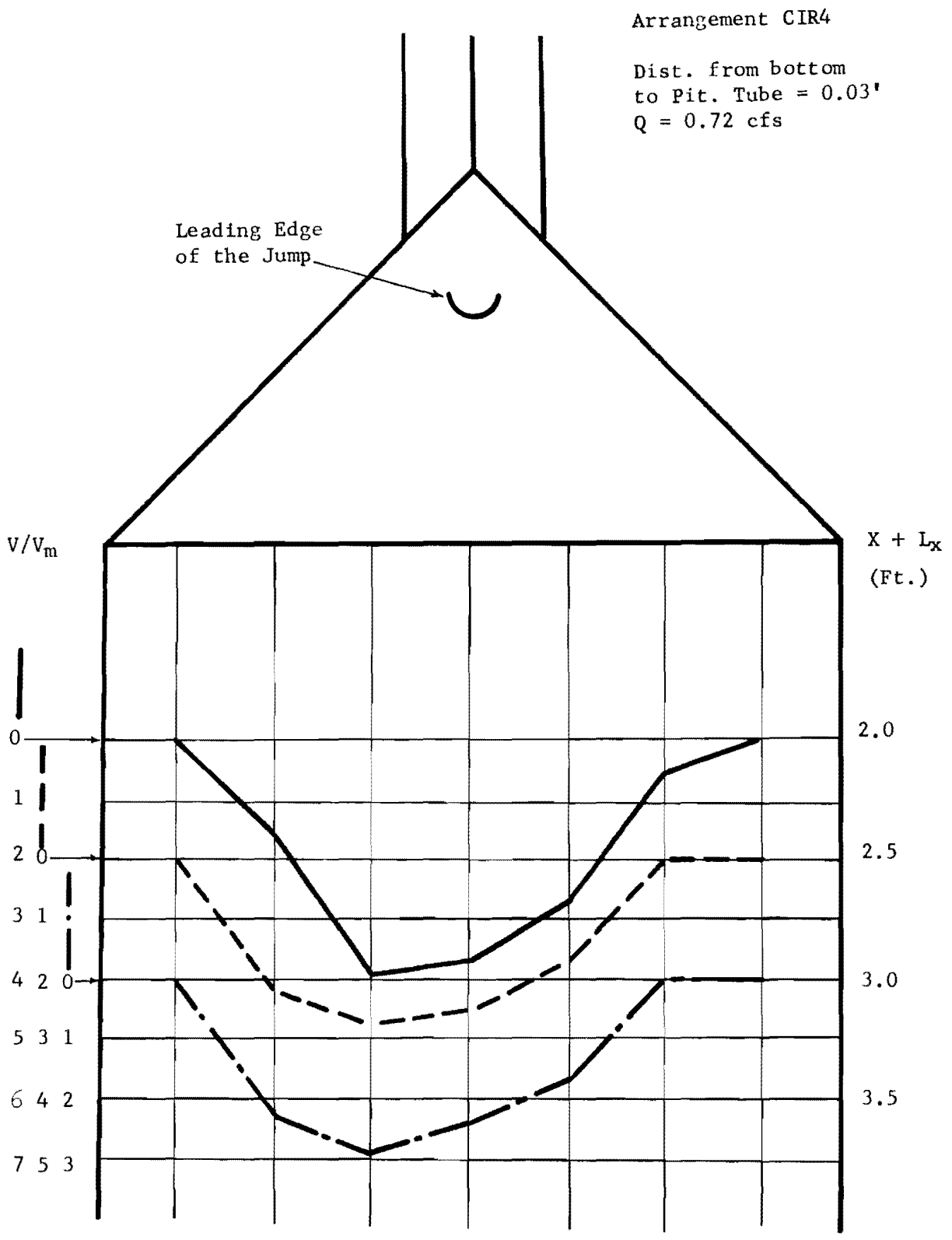

NOTE: Horizontal arrow along V/V_m scale indicates the section of velocity measurements in downstream channel.

FIG. 3-24 VELOCITIES IN DOWNSTREAM CHANNEL

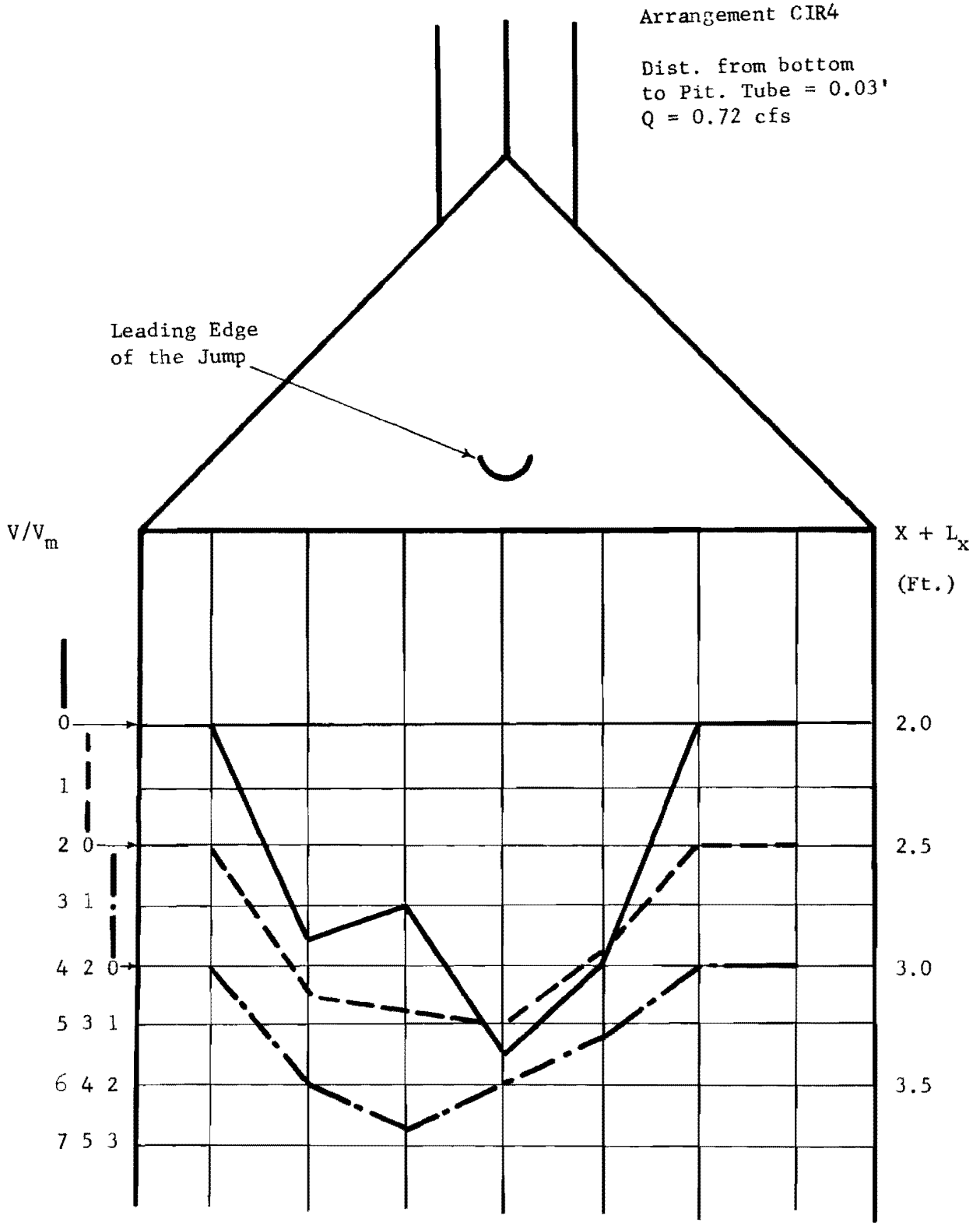

NOTE: Horizontal arrow along V/V_m scale indicates the section of velocity measurements in downstream channel.

FIG. 3-25 VELOCITIES IN DOWNSTREAM CHANNEL

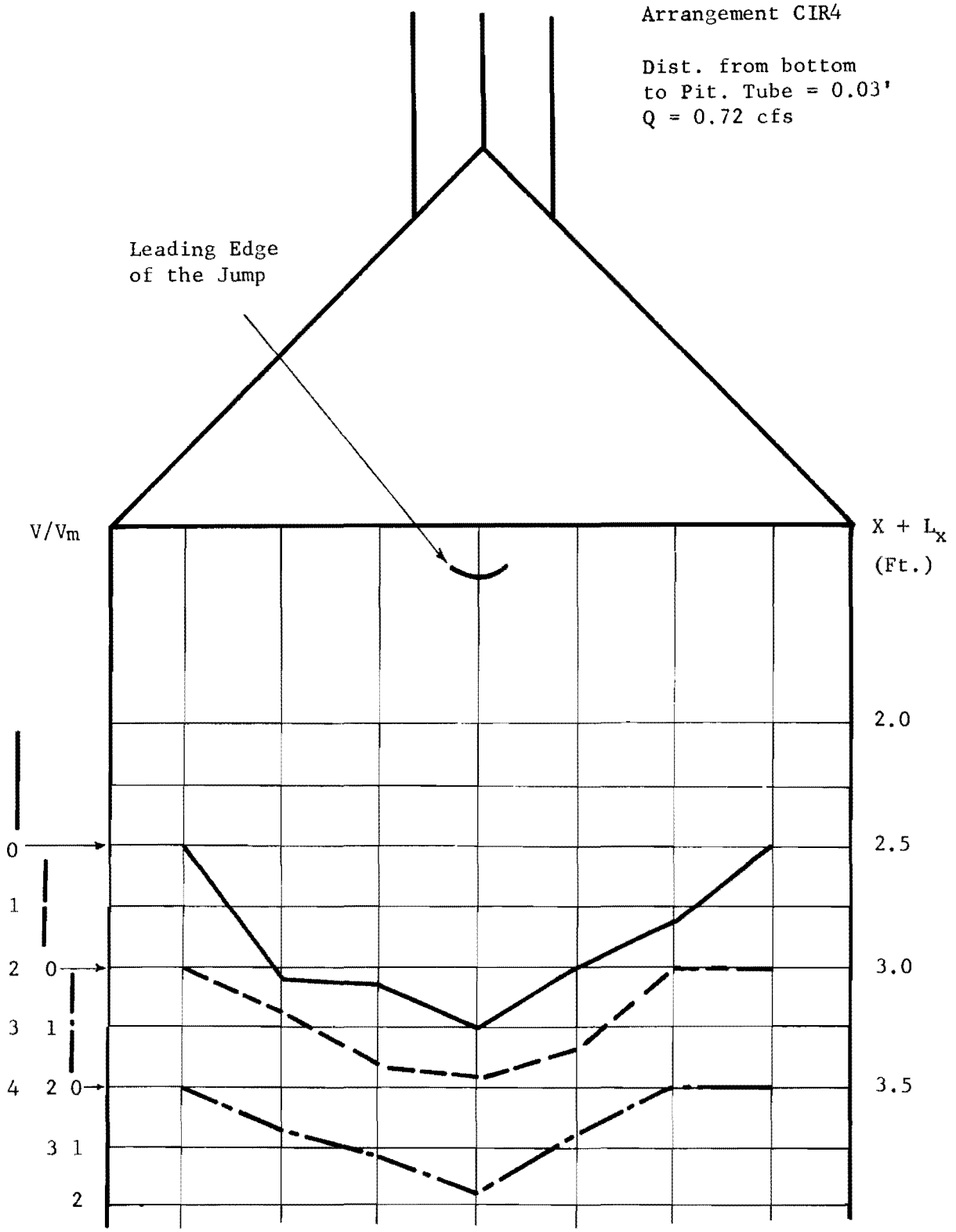

NOTE: Horizontal arrow along V/V_m scale indicates the section of velocity measurements in downstream channel.

FIG. 3-26 VELOCITIES IN DOWNSTREAM CHANNEL

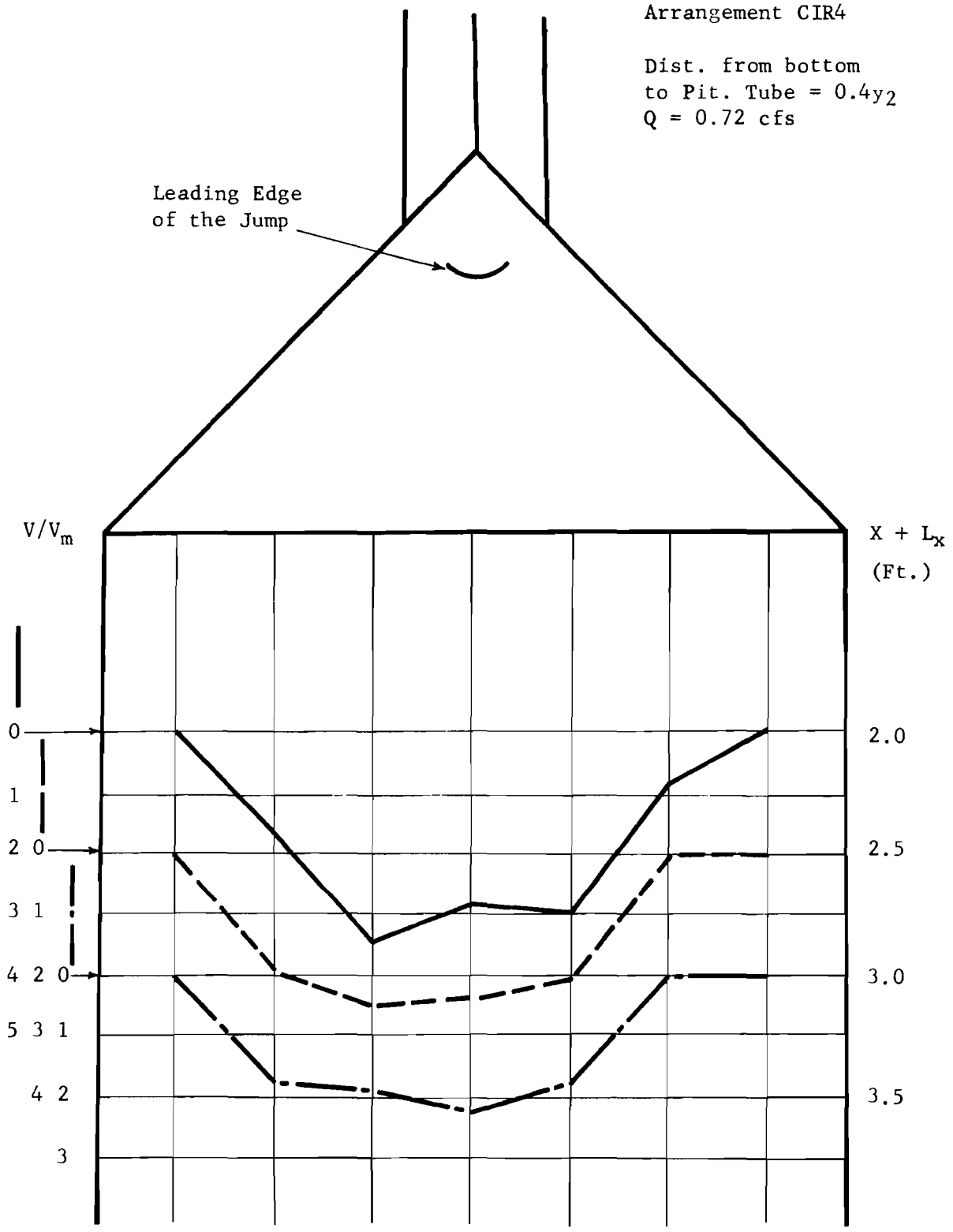

NOTE: Horizontal arrow along V/V_m scale indicates the section of velocity measurements in downstream channel.

FIG. 3-27 VELOCITIES IN DOWNSTREAM CHANNEL

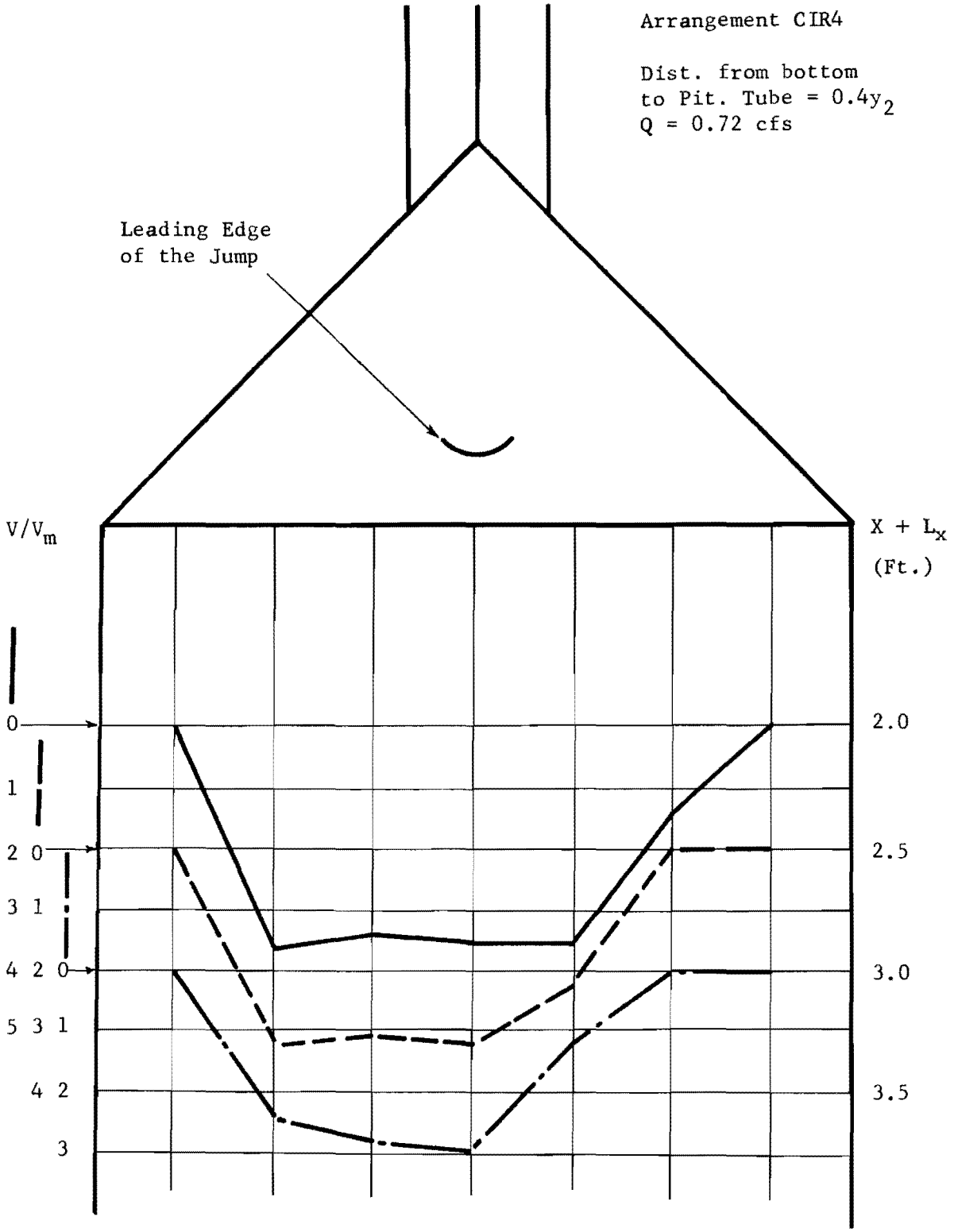

NOTE: Horizontal arrow along V/V_m scale indicates the section of velocity measurements in downstream channel.

FIG. 3-28 VELOCITIES IN DOWNSTREAM CHANNEL

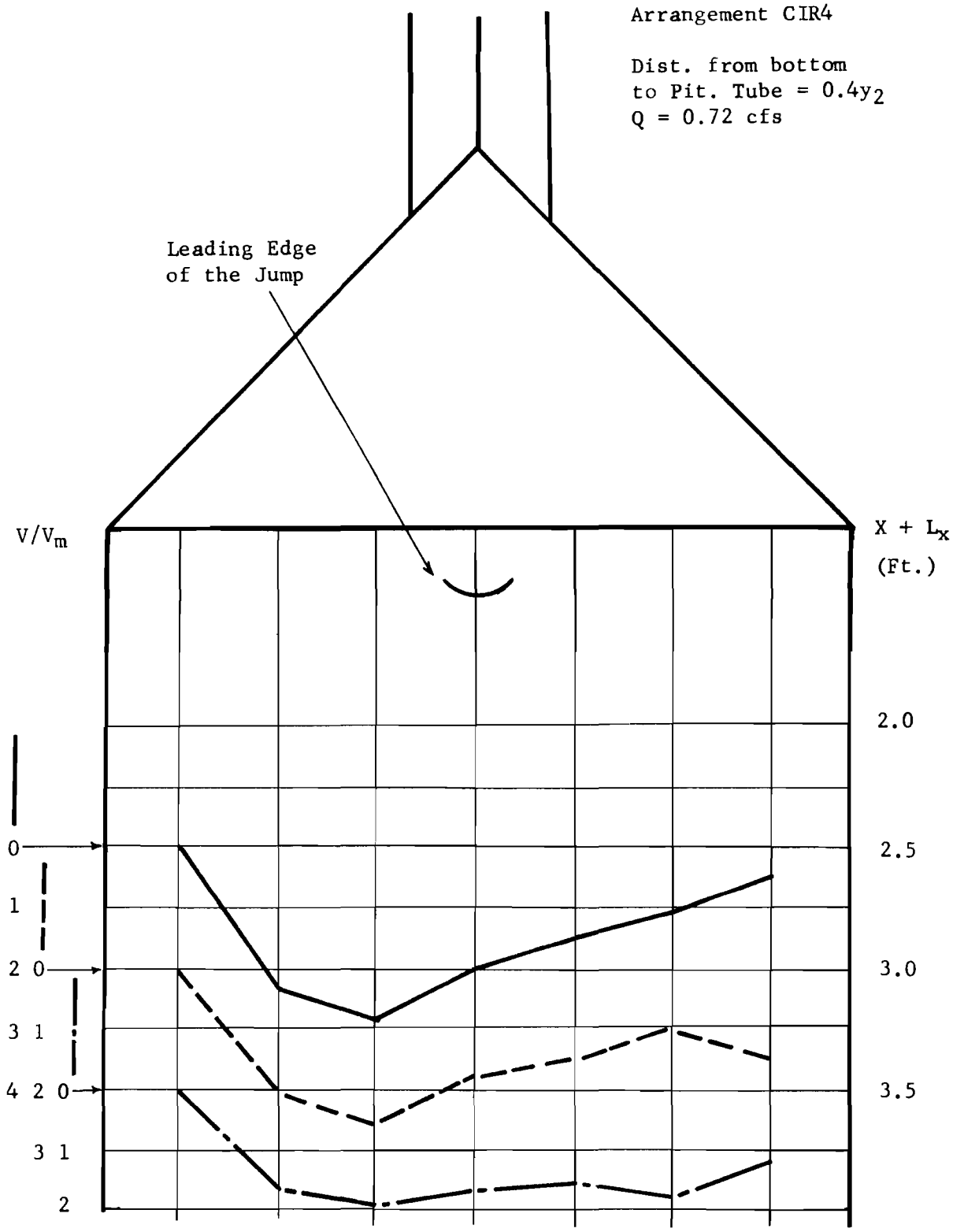

NOTE: Horizontal arrow along V/V_m scale indicates the section of velocity measurements in downstream channel.

FIG. 3-29 VELOCITIES IN DOWNSTREAM CHANNEL

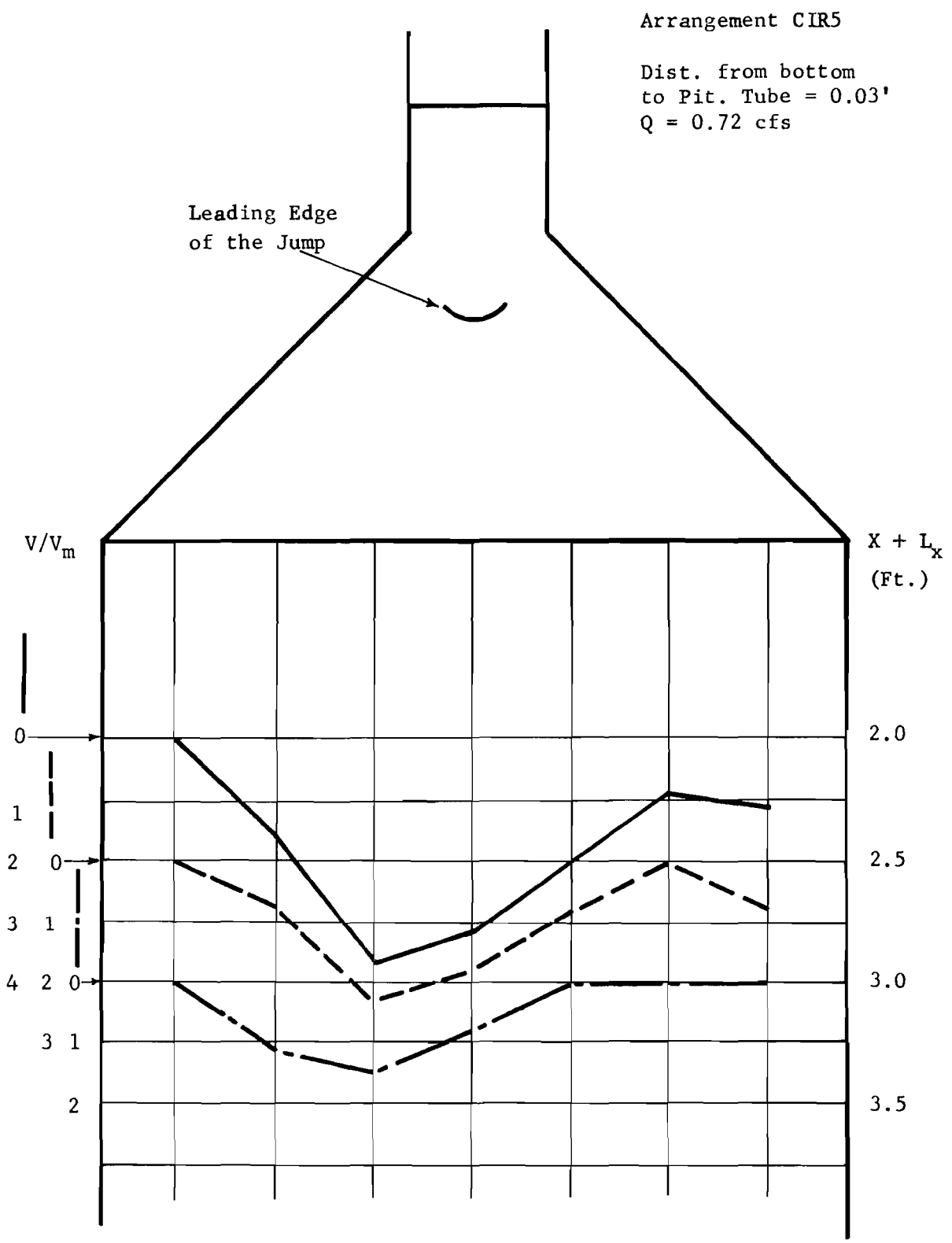

NOTE: Horizontal arrow along V/V_m scale indicates the section of velocity measurements in downstream channel.

FIG. 3-30 VELOCITIES IN DOWNSTREAM CHANNEL

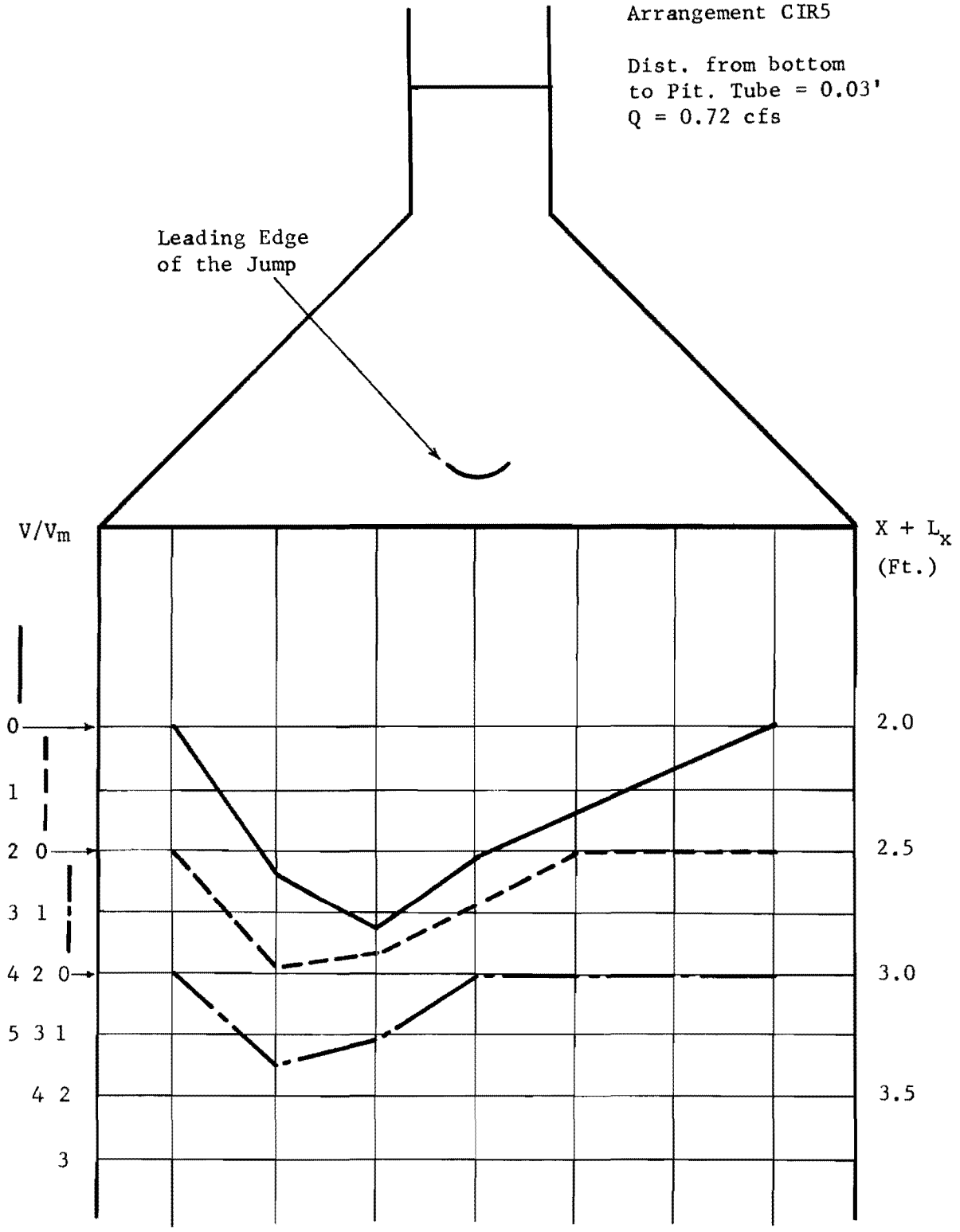

NOTE: Horizontal arrow along V/V_m scale indicates the section of velocity measurements in downstream channel.

FIG. 3-31 VELOCITIES IN DOWNSTREAM CHANNEL

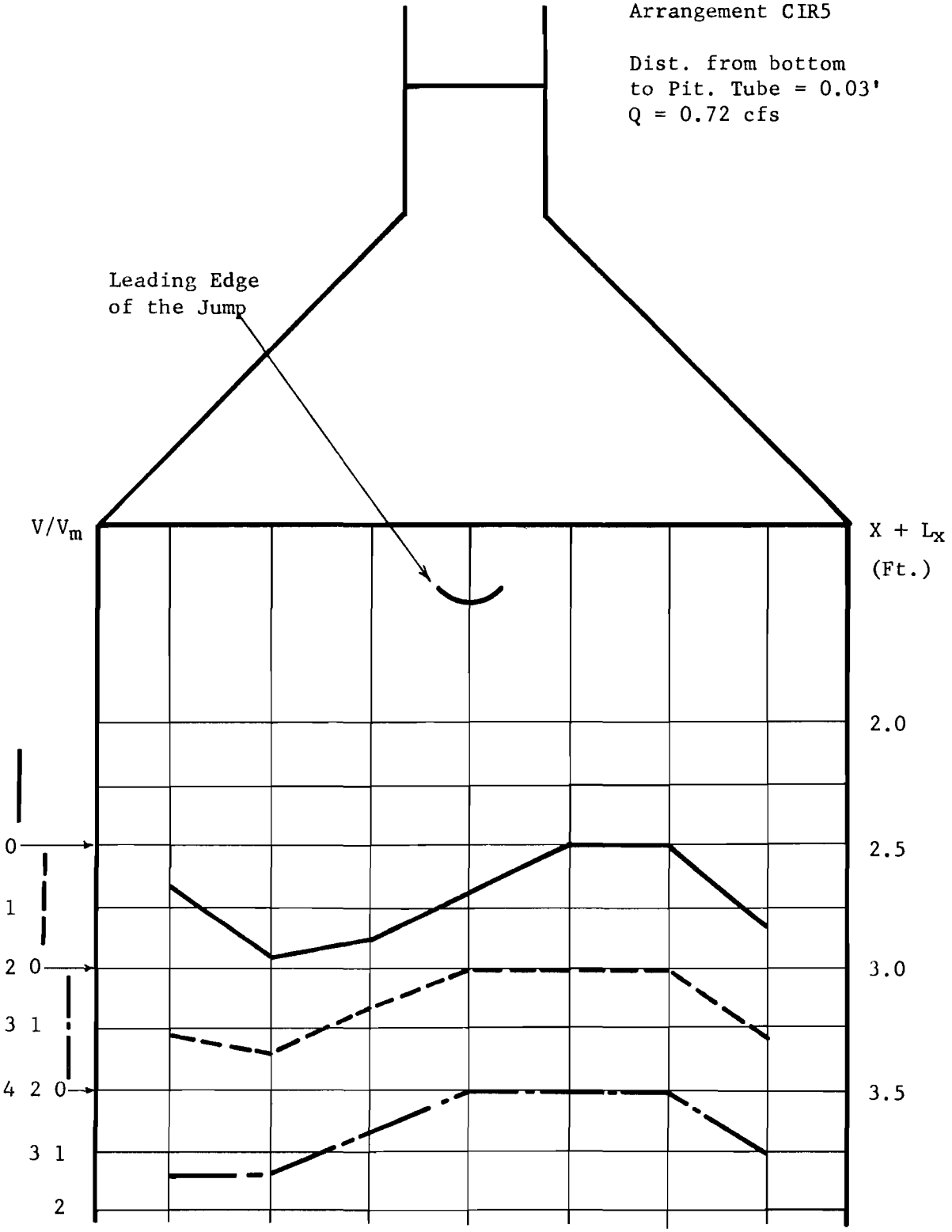

NOTE: Horizontal arrow along V/V_m scale indicates the section of velocity measurements in downstream channel.

FIG. 3-32 VELOCITIES IN DOWNSTREAM CHANNEL

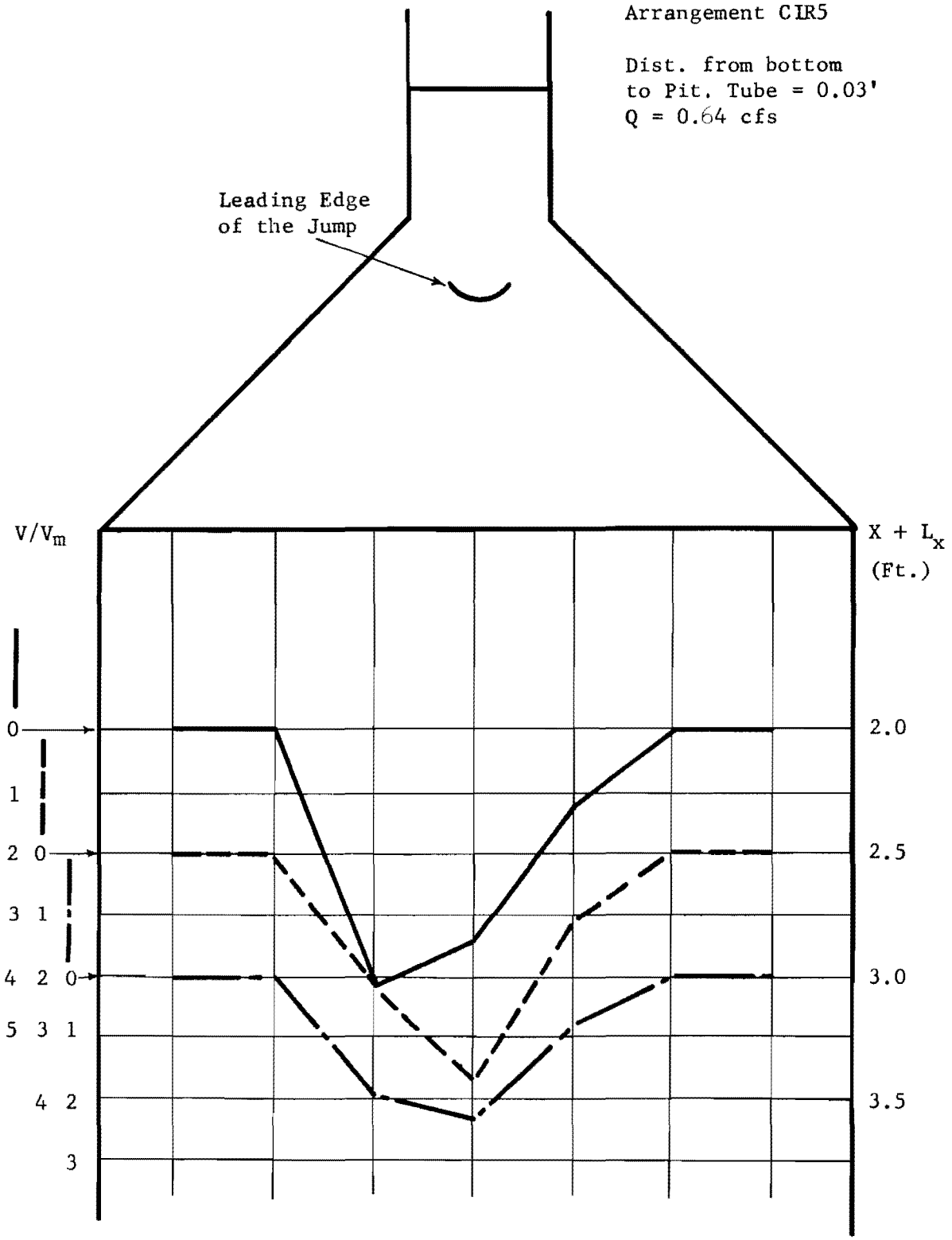

NOTE: Horizontal arrow along V/V_m scale indicates the section of velocity measurements in downstream channel.

FIG. 3-33 VELOCITIES IN DOWNSTREAM CHANNEL

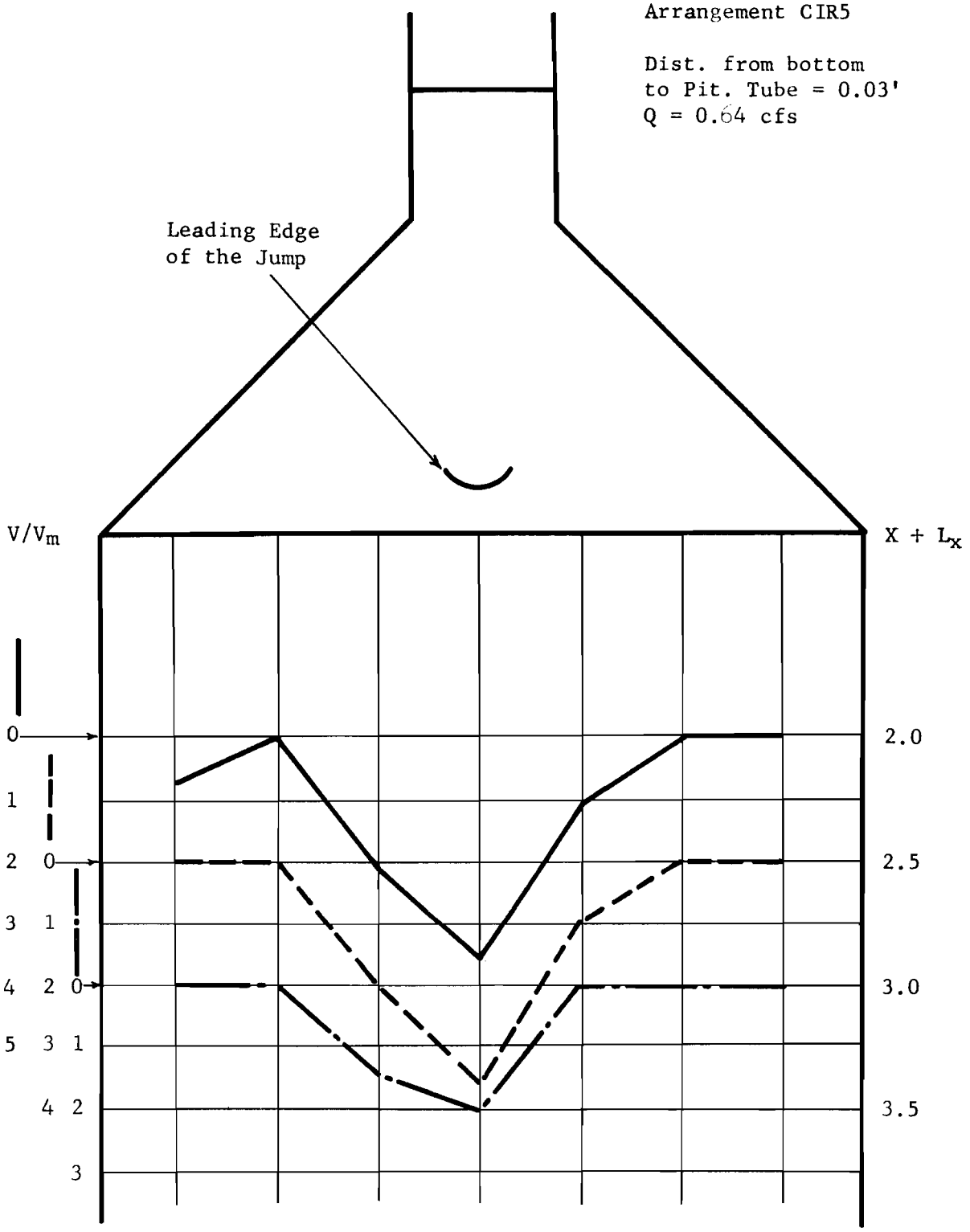

NOTE: Horizontal arrow along V/V_m scale indicates the section of velocity measurements in downstream channel.

FIG. 3-34 VELOCITIES IN DOWNSTREAM CHANNEL

It should be noted that arrangement CIR5 performed quite well only when the design flow conditions were prevailed, but a small increase in F_t shifted the point of impingement of the flow on the apron and resulted in a very unsatisfactory performance when the falling jet impinged too far downstream.

III - Structures with Box Culvert

The dimensional configuration and designation of these structures are shown in Table 2-1. The structures tested in this group consisted of arrangements BOX 1 and BOX 2. The basic difference between these structures and the ones studied previously is that the six inch diameter circular culvert of previous models was replaced by a six inch wide box culvert. The curved bottom channel for both structures had graduated "v" sections with vertical wingwalls for arrangement BOX 1 and slanted wingwalls for arrangement BOX 2. Distance "a" was zero in both structures. The criteria and the method of analyses in evaluating the dissipating ability and performance of the basin are similar to those of group I and II structures.

Water Surface Profile

Representative water surface profiles for these structures are plotted in Figures 3-35 and 3-36. The flow depth across any transverse section within the basin was rather nonuniform with centerline depth higher than the intermediate ones. Flow depth in the region of wingwalls was quite high especially in arrangement BOX 1. It was observed that along any radial line within the basin except along the wingwalls the flow depth was slightly higher in arrangement BOX 2 than BOX 1. The rearrangement of structure from vertical wingwalls to slanted wingwalls in the curved bottom channel did not change the general appearance of water surface profile appreciably. Therefore, no definite conclusion could be drawn with respect to superiority of one model to another. The economic considerations in the construction of these

BOX CULVERT (Arrangement B OX 1)

Q = 0.72 cfs Y_t = 0.31 ft.

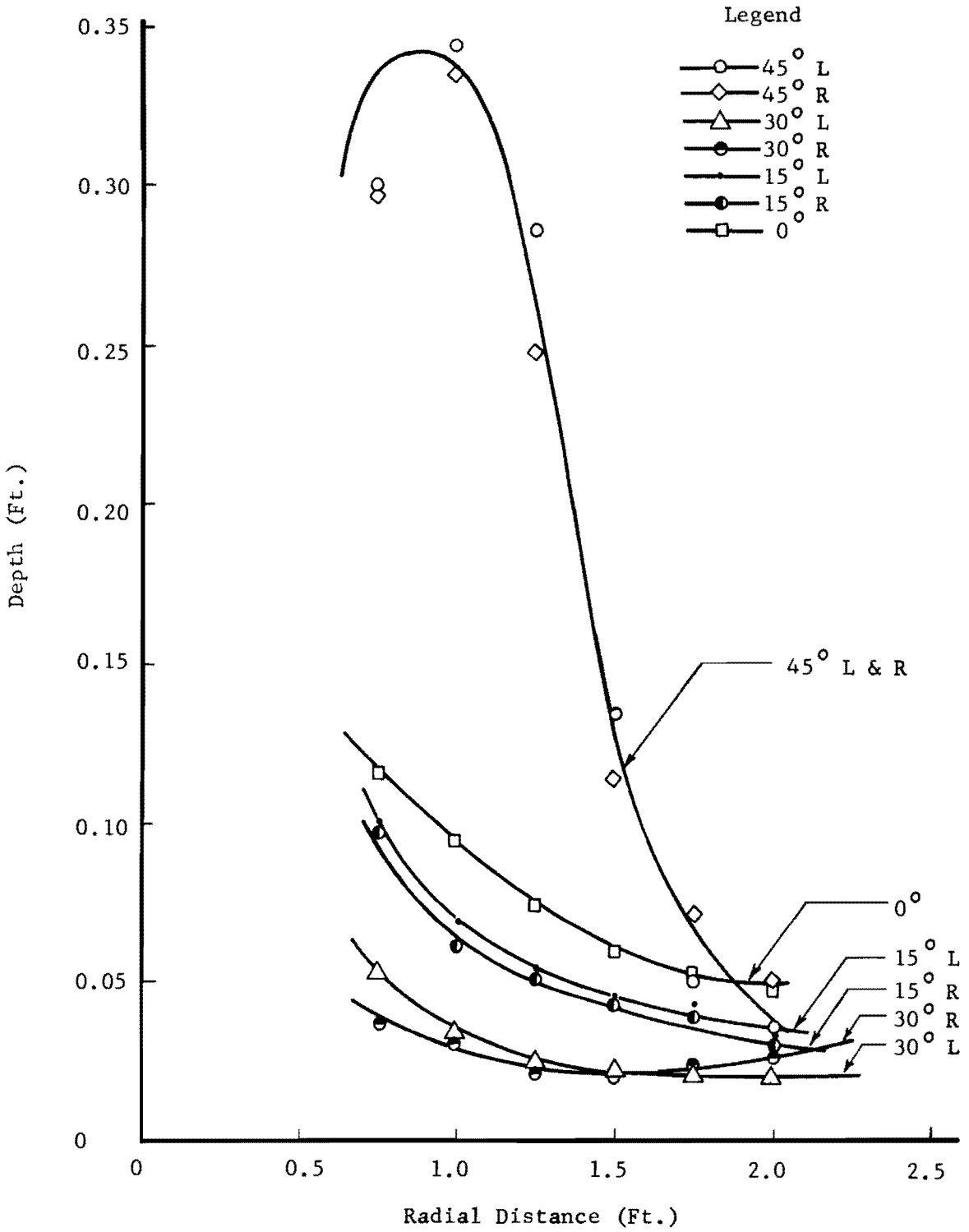

FIG. 3-35 WATER SURFACE ELEVATION OF SUPERCRITICAL FLOW ON APRON

BOX CULVERT (Arrangement BOX 2)

Q = 0.72 cfs Y_t = 0.31 ft.

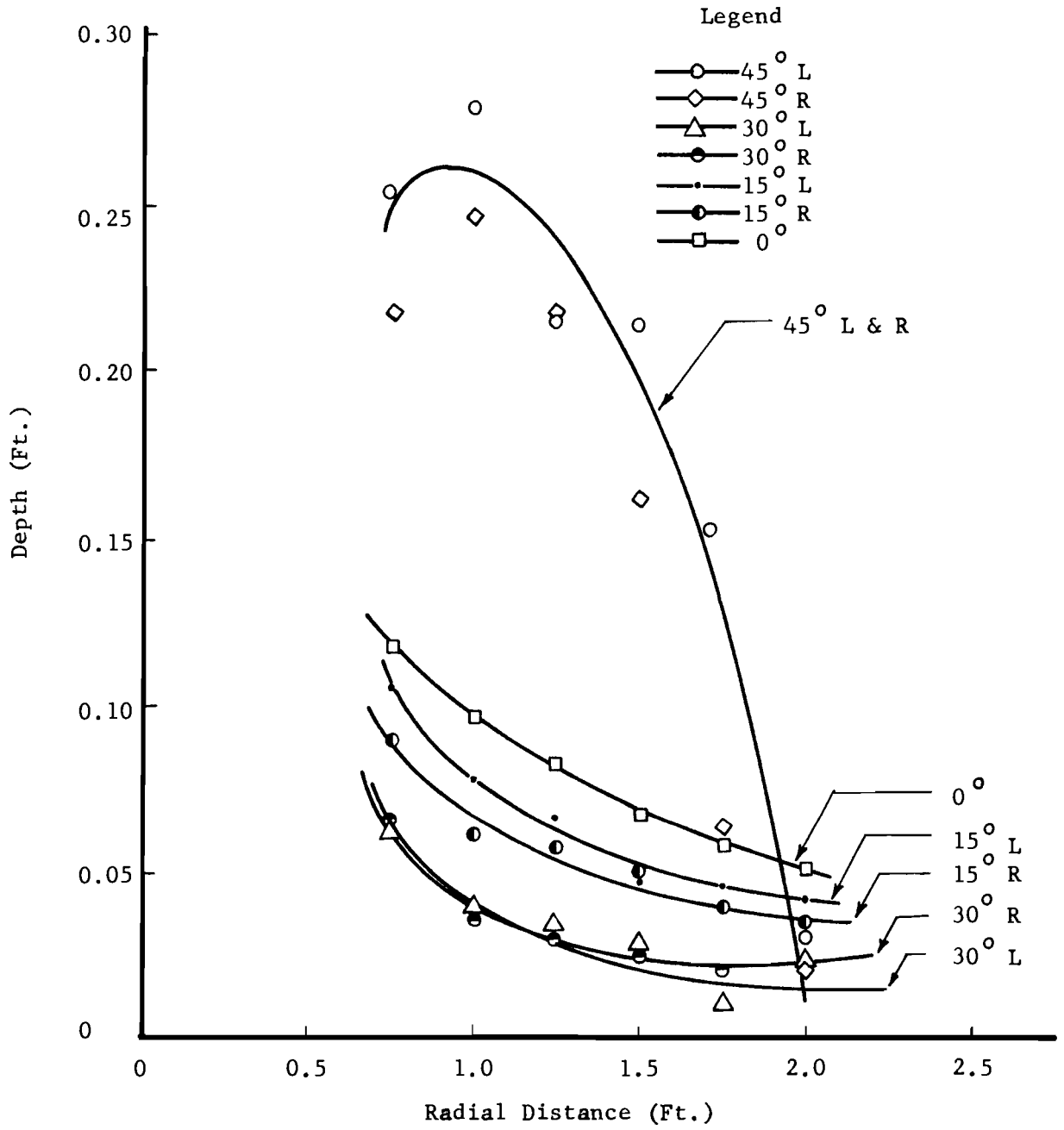

FIG. 3-36 WATER SURFACE ELEVATION OF SUPERCRITICAL FLOW ON APRON

structures is the only determining factor in the utilization of either type of geometric configuration so far as water surface profile is concerned.

Stability of the Hydraulic Jump

Curves of Y_2/Y_t vs. x/Y_t for both arrangements operating at F_t of 1.50 and 2.68 are shown in Figures 3-37 and 3-38. No significant difference was observed in the jump stability performance of the two arrangements when the jump was formed within the radial flow basin. However, when the jump moved downstream into the parallel flow channel, arrangement BOX 2 required a higher tailwater depth to stabilize the jump at a given section. It was expected that when F_t increased the required tailwater depth to stabilize the jump at a given section would also increase. This anticipated performance was experimentally verified and the results are shown in Figures 3-37 and 3-38. The absolute value of the slope of tangent to the curves of Y_2/Y_t vs. x/Y_t, which is the determining parameter of the stability characteristics, varied generally within a small range for any fixed value of x/Y_t in both arrangements and for different values of F_t. The tailwater requirements of the two structures were approximately the same for a given hydraulic condition except when value of F_t was increased to 2.68, and the jump moved into the downstream channel.

The tailwater depth required to stabilize the jump at a particular position was substantially increased when the jump moved into the downstream channel section. This performance could be due to the formation of cross waves in the supercritical flow upstream

BOX CULVERT (Arrangement BOX 1)

F_t = 2.68 Q = 0.72 cfs Y_t = 0.208 ft.
F_t = 1.50 Q = 0.72 cfs Y_t = 0.310 ft.

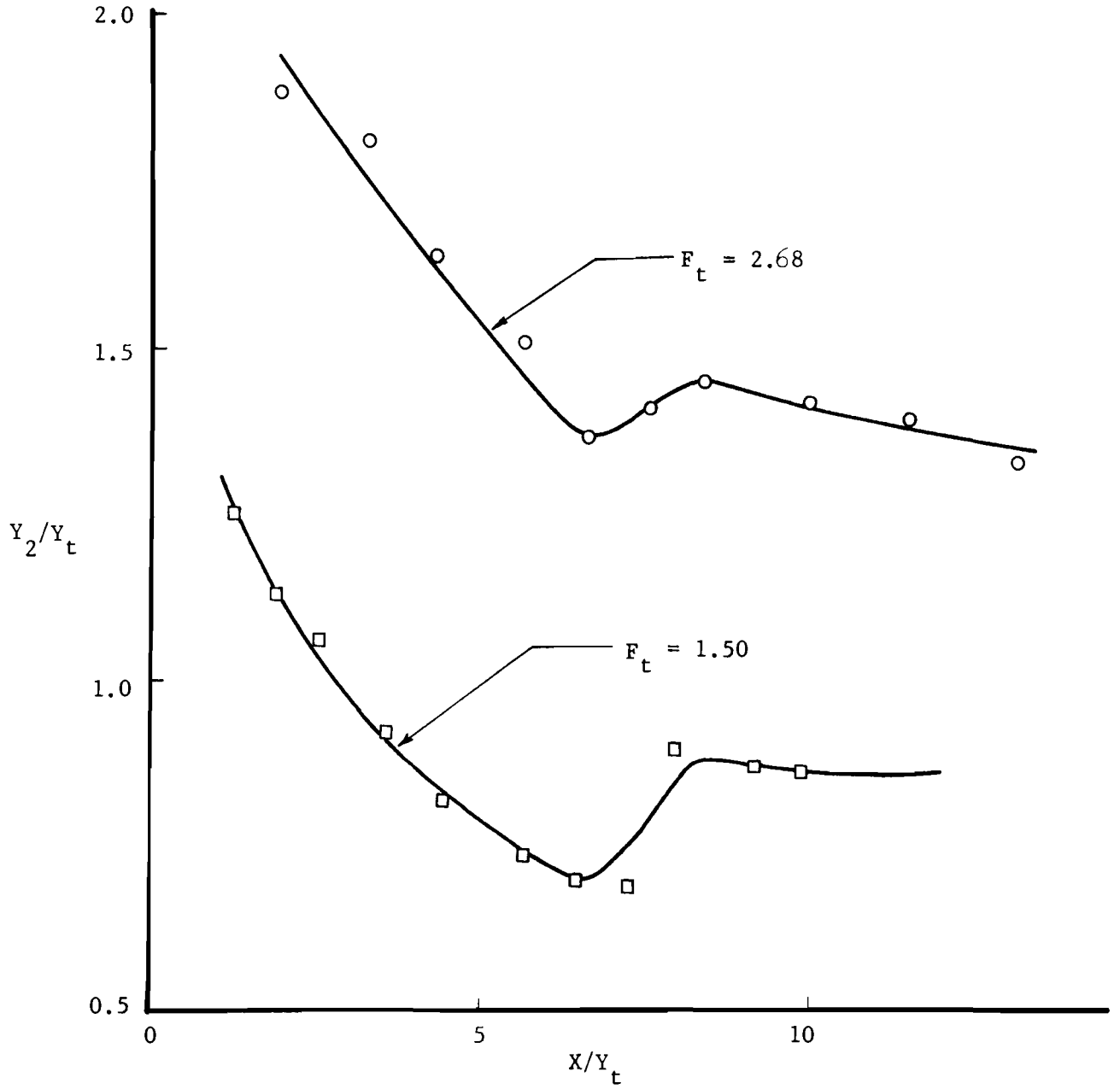

FIG. 3-37 TAILWATER DEPTH vs. JUMP POSITION

BOX CULVERT (Arrangement BOX 2)

F_t = 2.68 Q = 0.72 cfs Y_t = 0.208 ft.
F_t = 1.50 Q = 0.72 cfs Y_t = 0.310 ft.

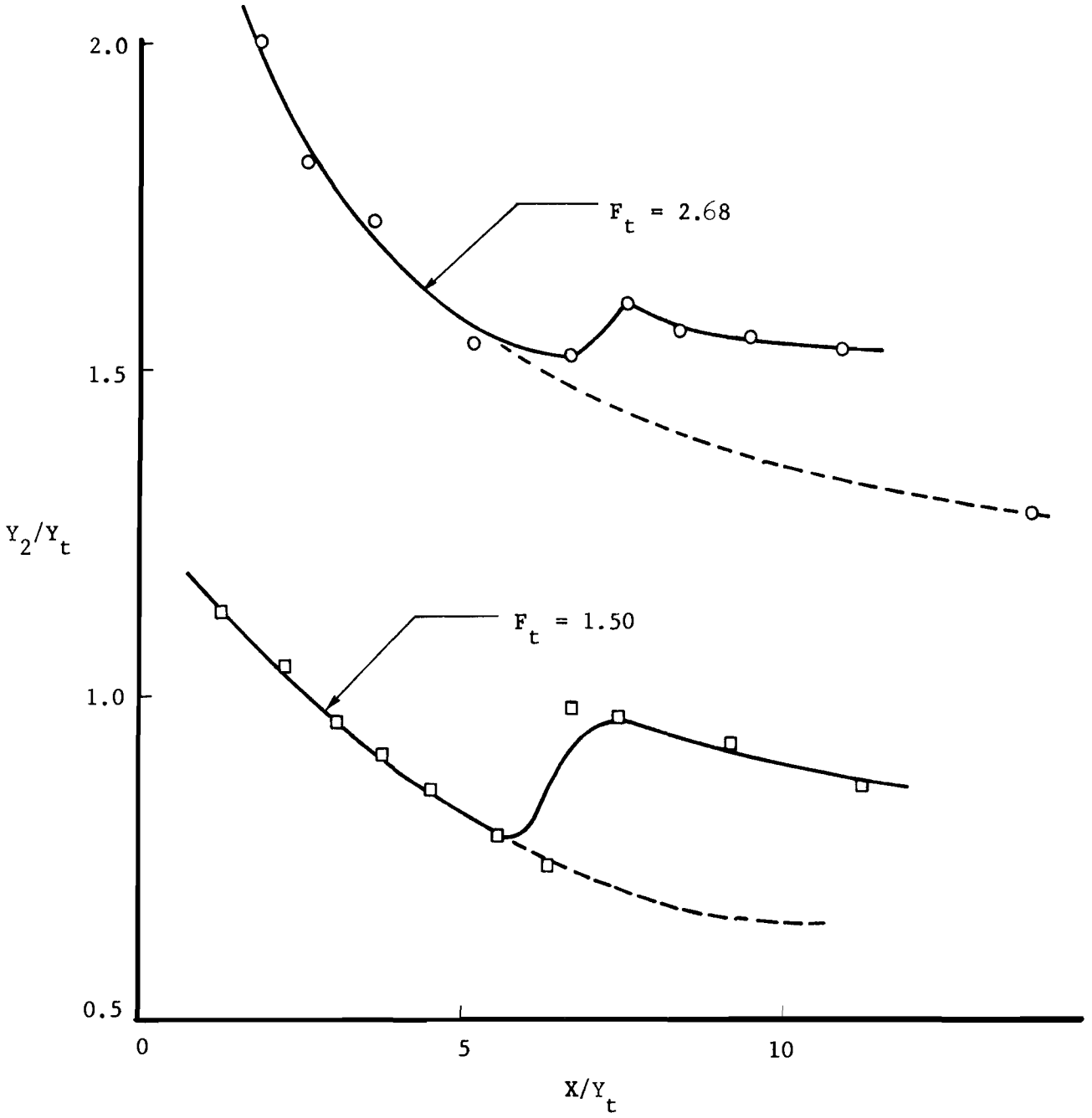

FIG. 3-38 TAILWATER DEPTH vs. JUMP POSITION

from the jump. These waves are usually found in supercritical flow in channels of nonlinear alignment or nonprismatic sections. Since the flaring wingwalls of tested structures terminated to parallel downstream channel walls, the channel was nonprismatic, and the cross waves were observed in the supercritical flow. The cross waves thus formed reflected back and forth between downstream channel walls and interferred with each other until they reached the leading edge of the hydraulic jump. These waves resulted in an increase in the initial depth of the hydraulic jump (Y_1) especially on the sides of the downstream channel. It was believed that the increase in the value of Y_1 caused an increase in the sequent depth (Y_2) of the hydraulic jump. Since this effect on Y_2 was more pronounced on the sides of the channel, it is possible that some error was introduced in determining the values of Y_2 by taking depth measurements on this region rather than the central portion of the channel. The increase in the sequent depth in turn required a higher tailwater depth to stabilize the jump at a given section.

The overall comparison of the performance of two structures indicated that arrangement BOX 1 was superior to arrangement BOX 2. Hence, slanted wingwalls in the curved bottom channel section did not improve the stability performance of the radial basin.

Velocity Distribution and Reduction

The method of velocity measurement and its representation was the same as that used in group I and II structures. Several representative plots of V/V_m are shown in Figures 3-39 through 3-50.

Analyses of these plots show the concentration of flow velocities within the central portion of the channel, zero velocities on the sides, and the highest velocities along the centerline at points nearest to the leading edge of the jump.

The velocity along the centerline at a section nearest the leading edge of the jump varied from 3 to 5 times V_m in arrangement BOX 1 and from 3.5 to 5.5 times V_m in arrangement BOX 2. Comparison of the velocity profiles of the two structures shows that usually the value of centerline velocity was slightly higher in arrangement BOX 2 than BOX 1. The upper limits of measured velocities indicated that channel protection might be needed for some natural channels in order to prevent the scour damage in the central section of the downstream channel. The necessity of channel protection would depend to a great extent on the type of material in the channel and a definite statement in regard to its applicability cannot be made. The velocity distribution in either structure was skewed to one side of the channel, which was a characteristic observed in most of the models tested in this experimental investigation. In view of the degree of velocity reduction arrangement BOX 1 was slightly preferable to arrangement BOX 2.

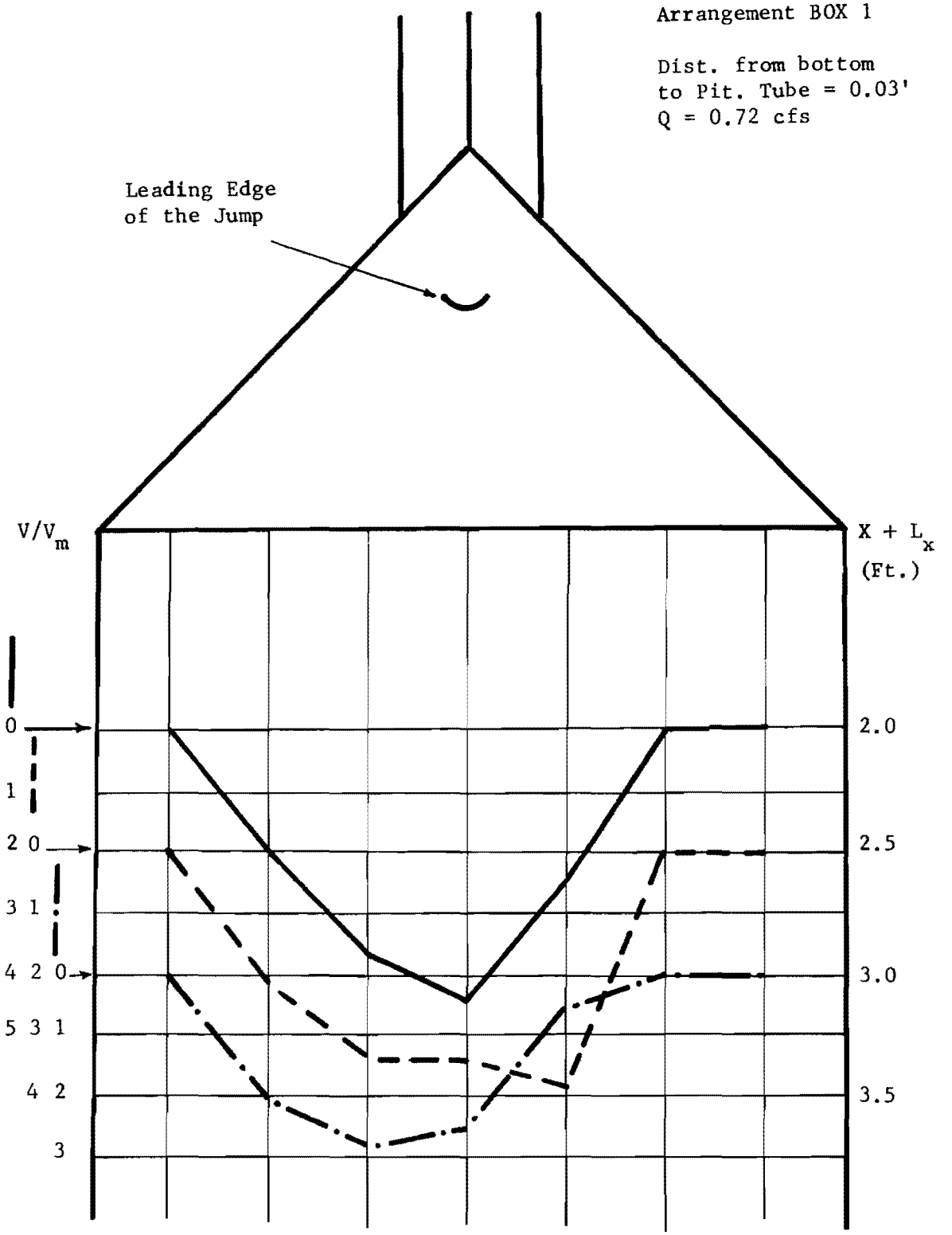

NOTE: Horizontal arrow along V/V_m scale indicates the section of velocity measurements in downstream channel.

FIG. 3-39 VELOCITIES IN DOWNSTREAM CHANNEL

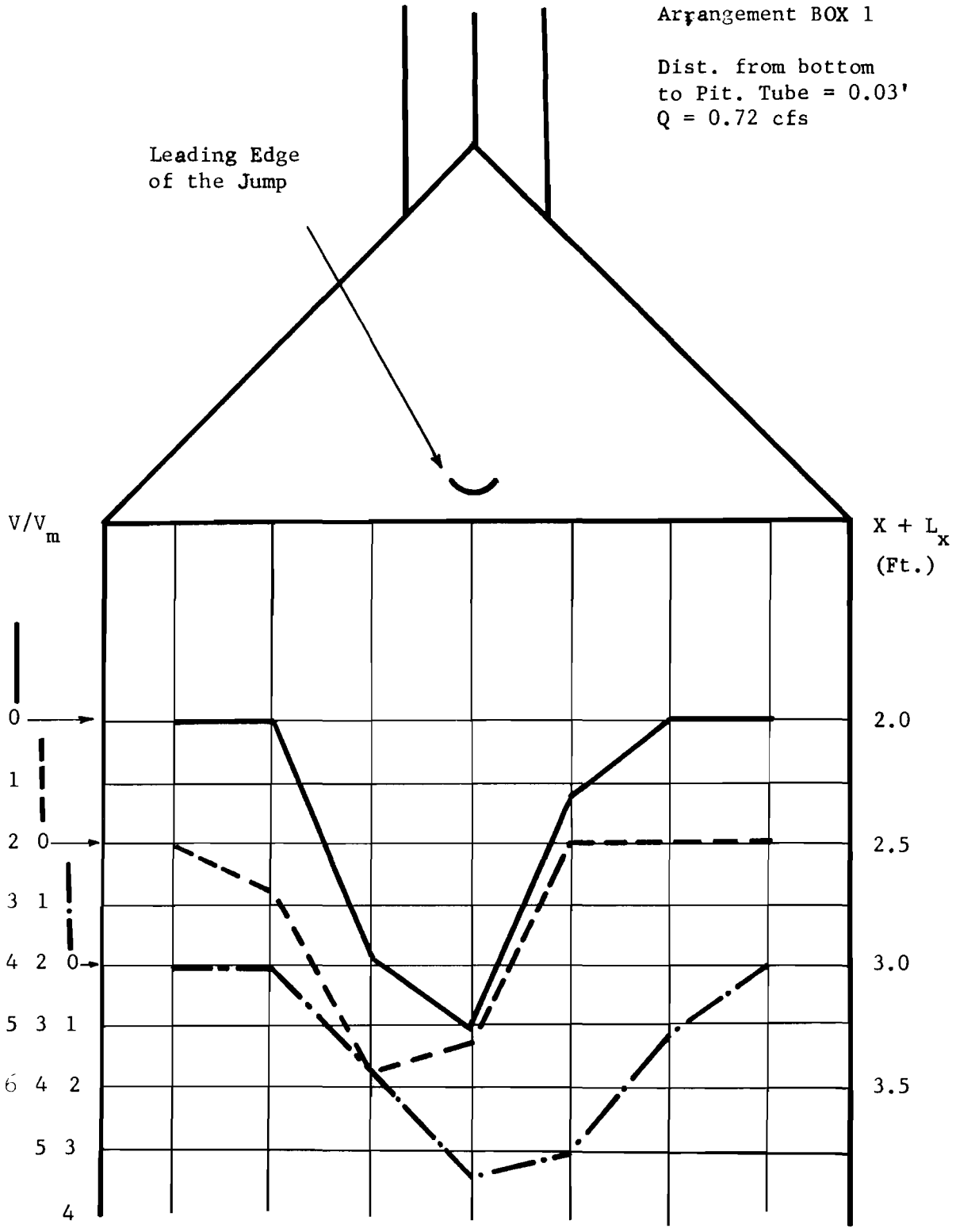

NOTE: Horizontal arrow along V/V_m scale indicates the section of velocity measurements in downstream channel.

FIG. 3-40 VELOCITIES IN DOWNSTREAM CHANNEL

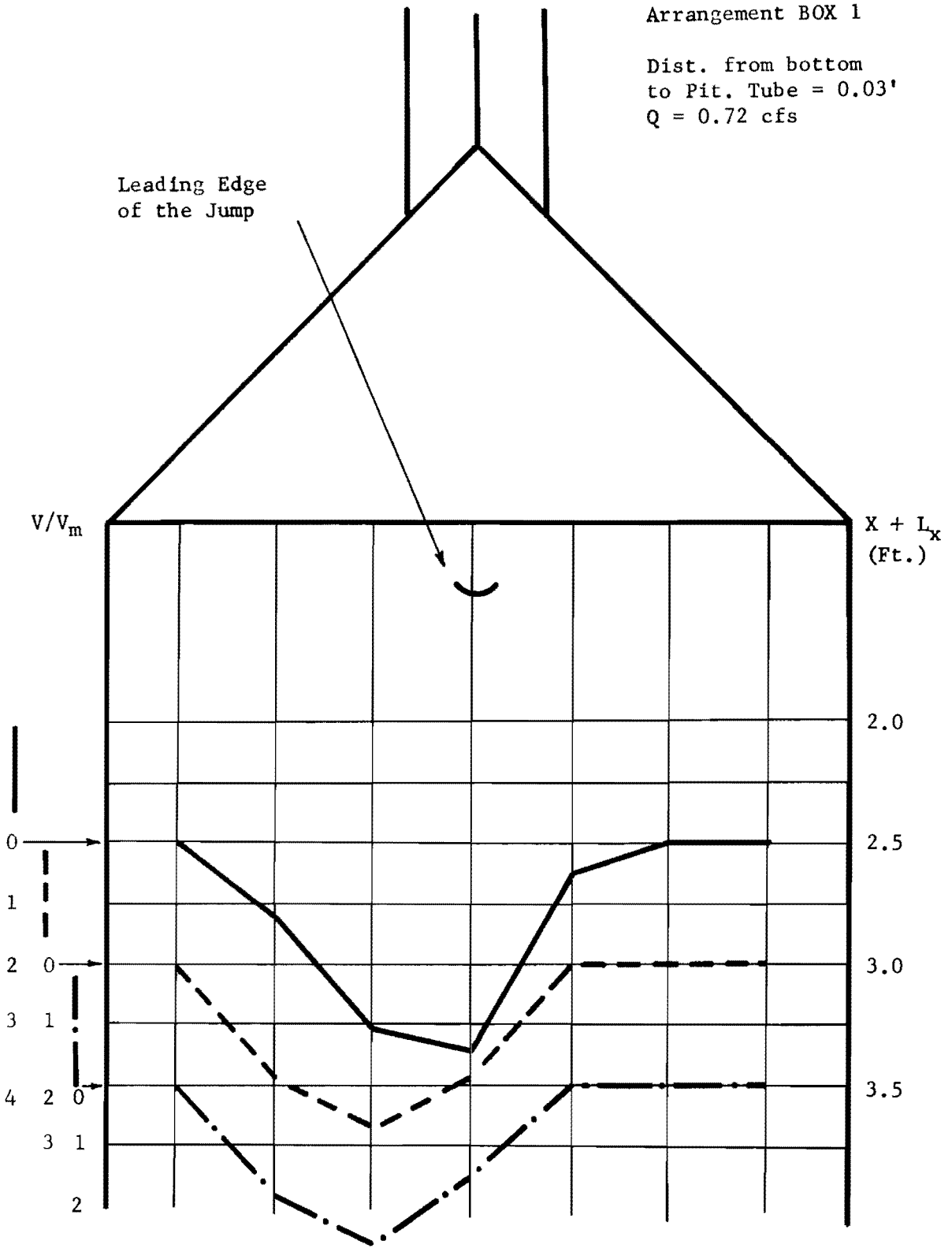

NOTE: Horizontal arrow along V/V_m scale indicates the section of velocity measurements in downstream channel.

FIG. 3-41 VELOCITIES IN DOWNSTREAM CHANNEL

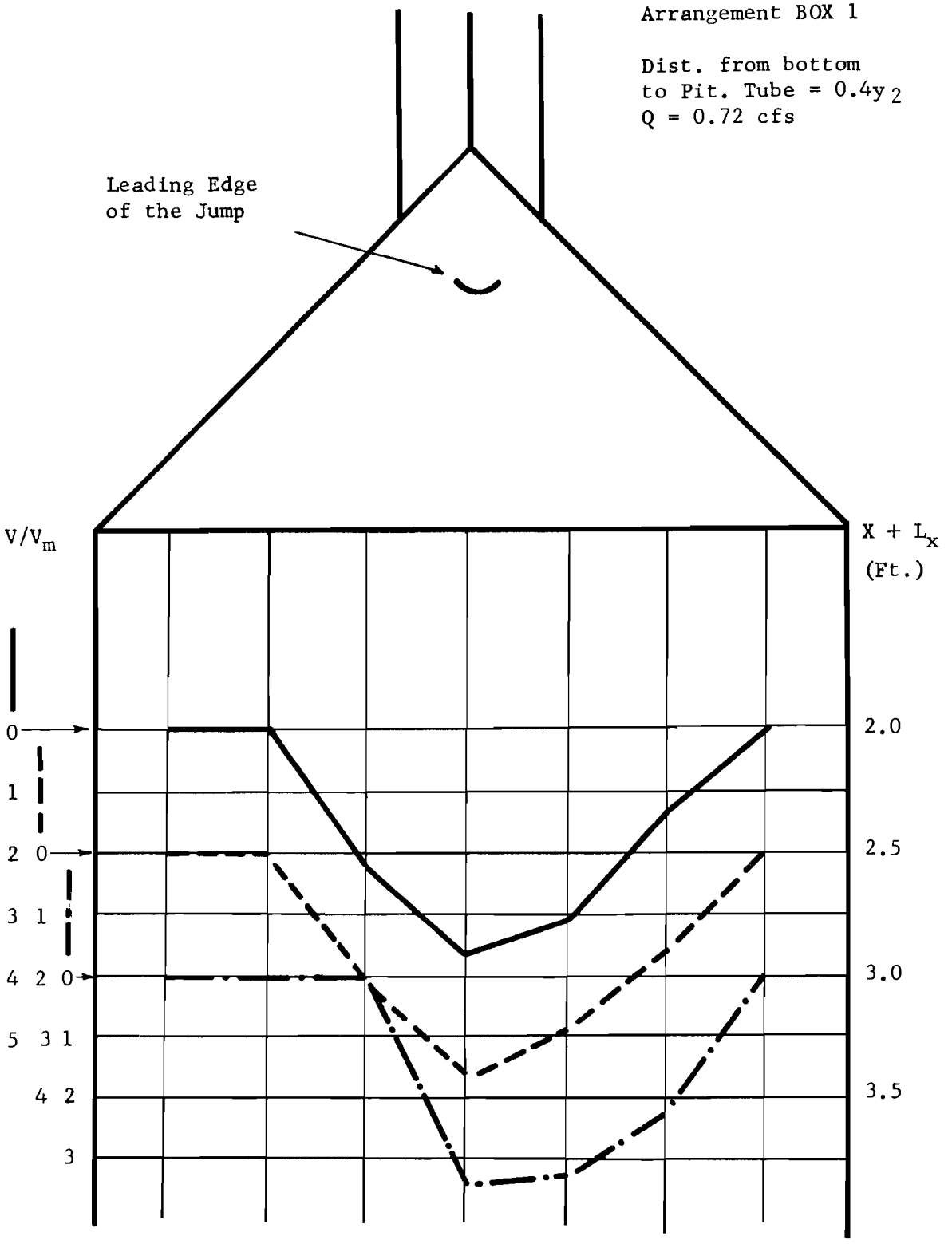

NOTE: Horizontal arrow along V/V_m scale indicates the section of velocity measurements in downstream channel.

FIG. 3-42 VELOCITIES IN DOWNSTREAM CHANNEL

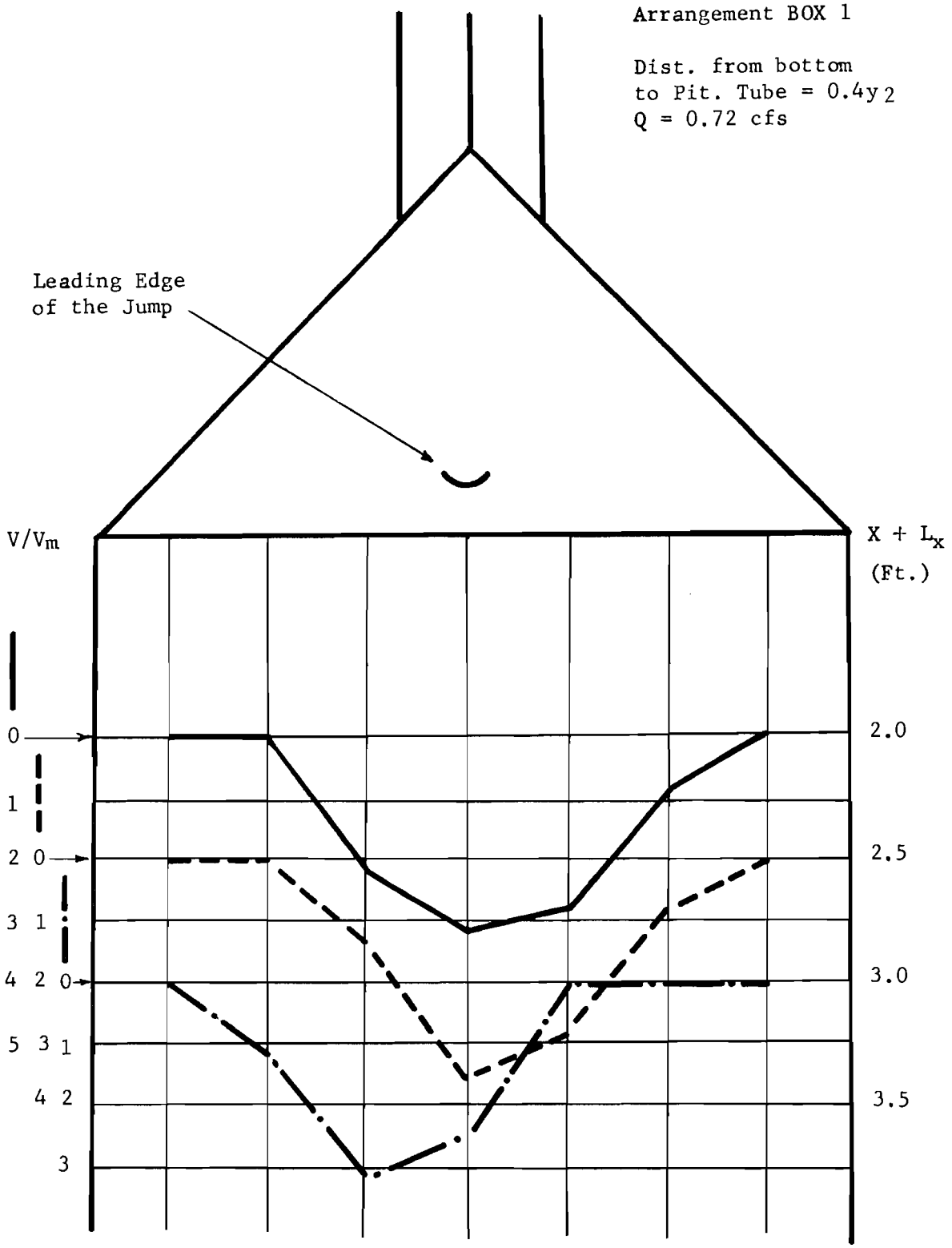

NOTE: Horizontal arrow along V/V_m scale indicates the section of velocity measurements in downstream channel.

FIG. 3-43 VELOCITIES IN DOWNSTREAM CHANNEL

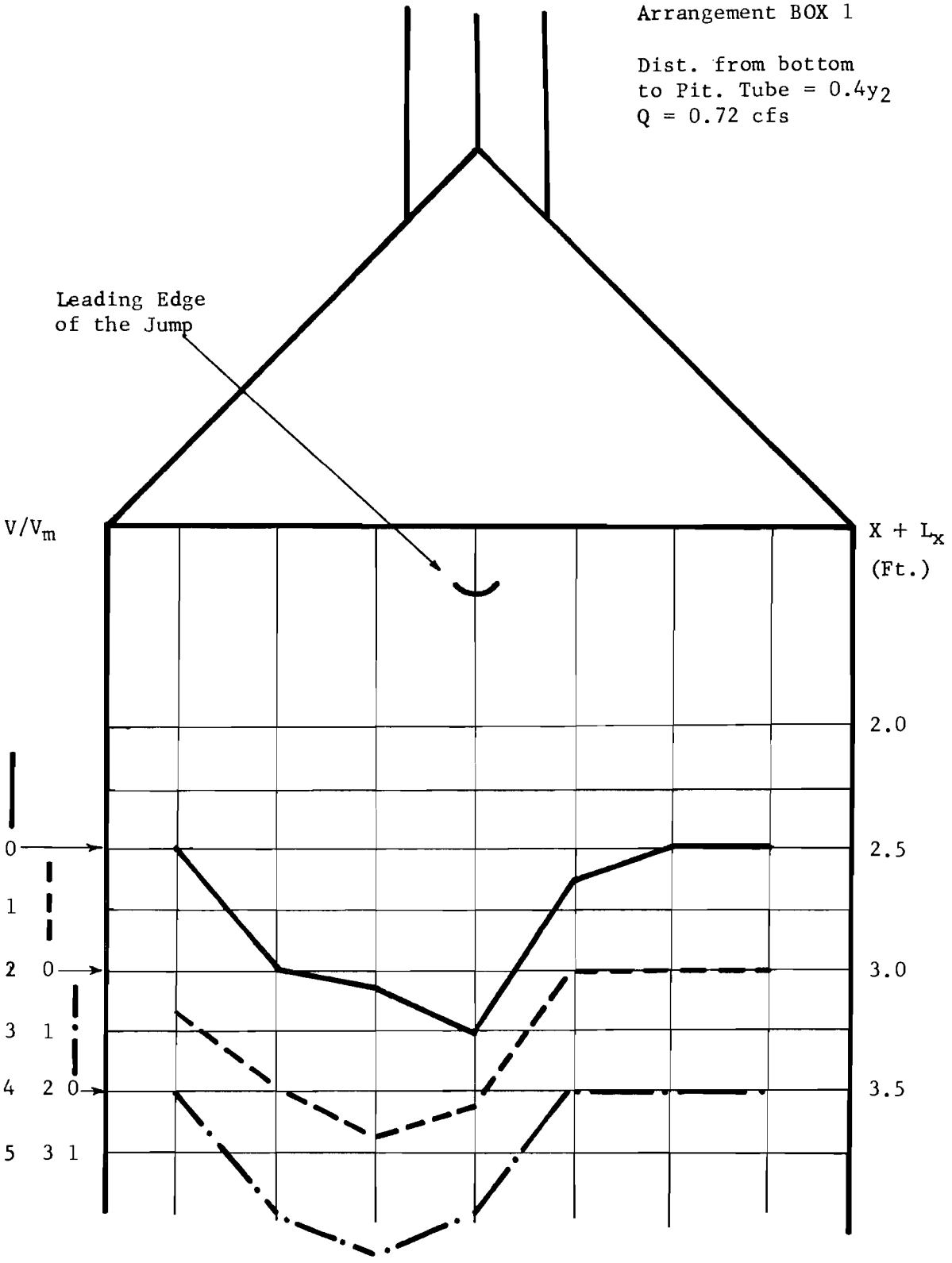

NOTE: Horizontal arrow along V/V_m scale indicates the section of velocity measurements in downstream channel.

FIG. 3-44 VELOCITIES IN DOWNSTREAM CHANNEL

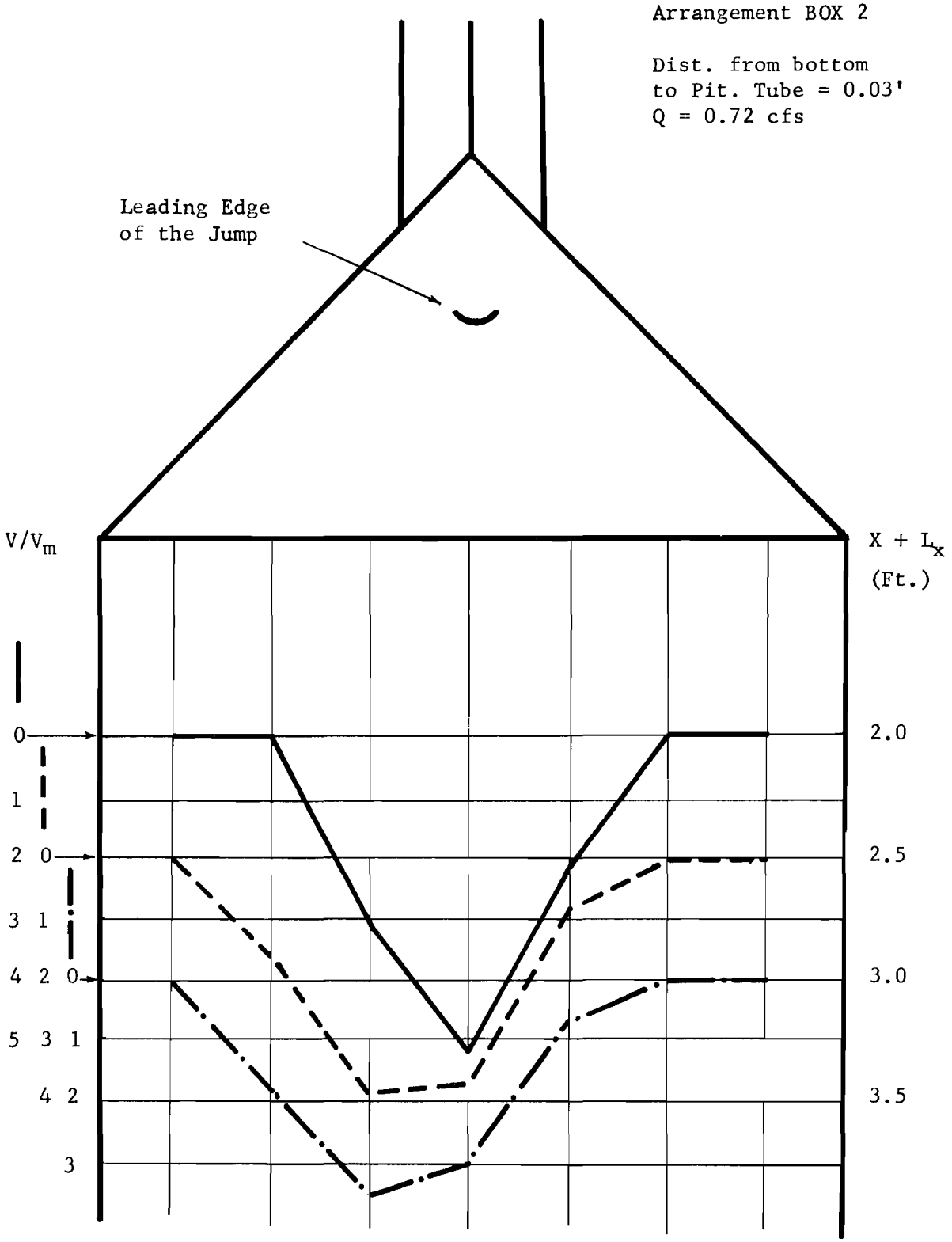

NOTE: Horizontal arrow along V/V_m scale indicates the section of velocity measurements in downstream channel.

FIG. 3-45 VELOCITIES IN DOWNSTREAM CHANNEL

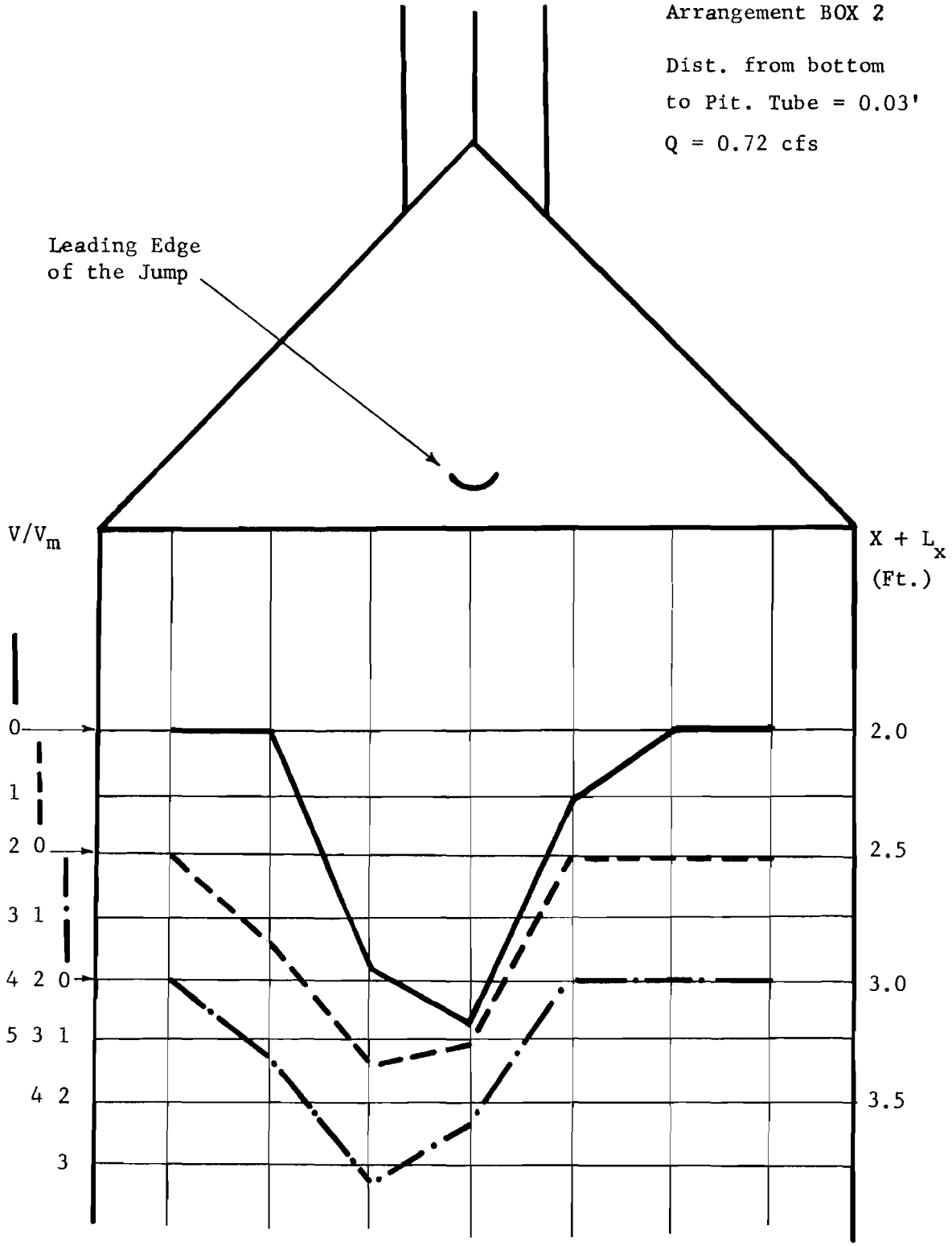

NOTE: Horizontal arrow along V/V_m scale indicates the section of velocity measurements in downstream channel.

FIG. 3-46 VELOCITIES IN DOWNSTREAM CHANNEL

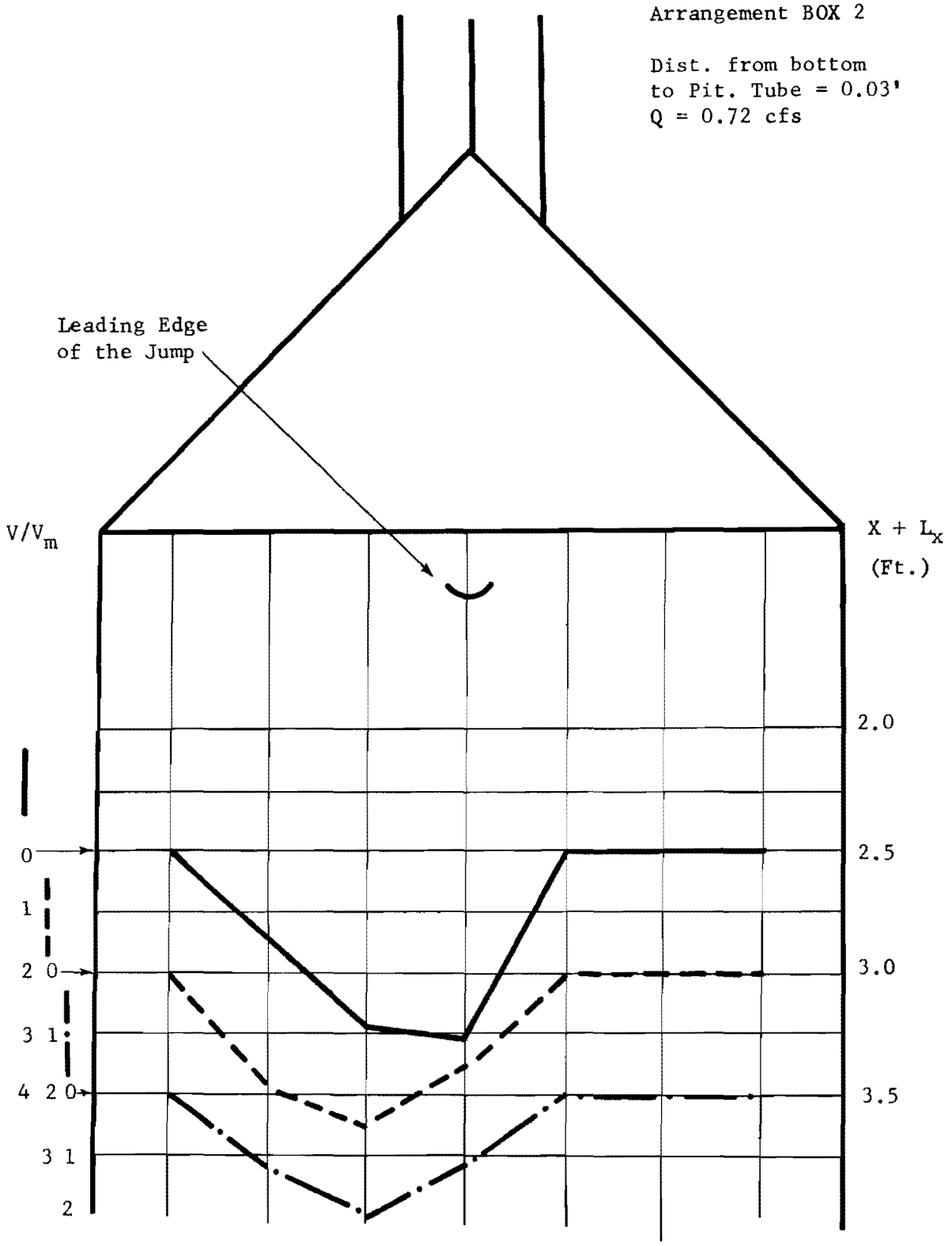

NOTE: Horizontal arrow along V/V_m scale indicates the section of velocity measurements in downstream channel.

FIG. 3-47 VELOCITIES IN DOWNSTREAM CHANNEL

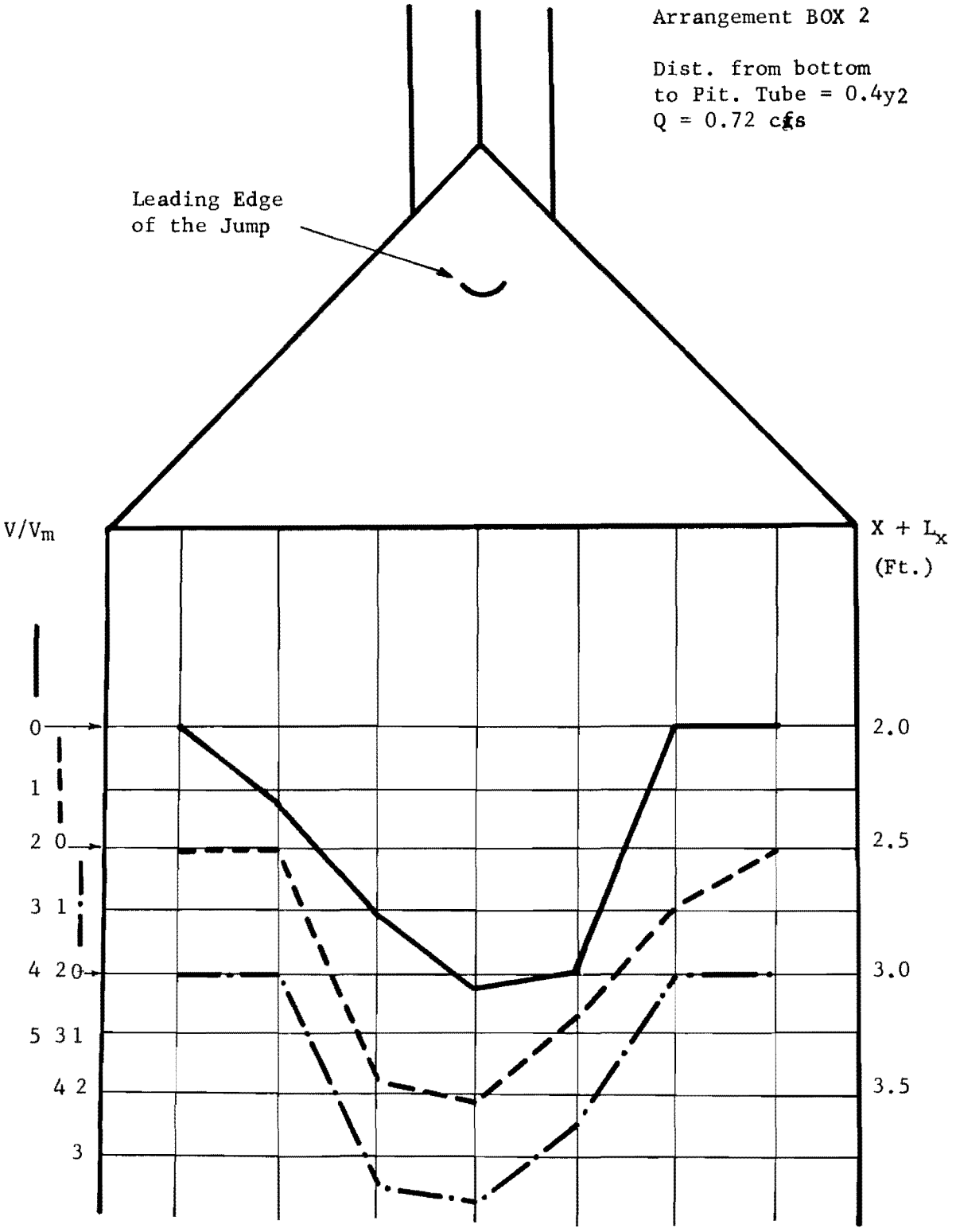

NOTE: Horizontal arrow along V/V_m scale indicates the section of velocity measurements in downstream channel.

FIG. 3-48 VELOCITIES IN DOWNSTREAM CHANNEL

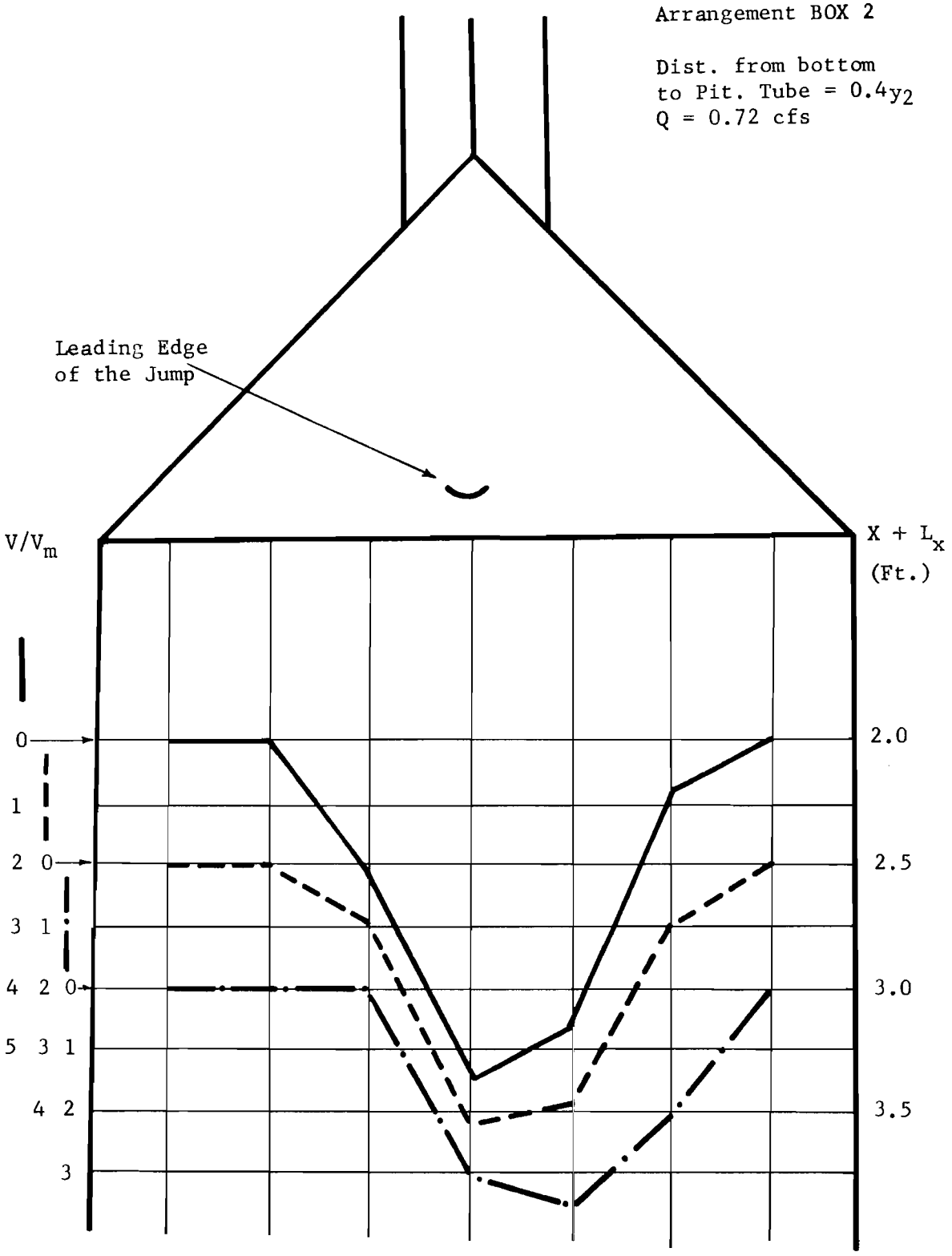

NOTE: Horizontal arrow along V/V_m scale indicates the section of velocity measurements in downstream channel.

FIG. 3-49 VELOCITIES IN DOWNSTREAM CHANNEL

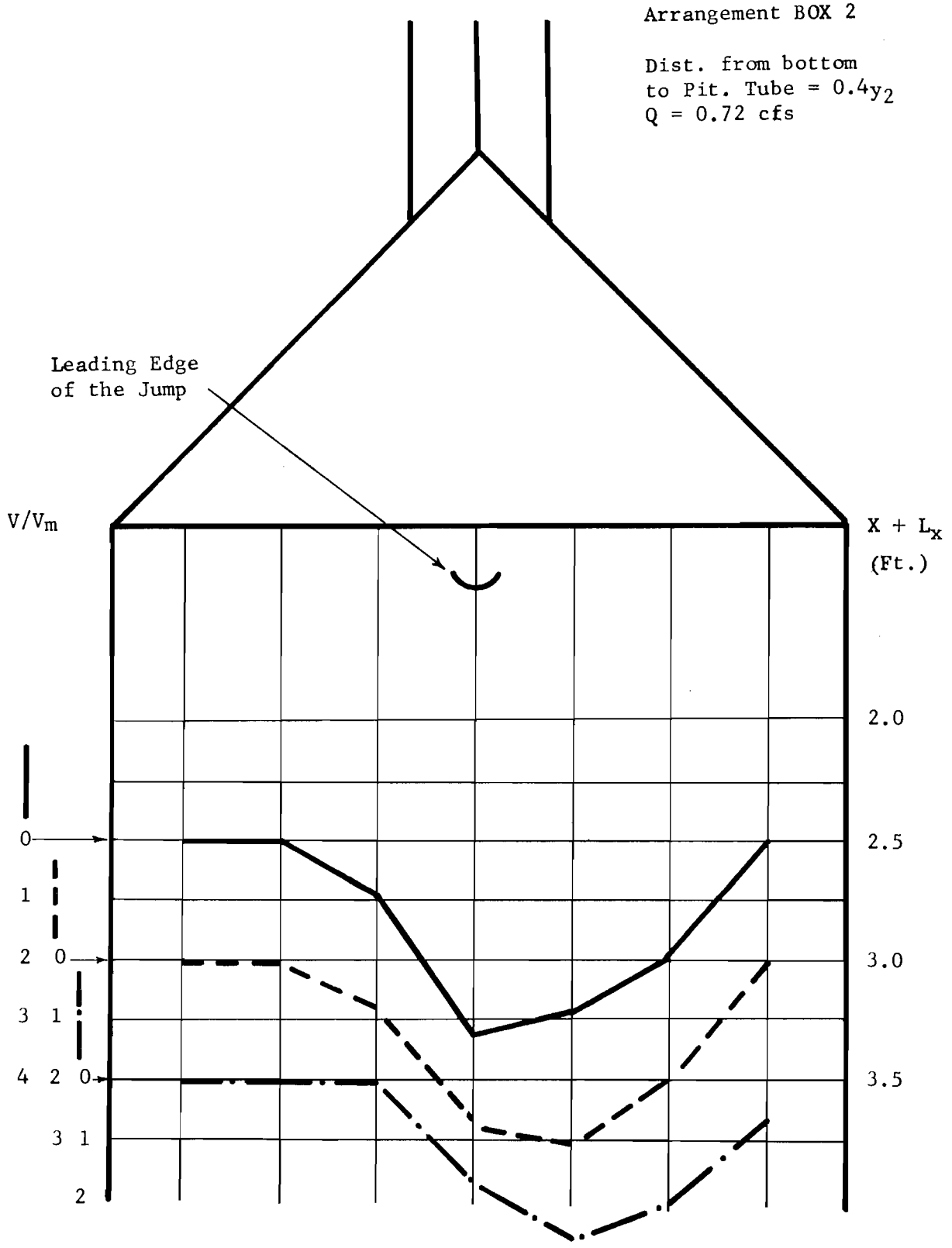

NOTE: Horizontal arrow along V/V_m scale indicates the section of velocity measurements in downstream channel.

FIG. 3-50 VELOCITIES IN DOWNSTREAM CHANNEL

CHAPTER 4

Conclusions

Since the adaptability of various geometric arrangement to the radial flow basin was not known prior to this investigation, the experimental work presented and analysed in this report has clarified certain questions with regard to the efficiency of performance and suitability of various configurations for such dissipators The results obtained herein have indicated the degree of spreading of the super-critical flow within the basin, the stability of the hydraulic jump, and the degree of velocity reduction as the flow passed over the basin for seven different geometric arrangements.

Table 4-2 shows the relative efficiency of various basins so far as the water surface profile, the hydraulic jump stability, and the degree of velocity reduction is concerned. It should be noted that in some cases it was rather difficult to make a definite distinction between the performance of some of the basins. However, the detailed investigation of their performance showed slight preference of one to another.

The best spreading action was observed in arrangement CIR5 followed by CIR1, indicating that increase in distance "a" did not improve the appearance of the water surface profile within the basin. Furthermore, the performance of the basin was satisfactory when the curved bottom channel was replaced by a simple vertical wall as in

arrangement CIR5. The least desirable water surface profile was resulted in arrangements BOX 2 and BOX 1.

Arrangement CIR1 and CIR5 displayed the highest degree of jump stability within the basin. The structural configuration having "a" of 0.5 inch performed with a little stability and was considered unsatisfactory. Stability characteristics of other arrangements were approximately the same with some minor variations.

The efficiency of the stilling action as measured by the degree of velocity reduction indicated that the most attractive basin was arrangement CIR1 followed by CIR5 and CIR4. The degree of velocity reduction in these basins indicated that the higher values of "a" were associated with lower desirable performance characteristics. So far as the velocity reduction is concerned arrangement CIR3 (a = 0.5") had the least order of performance in comparison to all other configurations.

The overall comparison of the performance of seven different configurations indicated that arrangements CIR1 and CIR5 had the best characteristics of radial flow energy dissipators. Arrangenents CIR4, BOX 1, and BOX 2 could also be effectively used as energy dissipators; however, their applicability depends to certain extent on the topography of the area, type of the culvert to be used, and the economic considerations. The performance of arrangement CIR3 was considered to be unsatisfactory.

The observed difference in performance between the various structural configurations were relatively small and the more complex

geometric forms showed no major improvement over the simple forms. The structure with the abrupt drop performed quite well for the design flow conditions, but a small increase in Froude number (F_t) caused a shift in the point where the falling jet impinged on the apron and resulted in a very unsatisfactory performance when the falling jet impinged too far downstream. From these results it appeared that the relative simplicity of construction was a strong argument in favor of the arrangements with the simple curved drop and straignt horizontal elements as in arrangement CIR1, and the simple curved bottom section used with a box culvert as reported previously by Aguirre[2].

TABLE 4-1

CLASSIFICATION OF VARIOUS GEOMETRIC ARRANGEMENTS ACCORDING TO THE ORDER OF PERFORMANCE

Order of Performance*	Water Surface Profile	Hyd. Jump Stability	Degree of Velocity Reduction
1	CIR 5	CIR 1	CIR 1
2	CIR 1	CIR 5	CIR 5
3	CIR 2	CIR 4	CIR 4
4	CIR 3	CIR 2	BOX 1
5	CIR 4	BOX 1	BOX 2
6	BOX 1	BOX 2	CIR 2
7	BOX 2	CIR 3	CIR 3

* Increasing numbers indicate decreasing performance characteristics.

BIBLIOGRAPHY

1. Chow, V. T., "Hydrologic Determination of Waterway Areas for the Design of Drainage Structures in Small Drainage Basins," Urbana, Illinois, University of Illinois, Department of Civil Engineering, Engineering Experiment Station Bulletin No. 462 (March, 1962).

2. Aguirre, R. G., and W. L. Moore, "Radial Flow Energy Dissipator for Culvert Outlets," Center for Highway Research, University of Texas, Austin, Texas, Report No. 92-1, (November 1967).

3. Wear, R. R., and W. L. Moore, "Culvert Outlet Energy Dissipator Incorporating Radial Flow and a Transverse Sill," Center for Highway Research, University of Texas, Austin, Texas, Report No. 92-3 (January 1968).